Dynamic Walking Principles Applied to Human Gait

by

Steven H. Collins

A dissertation submitted in partial fulfillment
of the requirements for the degree of
Doctor of Philosophy
(Mechanical Engineering)
in The University of Michigan
2008

Doctoral Committee:

Associate Professor Arthur D. Kuo, Chair
Professor Richard B. Gillespie
Professor Karl Grosh
Assistant Professor Riann A. Palmieri

Contents

List of Figures **iv**

Abstract **viii**

Chapter

1 Introduction **1**

1.1 Motivations 1

1.2 Dynamic walking 3

1.2.1 Passive dynamic walking

1.2.2 Dynamic walking

1.2.3 A model-based approach

1.3 Energetics 5

1.3.1 Inverted pendulum stance

1.3.2 The step-to-step transition

1.3.3 The impact of push-off

1.3.4 Step length and swing frequency

1.4 Stability 10

1.4.1 Not falling down

1.4.2 Limit cycles and Lyapunov stability

1.4.3 Sagittal stability is easy

1.4.4 Lateral stability is hard

1.5 Focus areas 15

1.5.1 Prosthetic foot to improve the step-to-step transition

1.5.2 The role of the upper extremities in gait

1.5.3 Determining risk of falls in elderly individuals

1.6 Thesis outline 17

2 Controlled Energy Storage and Return in a Prosthetic Foot **19**

2.1 Introduction 20

2.2 Methods 25

2.2.1 CESR foot prosthesis prototype

2.2.2 Experimental methods

2.2.3 Analysis

2.3 Results 33

2.4 Discussion 42

3 Swinging the arms makes walking easier **49**

3.1 Introduction 50

3.2 Methods 54

3.2.1 Model

3.2.2 Experimental methods

3.3 Results 60

3.4 Discussion 66

4 Age-related changes in balance-related step kinematics during overground walking **71**

4.1 Introduction 72

4.2 Methods 75

3.2.1 Experimental methods

3.2.2 Analysis

4.3 Results 79

4.4 Discussion 85

Appendix A **91**

References **99**

List of Figures

Figure 1.1 **7**
Fundamentals of energy use in dynamic walking.

Figure 2.1 **21**
a. Conventional prosthetic feet result in a dramatic reduction in ankle push-off work compared to the intact ankle (reproduced from Whittle (1996)).
b. Dynamic walking models predict that reduced push-off of the trailing leg (W+) will result in a disproportionately larger increase in collision negative work of the leading leg (W-) during the step-to-step transition (Kuo, 2002).

Figure 2.2 **22**
Center of mass (COM) work in intact gait, as estimated using the individual limbs method (Donelan et. al., 2002).

Figure 2.3 **24**
Hypothesized Center of Mass (COM) work rate in amputees (top) and proposed Controlled Energy Storage and Return pattern to reduce mechanical work requirements (bottom).

Figure 2.4 **27**
CESR prototype and mechanical function.

Figure 2.5 **30**
Experimental setup.

Figure 2.6 **34**
Metabolic rate was significantly reduced when wearing the CESR foot as compared to the Conventional foot prosthesis.

Figure 2.7 **34**
Subjects walked with a higher stride frequency in the Conventional condition than in the CESR condition.

Figure 2.8 **35**
Prosthesis work rate comparison.

Figure 2.9 **35**
Center of Mass (COM) work rates as estimated using the individual limbs method.

Figure 2.10 **36**
Average work rate during Collision, Rebound, Preload, and Push-Off phases of COM work as estimated using the individual limbs method.

Figure 2.11 **37**
Biological joint angles (top row), torques (middle row), and work rates (bottom row) as estimated using inverse dynamics.

Figure 2.12 **39**
Average work rates of the joints during clinical phases of gait, as estimated using inverse dynamics.

Figure 2.13 **40**
Lateral foot placement variability was greater in both simulated prosthesis conditions, while step width was greater with the CESR than with the Conventional foot.

Figure 2.14 **41**
Center of Pressure (COP) trajectories in the shank reference frame.

Figure 3.1 **55**
a. Illustration of the simple dynamic walking model with arms.
b. Frame-by-frame rendering of the Normal gait, where the ipsilateral arm and leg have the same shading.
c. Simulation results for selected arm swinging modes.

Figure 3.2 **56**
Illustration of the walking conditions tested experimentally.

Figure 3.3 **61**
Arm component of vertical angular momentum (**(a)** & **(b)**), total body angular momentum (**(c)** & **(d)**), and vertical moment at the stance foot (**(e)** & **(f)**). Double support is denoted by a shaded region in plots.

Figure 3.4 **62**
Net metabolic rate increased across conditions. Error bars represent standard deviations and asterisks indicate a statistically significant difference with a significance level of $p = 0.05$

Figure 3.5 **63**
Upper limb joint angles, torques, and powers for the Normal, Held, and Anti-Phase conditions over one stride.

Figure 3.6 **65**
Peak shoulder joint torques were always low, but increased in the Held condition. Error bars represent standard deviations and asterisks indicate a statistically significant difference with a significance level of p = 0.05.

Figure 3.7 **65**
Lower limb joint angles, torques, and powers for each of the conditions tested. No statistically significant differences due to arm swinging condition were observed within these measurements.

Figure 4.1 **75**
Method of data collection (left) and definition of step length and step width (box at right). Subjects wore a magnetic marker on each foot, placed above the third metatarsal (depicted as squares), as well as a marker near the sacrum (not pictured).

Figure 4.2 **77**
Decomposition of fore-aft foot placements, demonstrated with one sample trial.

Figure 4.3 **80**
Box plots of mean walking speed, step length, and step width.

Figure 4.4 **80**
Box plots of total foot placement variability and total stride period variability.

Figure 4.5 **82**
Box plot of short-term foot placement variability, defined as the standard deviation of short-term deviations (see figure 2).

Figure 4.6 **83**
Box plots of long-term speed, step length, and step width variabilities, defined as the standard deviation of their respective long-term fluctuations (figure 2).

Figure 4.7 **84**
Long-term fluctuations in step length vs. speed, for two sample subjects.

Figure A.1 **94**
Joint angle trajectories for the Most Anthropomorphic parameter set Normal mode of walking.

Figure A.2 **95**
Joint angle trajectories for the Most Anthropomorphic parameter set Bound mode of walking.

Figure A.3 **95**
Joint angle trajectories for the Most Anthropomorphic parameter set Anti-Phase mode.

Figure A.4 **96**
Joint angle trajectories for the Demonstration parameter set Normal mode of walking.

Figure A.5 **96**
Joint angle trajectories for the Demonstration parameter set Bound mode of walking.

Figure A.6 **97**
Joint angle trajectories for the Demonstration parameter set Anti-Phase mode.

Figure A.6 **97**
Joint angle trajectories for the Demonstration parameter set Anti-Phase mode.

Figure A.8 **98**
Joint angle trajectories for the Demonstration parameter set Parallel mode of walking.

Figure A.9 **98**
Joint angle trajectories for the Slow parameter set Double-Swing mode.

Abstract

The subject of this thesis is the application of the dynamic walking approach to human gait. This work is motivated by the needs of persons with disabilities and by a desire to expand basic understanding of human walking. We address human gait from the perspective of dynamic walking, a theoretical approach to legged locomotion which emphasizes the use of simple dynamical models and focuses on behavior over the course of many steps rather than within a single step. We build on results from prior dynamic walking research and develop new areas of exploration, with energetics and stability providing context. We focus on three areas: improvement of prosthetic foot design, the function of arm swinging, and evaluation of balance among the elderly. These issues are addressed by use of dynamic walking models and controlled human subject experiments. We propose a Controlled Energy Storage and Return (CESR) foot prosthesis to increase push-off work and reduce energy expenditure in amputees, and tested a prototype experimentally. To better understand the role of arms swinging in gait, we developed a simple dynamic walking model with free-swinging arms and performed human subject experiments in which subjects swung their arms in various ways. Finally, we studied the effects of aging on balance during walking using a computational model and a human subject experiment in which younger and older adults walked overground for hundreds of consecutive steps. These models and experiments each expand our understanding of the fundamentals of gait and indicate pathways toward assisting individuals with disabilities. Taken as a whole, this work emphasizes the utility of the dynamic walking approach.

Chapter 1
Introduction

1.1 Motivations

A wide range of health issues related to walking pose problems to individuals in the U.S. and throughout the world today. Additionally, some basic questions about why people walk the way we do still persist. We seek to address some of these problems and questions using a dynamic walking approach.

Millions of Americans are affected by limb loss, with hundreds of thousands of new amputations performed each year, most of which affect the lower extremities. The majority of amputations in industrialized nations result from vascular diseases such as diabetes, which now affects about sixteen million Americans and is becoming increasingly prevalent among all age groups. A small but disturbing portion of amputations are the devastating result of military conflict. Modern wars have produced proportionally greater numbers of amputees among casualties of war, as protective gear and life-saving medicine reduce the risk of death but increase the numbers of disabled veterans and civilians. While the amputee population has been increasing, prosthesis technologies have not kept pace with innovations in other medical fields. The most commonly prescribed foot prosthesis in the U.S. is still the Solid Ankle Cushioned Heel foot, which was designed in the 1950's to improve upon prior wooden feet by the inclusion of a rubber wedge at the heel. The SACH foot was popularized by the Ohio Willow Wood Company, so named for the type of wood they used as the primary building material for these feet. Many newer foot prosthesis designs incorporate modern engineering materials such as carbon fiber composites to improve comfort, an innovation which took place in the mid 1980's. However, amputees still require significantly greater effort to accomplish the same ambulatory tasks as intact individuals. We sought to

develop greater understanding of the factors which affect energy use in amputee gait and to apply this understanding, and modern technologies such as the microprocessor, to prosthetic feet with the aim of increasing mobility in the growing amputee community.

Falls during walking also present a growing health risk among the aging populations of industrialized nations. Falls can result in serious injuries such as hip fracture, which also increase the risk of pneumonia and other complications during hospitalization. Elderly individuals are more likely to fall than the general population, and are more likely to become injured during a fall. Most falls occur during walking. Interventions with individuals who are at an increased risk of falls may provide a crucial means of prevention, and many researchers have attempted to develop tools for predicting the likelihood of falls as a means of identifying at-risk individuals, with limited success. Evaluation methods often require significant laboratory time and instrumentation, and current metrics have produced mixed results. We sought to apply a modeling approach to help identify the parameters most related to balance and to fall likelihood, with the aim of developing a device to monitor fall risk more effectively and easily.

In addition to solving these concrete health problems, we are also interested in answering some persistent questions about why people walk the way they do. For instance, why do people swing their arms during walking? As everyone knows, people swing their arms as they walk, with the left arm following the pattern of the right leg and vice versa. For more than one hundred years, biomechanics researchers have puzzled over the reasons for this peculiar motion, if any, but have not presented a convincing case for any singular hypothesis. We sought to use simple dynamic walking models and controlled human subject experiments to help explain the underlying reasons for arm swinging.

We used an approach that utilized mathematical models, human subject experimentation, and, where possible, technology development. We used simple mathematical models to gain abstract insights into walking. These mathematical models allowed for rapid and highly controlled examination of the modeled systems, facilitating development of theories that describe the phenomena of interest. Energetics and stability were a primary

focus. Guided by the understanding gained from these models, we designed controlled human subject experiments. In these experiments, we evaluated the relevance of our models and studied the effects of theoretically relevant parameters on actual human gait. Where possible we capitalized on useful trends, using mechanical engineering design to develop assistive technologies.

1.2 Dynamic walking

Dynamic walking is a theoretical approach to legged locomotion which emphasizes the use of simple dynamical models and focuses on behavior over the course of many steps, rather than within a single step, typically in an attempt to understand or promote stability and energy economy. It is useful to begin a discussion of dynamic walking by describing passive dynamic walking, from which the approach originated.

1.2.1 Passive dynamic walking

Passive dynamic walking was first proposed by Tad McGeer (e.g. McGeer, 1990) in the late 1980's as a simpler and more efficient alternative to popular approaches to the control of bipedal gait in walking robots. The prevailing approach to walking robots at the time was to use continuous-time high-gain feedback control to move joints through a pre-specified trajectory, an approach that resulted in slow walking speeds, high energy use, and high control costs (e.g. Hirai et. al., 1998). McGeer proposed that control of walking robots would be simplified if the machine were designed such that gait were a natural oscillation of the system, just as swinging back and forth is a natural oscillation of a pendulum. He created mathematical models to test this idea and found that a remarkably simple system, consisting of two rigid legs connected at the hip by a pin joint, could produce a motion remarkably similar to human leg motions during gait. He built a robot based on the model's parameters and found that indeed a machine with no control and no actuation could produce a walking motion very similar to human gait. McGeer's machines walked down shallow slopes to recover energy lost in collisions, but he theorized that power could be added to allow for level-ground walking. He took his inspiration from the Wright brothers, who before building powered airplanes first learned to build good gliders by studying the natural dynamic interactions of air and foil.

Advantages of the passive dynamic approach included the simplicity of the root models, the use of practical stability measurements, and energy economy. Passive dynamic models were morphologically simple, requiring few parameters to describe each model (e.g. McGeer, 1991; Garcia et. al., 1998; Kuo, 1999). This allowed for a more thorough exploration of parameter space than in complex high-parameter models. It also meant that the results were easier to interpret, which made it easier to develop an understanding of the principle factors underlying the systems. Instead of focusing on the stability of the continuous task of following prescribed joint trajectories within a step, passive dynamics considered stability of many steps over time (e.g. McGeer, 1989; Coleman and Ruina, 1998; Garcia et. al., 1998; Kuo, 1999). Since the simplest passive dynamic models had no control or actuation, continuous closed-loop feedback was not even a consideration. Instead, model parameters were selected which resulted in the most stable gait over many steps. A digital controls approach was used, considering each step as a unit, sampling the system at each heel strike, and tracking changes in the system state. This approach was girded by the use of nonlinear mathematics methods such as limit-cycle analysis, with eigenvalues quantifying a gait limit cycle's stability. In other words, the analysis was focused on whether the machine would fall eventually, rather than whether a particular joint trajectory could be temporarily perturbed. Finally, the approach resulted in models and machines which used remarkably little energy (e.g. McGeer, 1990; Coleman and Ruina, 1998; Collins et. al., 2001). Since the joints were un-powered, the only source of energy dissipation was the transition from one pendulum-arc step to the next, supplied by a slight descent in gravity on each step. Dynamic walking utilizes these strengths in systems that include some measure of active powering.

1.2.2 Dynamic walking

Dynamic walking builds on the passive dynamic approach by carefully adding simple forms of actuation and control. The strengths of the passive dynamic walking approach still hold, and indeed may be improved upon, by these additions as long as the natural dynamics of the system are not overwhelmed. For instance, high-frequency feedback position control is generally avoided. Success in such control schemes usually results in

a system that has little or no dynamics of its own. Typically, this type of position control also requires high-power high-bandwidth sensors and actuators which are cumbersome, consume large amounts of energy, and are quite unlike human nerves and muscles. Instead, dynamic walking models are powered by springs, impulses, and simple forcing functions. This allows exploitable dynamics to persist and yields results that lend themselves to comparisons with human gait.

1.2.3 A model-based approach: prediction and observation

Human subject experiments based on dynamic walking are implicitly model-based as opposed to observation-based. Classically, many theories developed in the biomechanics community regarding the underlying principles of human walking have been based almost entirely on observations of unaffected gait. For instance, the "six determinants of gait" (Saunders et. al., 1953) were based on observations of patients and subjects as they walked naturally in a gait laboratory, rather than upon experiments in which parameters hypothesized to impact energy use were controlled and varied across conditions. By contrast, the dynamic walking approach uses models to guide human subject experiments, with model results suggesting parameter studies to be conducted or interventions to be applied. Additionally, dynamic walking models have shown predictive validity for human gait in many cases (e.g. Kuo, 2001; Bertram and Ruina, 2001; Donelan et. al., 2002b). Dynamic walking models have been particularly effective at increasing our understanding in the important areas of energetics and stability.

1.3 Energetics

Keeping energy use low during walking is highly desirable. People and machines that walk are mobile and autonomous by nature, and so must carry their energy supply with them. For a given energy supply, the maximum range of travel before exhaustion is inversely proportional to the rate of energy expenditure. Using less energy per unit distance per unit weight, a quantity termed cost of transport (e.g. Tucker, 1975), leads to greater mobility. Often, energy stores are determined by the needs of the task, e.g. the distance or time between refueling. The slower energy is consumed, the less must be carried about in the form of fat, batteries, or fuel. Both of these factors lead to the

hypothesis that energy economy has been an important selection criterion in the evolution of humans and other animals (e.g. Alexander, 2003). People and machines also have maximum systemic power production capacities. Humans are limited by their maximum rate of production of metabolic energy, or biochemical food energy, in their bodies, a process which is limited by the capacity of the cardiovascular system to absorb and distribute oxygen throughout the body. Likewise, machines are often limited by the maximum rate of battery discharge or power transmission through conductive elements. In general, energy use tends to increase rapidly with speed of travel during locomotion, so a limit in power translates into a limit on speed. By reducing energy use at a given speed, maximum speed is generally increased. To keep range and maximum speed high, and to keep fuel carry low, energy use must be kept low. Dynamic walking models have lent insight into the factors that impact energy use.

Previous dynamic walking models have demonstrated the utility of an inverted pendulum stance phase, as well as relationships between step length, step frequency, and the mechanics of energy addition, trends that have been confirmed through human subject experiments.

1.3.1 Inverted pendulum stance

Dynamic walking models predict that using the stance leg as inverted pendulum can minimize energy use during walking by concentrating leg work in step-to-step transitions. There are, of course, many conceivable strategies for the coordination of walking, even in a very simple model of the body. One strategy which is still accepted by many in the biomechanics community is minimization of the vertical excursion of the center of mass during the course of a step (Saunders et. al., 1953). By reducing fluctuations in potential energy from the body moving in the gravitational field, it has been proposed that mechanical energy requirements could be reduced. However, this type of strategy actually requires significant energy production and absorption by the legs, since they must lengthen and shorten under load throughout stance (Figure 1.1a, right). A similar approach is used by many walking robots based on so-called zero moment point control, which typically results in a cost of transport that is ten times greater than in humans

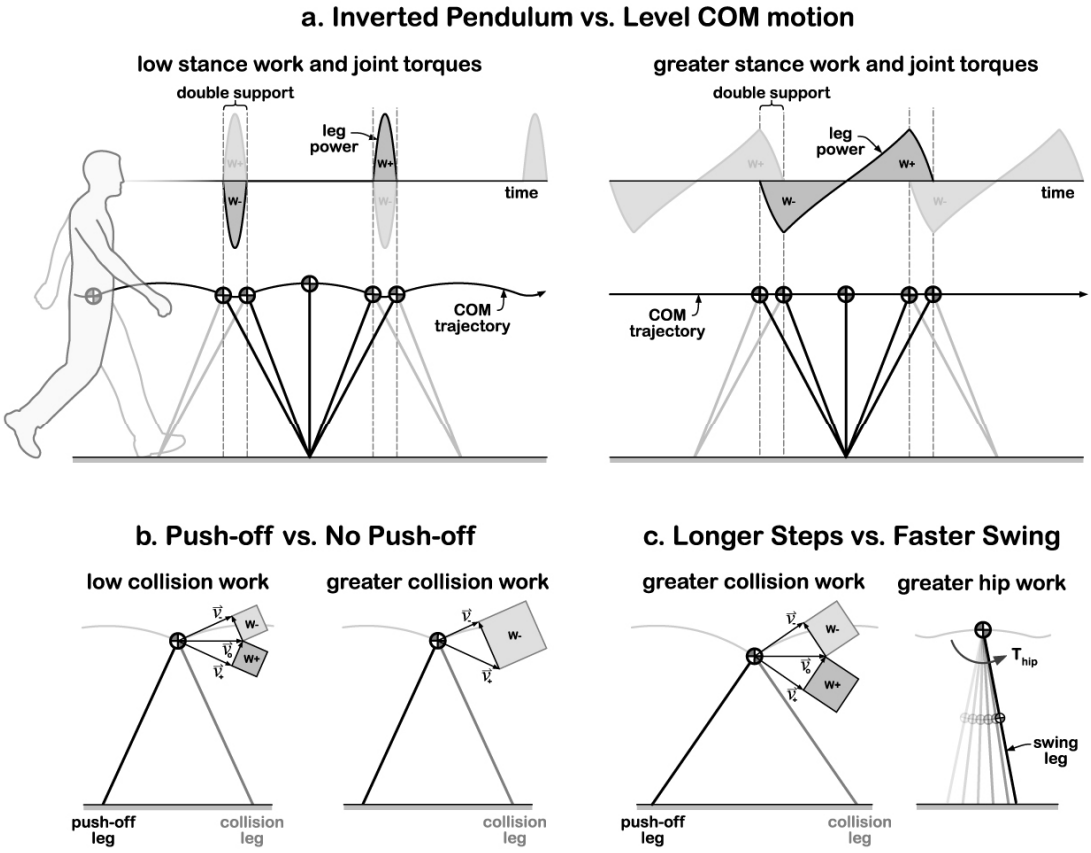

Figure 1.1: Fundamentals of energy use in dynamic walking. (a.) Walking with inverted pendulum stance phases requires less energy use than maintaining constant center of mass (COM) height. In pendular gait the stance leg changes length little during single-support, which requires little mechanical work and allows for a relatively straight leg and low joint torques. Substantial work is only required at the step-to-step transition, during which the COM velocity is redirected from one arc to the next. This is significantly less work than in level COM gaits, where leg length changes throughout stance under body-weight forces. Leg length is also shortest at mid-stance, requiring greater joint flexion and leading to greater joint torque requirements. For the simple point-mass models depicted here, the pendulum gait uses less than half as much energy as the level COM model. (b.) Push-off of the trailing leg before and during the step-to-step transition reduces energy use. Preemptive push-off can reduce the COM redirection vector of the collision by as much as a factor of two, which results in a factor of four reduction in the energy dissipated in the collision. Powering gait in other ways, such as with the hip during single-support, is less economical because it requires more positive work to compensate for the larger collision. (c.) For a given speed, taking longer steps increases collision losses, while taking shorter steps with faster leg swinging increases energy used in swinging the leg. The optimum combination employs some amount of leg powering, and changes with the mass properties of the legs and the mechanics of the step-to-step transition.

(Collins et. al., 2005). Utilizing a pendulum stance phase eliminates this mid-stance leg work. Potential and kinetic energy do change as the body rises and falls over the rigid stance leg, but since the legs do not perform work by lengthening or shortening, there is no dissipation and the total energy remains constant (Figure 1.1a, left). Energy is

required to redirect the center of mass velocity during the step-to-step transition, but this energy requirement is much lower than the energy savings mid-stance, resulting in a more economic gait. In fact, a comprehensive optimization of one model of this type demonstrated that the inverted pendulum approach is the energetically optimal approach among all strategies (Srinivasan and Ruina, 2006). In order to better understand energy use in inverted pendulum gait, it is useful to further explore the mechanics of this step-to-step transition between pendulum arcs.

1.3.2 The step-to-step transition

In most models of dynamic walking, the majority of the mechanical work is produced or absorbed during the step-to-step transition, which therefore has a great impact on the energy used in gait. During the step-to-step transition, the center of mass velocity is redirected from the pendular arc of the trailing leg to the arc of the leading leg, a process which directly requires the dissipation of mechanical work. This process may be usefully considered in terms of an instantaneous collision in a point mass model (Figure 1.1b). In this simplest dynamic walking model, the mass of the biped is concentrated in a point at the hip, while rigid legs with negligible mass make intermittent contact with the ground. During the step-to-step transition, the leading leg dissipates energy through a collision impulse, where the magnitude of the energy loss is proportional to the square of the impulse (Garcia et. al., 1998; Kuo, 2001). This results from the geometric relationship between the initial and resultant velocity vectors. The velocity change vector must be collinear with the impulse vector, which in turn must be collinear with the mass-less leg. This forms a right triangle with the initial, resultant and change velocity vectors composing the three sides. The initial and resultant kinetic energies are proportional to the square of the initial and resultant velocities, with their difference being the energy lost in the collision. By use of the Pythagorean Theorem, it can be seen that the energy loss is proportional to the square of the magnitude of the velocity change vector. The mechanics of this collision are therefore greatly affected by geometry resulting from walking speed and step length.

Since walking at a stead speed on level terrain is an energy-neutral task, i.e. the average energy does not change over many steps, all negative work or energy dissipation produces an energy debt that must be replaced through positive work or the production of mechanical energy. Therefore, collision losses are an effective measure of the energy use dictated by the step-to-step transition. Reducing collision losses can be an effective means of reducing energy use overall, and can be accomplished through carefully-timed energy addition as well as by modulating step frequency.

1.3.3 The impact of push-off

Energy dissipated in collisions is most usefully restored by positive work of the trailing leg during the step-to-step transition because this can reduce the collision loss. Energy to replace collision losses must be supplied at some point during gait. If it is provided in the form of positive mechanical work by the trailing leg, or push-off, just prior to the collision of the leading leg, the result can be a smaller collision and therefore less energy consumed overall (Kuo, 2001; Figure 1.1b). In the simplest dynamic walking model described here, the optimal push-off results in an intermediate resultant velocity vector that is purely horizontal, roughly halving the velocity change vectors for both push-off and collision. Since the change in energy is proportional to the square of the velocity change vector, this reduces the collision loss by a factor of four. In humans, the step-to-step transition occurs over a finite time and push-off of the trailing leg does not occur entirely before the collision of the leading leg, but it is likely that humans benefit to some extent from this effect. Collision losses may also be reduced by taking shorter steps, up to a point.

1.3.4 Step length and swing frequency

Simple models of dynamic walking also demonstrate that taking shorter steps can reduce collision losses, but at the cost of increased energy to produce leg swing. It can be inferred from the geometric relationships above that the amount of energy dissipated in collisions is reduced as steps become shorter, even while maintaining the same walking speed (Kuo, 2001; Figure 1.1c). This can be accomplished by providing mechanical work at the hip joint to swing the leg faster than its natural frequency. For a given speed,

very large step lengths and slow leg swinging produce very high collision costs, while short step lengths and very fast leg swinging produce very high leg swinging costs, and an optimum lies between. That is, some amount of work to increase leg swing frequency is better than passive leg swing. These results have been confirmed in humans walking (Donelan et. al., 2002a; Donelan et. al., 2002b; Doke et. al., 2005). Further, it is worth noting that the optimum balance between step length and swing frequency can be altered by changing the mechanics of the step-to-step transition or the mass properties of the swing leg. If the step-to-step transition mechanics were worsened, for instance by reducing or removing push-off, the optimal step length for a given speed should be shorter to partially compensate for the increased collision losses. Likewise, if leg swinging were made more costly, for instance by increasing the work requirements of swing by adding mass at the foot, the optimal step length would be longer. A similar effect can be observed in step width in three-dimensional models and in human gait, where collision costs increase with increasing step width (Donelan et. al., 2001). These factors will be of interest when we consider interventions that may change the step-to-step transition mechanics and leg inertia.

In addition to energy use, stability is essential to effective walking. Previous work with dynamic walking models has resulted in similarly useful tools for predicting trends in gait stability.

1.4 Stability

Stability is essential to functional gait. Getting from one place to the next is more energy consuming, takes longer, and may be more dangerous if one is continually falling down. Falls often result in injury in humans, other animals and machines, with very costly effects. Fall avoidance is therefore an essential goal in walking. Many definitions of stability are used when considering walking, the most useful of which to our discussion are: (1) not falling down, and (2) Lyapunov stability of limit-cycle behavior.

1.4.1 Not falling down

Removing the nonlinear controls jargon that will clutter the following sections, we have a very simple functional definition of stability: not falling down. All else being equal, this accurately summarizes the stability goal in walking. It is not essential to follow a specific trajectory through time or space with a high degree of accuracy, but rather only for the realized trajectory not to intersect the ground unexpectedly. Often, walking occurs in the presence of perturbations, or disturbances to the behavior of the system resulting from unplanned internal or external excitations. We will call the ability to resist falling down in the presence of disturbances robustness. A robustly stable walking person or machine can tolerate significant perturbations such as a push or a small dip in the ground without falling down. Of course, these simple definitions can only get us so far, and in order to begin quantifying degrees of stability or robustness, we must use tools from nonlinear systems theory.

1.4.2 Limit cycles and Lyapunov stability

A limit cycle describes a periodic oscillation of a nonlinear dynamical system, such as a dynamic walking model, and provides a framework for quantifying stability in the Lyapunov sense through the use of Poincaré mapping, linearization, and eigenvalue analysis. The state of a system describes the system's past and future behavior completely. In the case of a dynamic walking model, the state is often comprised of the configuration and time rate of change of the configuration, e.g. the positions and velocities of all the degrees of freedom. Ideally, the configuration is expressed in terms of generalized coordinates which describe the configuration completely in the minimum number of variables. As a nonlinear dynamical system oscillates in a periodic behavior, the state of the system follows a closed loop through state space, which under most circumstances constitutes a limit cycle. If trajectories which start nearby the limit cycle in state space approach the limit cycle over time, the limit cycle is asymptotically stable, whereas if they deviate over time the limit cycle is unstable. (If trajectories remain in some neighborhood near a path, but do not approach a particular path, this describes quasi-periodic or chaotic behavior, a distinction that is generally useless in any practical application.) To determine whether states nearby the limit cycle are attracted towards it,

it is useful to take a slice through state space in what is called a Poincaré section. The Poincaré section is taken at a well-defined manifold in state space, for instance at the moment of heel strike in a dynamic walking model, and each time the state trajectory passes through this section a new point is added to the Poincaré map. In this way, the continuous nonlinear system is discretized and collapsed onto a lower order space. This new discrete system, consisting of states surrounding the intersection of the limit cycle with the Poincaré section, lends itself to linearization. In the linearized system, the limit cycle crossing can be considered as a fixed point, which is the discrete equivalent of a limit cycle trajectory. Linear systems methods such as eigenvalue decomposition may then be applied to the linearized discrete state transition matrix to quantify local stability. Eigenvalues in this discrete linear system describe the growth or decay of perturbations in the corresponding eigenvector direction after a single cycle. Eigenvalue magnitudes greater than unity indicate growth and less than unity decay, with faster growth or decay occurring at magnitudes closer to infinity and zero, respectively. In the unusual case of an eigenvalue of magnitude unity, we have neutral stability, and points near the fixed point along the corresponding eigenvector are also fixed points. The stability behavior of the discrete linear system is characteristic of the behavior of the states surrounding the limit cycle, and so we may use the eigenvector analysis to characterize stability of the limit cycle. More detailed consideration of these concepts and techniques have been presented by, e.g., Strogatz,1994 and McGeer , 1990.

Related techniques such as Newton's method can be used to find limit cycles and track how they change as model parameters are varied. Newton's method is an iterative optimization technique that is used to find zero-crossings of a curve by taking a finite-difference estimate of the slope at a given point and using it to guess at the zero-crossing point of the curve by assuming a first-order system (i.e. a straight line). If the initial guess is close enough to the zero-crossing, i.e. near the linear region, then the optimization will converge on the zero-crossing after a few iterations. This can be used to find limit cycles by performing Newton's method on the difference between one state and the next in the Poincaré map. The zero-crossing of this quantity corresponds to a state that repeats itself on the Poincaré map, i.e. a fixed point of the discrete mapping or a

limit cycle of the nonlinear system. However, the initial guess must be close to the fixed point or the method will not converge, and the search space of even a relatively simple dynamic walking model may be quite large. Some researchers in dynamic walking have attempted to fully search the parameter space of their model for fixed points (e.g. Coleman and Ruina, 1998), but with very limited success. More practically, it is useful to start with a fixed point for a model that is already known and slowly change the parameters or morphology until the desired model or behavior is observed (Gomes and Ruina, 2005).

In dynamic walking, a limit cycle represents a particular gait exhibited by a particular model. Each model may exhibit many qualitatively distinct gaits, and each gait may change quantitatively over a range of model parameters. Each gait can be characterized in terms of speed, energy use, and stability. Here, stability is often quantified as the largest eigenvalue of the linearized discrete step map, which indicates whether the gait will persist in the face of small perturbations or will be knocked into a different stable mode, most often a prone position on the ground. By studying these eigenvalue indicators of stability and robustness, and the way that they change as parameters are modified, we have been able to gain some insights into the stability of dynamic walking.

1.4.3 Sagittal stability is easy

Dynamic walking models have demonstrated that for a wide range of model morphologies, legged walking within the sagittal plane can be stable without any additional control. Various models (e.g. McGeer, 1991; Garcia et. al., 1998; Kuo, 2001; Wisse, 2004) and walking robots (e.g. McGeer, 1989; Garcia, 1998) have demonstrated a variety of stable gaits within the sagittal plane. In these models, the maximum eigenvalues are all less than unity, such that small perturbations are gradually removed. This self-stabilization seems to primarily result from the motion of the swing leg towards the end of stance and its impact on the step-to-step transition, and can be understood to some extent by a consideration of energy dissipation. Just before heel strike in stable sagittal plane gaits, the swing leg has already reached its maximum forward excursion and has begun to move backwards. The longer the swing foot remains above the ground,

the further back it moves. When a perturbation increases the energy of the system by a small amount, the typical result is that the speed of the center of mass increases, forcing an earlier heel strike. This leads to a longer step, which dissipates more energy, moving the energy balance back towards the limit cycle energy. Likewise, an energy removing perturbation results in a shorter step, dissipating less energy and increasing the net energy for the step. So, collision losses can actually lead to stability in gait. This property only holds for relatively small perturbations, but may nevertheless reduce the control task for humans during gait.

Even greater robustness in the sagittal plane can be achieved through the use of the simple and largely open-loop control strategy of simply stopping the swing leg at the same hip angle at the end of each step. This control strategy has been demonstrated in simulation and in walking robots to further increase robustness such that larger external perturbations may be tolerated without falling over (Wisse and Frankenhuyzen, 2003). The strategy is based on the simple notion that a biped cannot fall over if a leg is in the way. This results in a situation where stability is closer to neutral than in the case of an unactuated swing leg, but is more robust to zero-centered external perturbations. However, new and troubling questions arise when considering the stability of three-dimensional dynamic walking models.

1.4.4 Lateral stability is hard

Unlike gaits in two-dimensional dynamic walking models, three-dimensional dynamic walking models exhibit gaits that are unstable, mostly in lateral motions. The three-dimensional anthropomorphic model described by Kuo (1999) demonstrated gaits in which all eigenvalues were stable save one, which had a corresponding eigenvector that lay primarily in the direction of side-to-side motions. Without stabilizing control, the model would quickly fall over sideways. The magnitude of the unstable eigenvector could be reduced by walking with wider steps, which would result in a slower deviation from the limit cycle and might make corrective control easier. (One dynamic walking model described by (Coleman et. al., 2001) demonstrated passive stability in three dimensions, but had a strange morphology which prevents useful comparison with

humans.) Since three-dimensional models seem to lack self-stable limit cycles, feedback control seems to be required to obtain stability.

Feedback-controlled lateral foot placement can stabilize gaits in three-dimensional dynamic walking relatively efficiently. Since the gait is not self-stable, corrective actions must be taken as a function of the deviation from the (passively) unstable limit cycle. Many types of corrective actions could be taken, but foot placement takes advantage of the step-to-step transition collision to produce a significant corrective effect without requiring significant mechanical work from actuators. Most means of removing lateral perturbations, such as ankle torques or torso motions, would require mechanical work equal to the energy of the perturbation. Foot placement, on the other hand, requires very little mechanical work in moving the foot slightly medially or laterally. These small changes can have a big impact, however, since the results of the step-to-step transition are very sensitive to changes in the configuration at the time of collision. So, lateral foot placement can provide an effective means of stabilizing three-dimensional gaits. Indeed, human subject experiments suggest that such control is ongoing during human gait and that this control may have a measurable metabolic cost (Donelan, 2004). However, any feedback control strategy will require knowledge of the state of the walking system.

Lateral foot placement variability may be a good means of quantifying the effectiveness of lateral stabilization in three-dimensional walking gaits, such as in humans. Given imperfect sensors or nerves and actuators or muscles, active foot placement control would be expected to exhibit variability, especially in the lateral direction.

Stability and energy use in gait are factors which will provide an important context as we consider the areas of focus for the body of work presented in this thesis.

1.5 Focus areas

We used a dynamic walking approach with an emphasis on energetics and stability to address three focus areas: prosthetic foot design, the role of the arms, and balance among the elderly. In each case, we used dynamic walking models to develop our understanding

and make predictions, then tested our theories in human subject experiments. Our results improve our basic understanding of walking, and may provide a path for developing or improving assistive devices.

1.5.1 A prosthetic foot which improves the mechanics of the step-to-step transition

Amputees consume more energy to walk, likely due to deficiencies in conventional prosthetic feet. Dynamic walking models suggest a means of altering the mechanics of the step-to-step transition to reduce overall energy use; energy may be stored during collision and returned in the successive push-off. We developed a foot prosthesis which provided this function, and demonstrated in a controlled human subject experiment that it reduced energy requirements as compared to a conventional prosthetic foot. Stability is also greatly affected by the mechanics of the step-to-step transition, so care was required to prevent destabilizing fore-aft motions or increasing the open-loop instability in lateral motions. The prototype foot successfully reduced energetic costs without reducing balance, suggesting that this type of technology may be useful as a commercial device.

1.5.2 The role of the upper extremities in gait

People typically swing their arms as they walk, a curious behavior which is unknown in other animals and not required in humans. No one really knows why. Some have speculated that the motion stems from neural pathways that are evolutionary relics from our quadrupedal ancestors, while others have proposed the motion is used so as to reduce "jerkiness". We developed a simple three-dimensional dynamic walking model with arms and systematically searched for gaits. We found several gaits with qualitatively different modes of arm swinging, all neutrally stable, including the normal mode exhibited by humans. Normal arm swinging reduced vertical angular momentum and vertical ground reaction moments, indicating a possible source of metabolic energy savings in humans. We conducted controlled human subject experiments in which subjects walked with their arms swinging in various ways and confirmed the predicted trends in angular momentum and energy use. Subjects used significantly more energy to walk without arm swinging, even if their arms were held at their sides with passive restraints. These results suggest that, rather than a facultative relic of the locomotion

needs of our quadrupedal ancestors, arm swinging appears to be an integral part of economical human gait.

1.5.3 Determining risk of falls in elderly individuals

Humans experience reduced balance with age, leading to an increased risk of falls and injury. Preventative interventions may help reduce the risk of injury, but require accurate identification of individuals with reduced balance. Dynamic walking models predict that lateral balance may be the most difficult control aspect of walking, with lateral foot placement variability being a useful indicator of balance ability. We conducted a controlled human subject experiment in which younger and older subject groups walked overground with their eyes either open or closed while foot placements were measured. As expected, the effect of reducing sensory information by closing the eyes or through the effects of aging were to increase variability in lateral foot placement. These results suggest that a mobile device monitoring lateral foot placement variability might assist in preventing falls and fall-related injuries among older populations.

1.6 Thesis Outline

The remainder of the thesis is broken into three chapters related to the above focus areas:

Chapter 2 presents the concept of Controlled Energy Storage and Return (CESR) as a means of improving step-to-step transition mechanics, describes the prototype CESR foot design, and presents the results of a human subject experiment in which the prototype was compared to a conventional foot prosthesis and to intact gait.

Chapter 3 presents a three-dimensional dynamic walking model with free-swinging arms, describes the modes of oscillation observed in simulation, and presents the results of a human subject experiment in which mode of arm swinging was a controlled condition.

Chapter 4 presents the results of a human subject experiment in which foot placement was measured as sensory information was selectively removed among young and elderly subject populations.

Appendix A presents a more detailed examination of the dynamic walking model with free-swinging arms.

Chapter 2

Controlled Energy Storage and Return in a Prosthetic Foot

Abstract

Lower limb amputees require significantly more energy to walk than intact individuals, reducing their mobility. Prosthetic feet designed with the aim of reducing metabolic energy expenditure have not been found to cause significant improvements, possibly because conventional prosthetic feet produce very little push-off work compared to the intact ankle. We propose a Controlled Energy Storage and Return (CESR) foot prosthesis which stores energy at the heel during the beginning of stance, then returns the energy at the toe during the end of stance to increase push-off work. We developed a prototype CESR foot prosthesis and tested it experimentally on able-bodied subjects wearing a prosthesis simulator boot as they walked on an instrumented treadmill. We compared metabolics and mechanics between intact gait, the CESR foot, and a conventional foot prosthesis. We found that the CESR foot was able to store energy that would otherwise be dissipated during the beginning of stance and return it usefully during push-off, providing more than twice as much push-off work as the conventional foot. The CESR foot reduced metabolic cost by 9.4% as compared to the conventional foot, roughly halving the metabolic penalty. This improvement was accompanied by reduced mechanical work in both affected and contralateral limbs. These results suggest that CESR technology may be usefully applied to prosthetic feet in order to reduce energy use during walking and improve mobility in lower limb amputees.

2.1 Introduction

Over one million individuals in the U.S. are affected by limb loss, with over one hundred thirty thousand new amputations performed each year (Dillingham et. al., 2002). The majority of these persons are lower extremity amputees, many of whom use an artificial foot. Lower limb amputees expend more metabolic energy than intact individuals to walk at the same speed or to travel the same distance. Unilateral below-knee amputees use 20-30% more metabolic energy than their intact counterparts (Molen, 1973; Herbert et. al., 1994) while above-knee and bilateral amputees require still more (Waters et al., 1999; James, 1973; Gailey et. al., 1994). More than 70% of these patients have cardiovascular problems that limit their energy producing capacity, further reducing mobility (Powers et. al., 1996). Amputees experience substantially limited mobility and would benefit significantly if their walking economy could be improved.

Prosthetic foot designs have been proposed with the aim of reducing energy expenditure, but these have achieved limited success. The most commonly prescribed prosthetic foot is the Solid Ankle Cushioned Heel (SACH) foot, comprised of a rigid forefoot and rubber heel wedge, which originated in the Berkeley biomechanics laboratory in the 1950's (Adams & Perry, 1992). Dynamic Elastic Response (DER) feet, such as the Flex-Foot®, incorporate plastic or composite toe and heel keels which deform elastically during stance. These designs have been available since the 1980's and are intended to provide increased comfort as well as improved energetic performance. Although many novel prosthesis designs have improved comfort for amputees, none have significantly reduced the energy requirements of gait as compared to the SACH foot (Nielsen et. al., 1988; Barth & Schumacher, 1992; Colbourne et. al., 1992; Lehmann et. al., 1993a & 1993b; Torburn et. al., 1995; Thomas et. al., 2000). We might gain insight into the reasons for this persisting energetic penalty by considering the work performed by the ankle during gait.

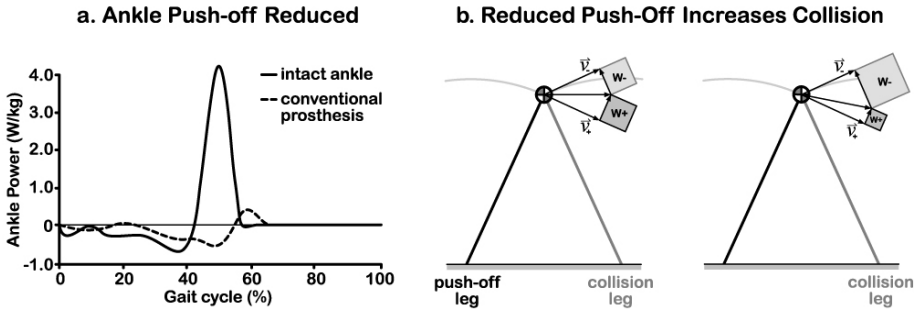

Figure 2.1: a. Conventional prosthetic feet result in a dramatic reduction in ankle push-off work compared to the intact ankle (reproduced from Whittle (1996)). **b.** Dynamic walking models predict that reduced push-off of the trailing leg (W+) will result in a disproportionately larger increase in collision negative work of the leading leg (W-) during the step-to-step transition (Kuo, 2002). This work debt must then be repaid with positive leg work during mid-stance, resulting in an overall increase in mechanical work requirements. Reduced push-off ability may therefore partially explain the increased metabolic energy requirements in amputee gait.

Conventional prosthetic feet produce dramatically less work during push-off than the intact ankle, which may lead to increased mechanical work requirements overall. A wide variety of conventional prosthetic feet have been shown to absorb energy in a manner similar to that of the intact ankle during early and mid-stance, but to produce far less positive work during the end of stance or push-off (Figure 2.1a; Barr et. al., 1992; Lehmann et. al., 1993a; Prince et. al., 1998; Geil et. al., 2000). Simple dynamic walking models predict that a reduction in push-off work may increase the overall mechanical work requirements in walking (Figure 2.1b; Kuo, 2002). During the double-support period when weight is transferred from one leg to the other (step-to-step transition) the trailing leg does positive mechanical work on the center of mass (push-off) while the leading leg does negative mechanical work (collision). Proper balance of push-off and collision can minimize the work required at the step-to-step transition. However, if push-off is reduced, the collision of the leading leg will be disproportionately increased. Since positive work must balance negative work in steady-state walking, this increased collision loss creates an energy deficit that must be fulfilled during single support, thereby leading to greater positive work requirements. Thus, the reduced push-off observed in prosthetic feet may lead to increased mechanical work, and therefore increased metabolic rate, among amputees.

A more detailed examination of center of mass work is required to apply the results of simple dynamic walking models to human gait. Center of Mass (COM) work can be separated into the contributions of the individual legs and further divided into distinct phases (Figure 2.2). During double support, the leading leg accepts the load of the body while shortening, thus performing negative work in the Collision phase. This Collision helps redirect the COM velocity from one pendulum-arc stance phase to the next. During the beginning of single-support, the stance leg lengthens slightly under load, producing positive mechanical work in Rebound. Towards the end of single-support, the stance leg shortens under load, absorbing energy in Preload. Finally, during double-support, the trailing leg lengthens under load, producing positive mechanical work in Push-off. This Push-off may be reduced in amputees, which may lead to increased Collision in the contralateral limb, thereby requiring an increase positive mechanical work during the ensuing stance phase (Figure 2.3a).

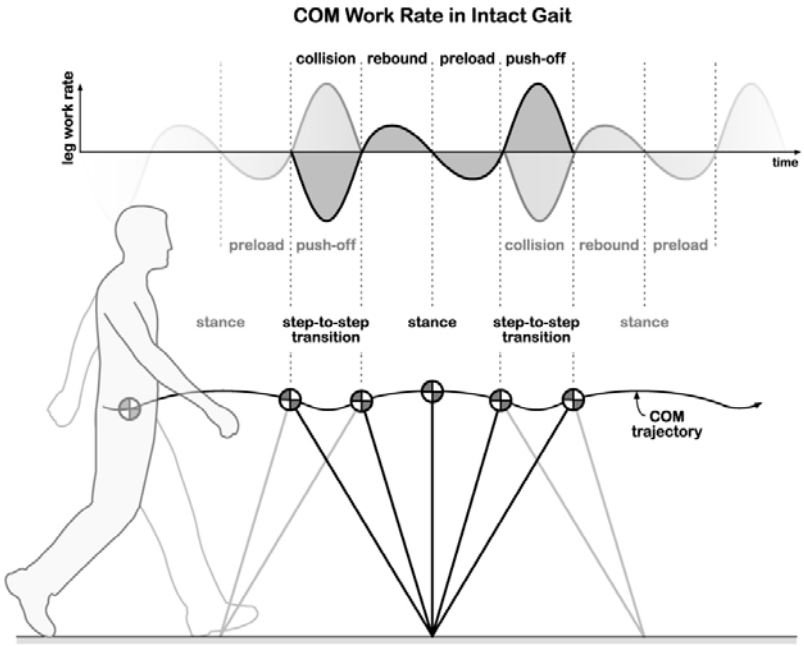

Figure 2.2: Center of mass (COM) work in intact gait, as estimated using the individual limbs method (Donelan et. al., 2002). Each leg undergoes four phases of work production or absorption: Collision, in which the leading leg does negative work on the COM during the step-to-step transition; Rebound, in which the stance leg provides a small amount of positive work during the first part of single support; Preload, in which the stance leg absorbs a small amount of energy; and Push-off, during which the trailing leg provides substantial positive work to redirect the COM during the step-to-step transition.

Providing increased Push-off using a prosthetic foot could reduce overall mechanical work requirements, but the energy for this Push-off must come from somewhere. Energy could be provided directly by an electric motor or other high-power actuator, but this would require a significant power source. Battery weight or tether length could limit mobility and autonomy, while peak power requirements might also result in a large, heavy foot. On the other hand, since equal amounts of energy are generated and dissipated by the limbs during a single stride of steady walking, perhaps energy could be stored in the foot prosthesis during negative work phases for use during Push-off.

We proposed that a prosthetic foot which performed Controlled Energy Storage and Return (CESR) could reduce overall mechanical work in amputee gait, leading to reduced metabolic cost. The foot would store energy in a high-efficiency mechanical element during Collision, replacing negative work typically done by the intact limb. Instead of returning this energy spontaneously, the foot would retain it until Push-off, the optimal time of release. During Push-off of the affected limb, the CESR foot would add to the work of the biological limb, resulting in greater total Push-off (Figure 2.3b). We propose that this increased Push-off work could reduce Collision losses and Rebound work in the contralateral limb, thereby reducing the overall mechanical work and metabolic energy requirements of walking.

However, a number of factors could complicate the evaluation of the CESR foot's performance. Significant Push-off without direct user control could make adaptation and balancing difficult, possibly increasing metabolic cost. Effective roll-over shape can be difficult to predict a priori, but may strongly effect metabolic cost (e.g. Adamczyk et. al., 2007). Mechanical comparisons between the CESR foot and a conventional prosthesis could also be complicated by subjects' choice of step frequency. Humans tend to pick a stride frequency that minimizes the sum of step-to-step transition costs and leg swinging costs (Kuo, 2001). The CESR foot should reduce the mechanical work of the step-to-step transition, resulting in an optimal stride frequency that is slower than in the conventional foot. Thus, leg swinging could constitute a significant portion of the metabolic difference between the feet (Doke, 2005), while differences in step-to-step transition work could be

apparently reduced. Testing amputee subjects could present additional challenges. Direct paired comparisons to intact gait are impossible with amputees. Amputee patients could also be more vulnerable to injury or complications should the novel prosthesis prototype fail or exhibit unexpected behavior. These issues can be avoided by testing intact individuals wearing prosthesis simulator boots (Lemaire et. al., 2000; Adamczyk et. al., 2007, Figure 2.5).

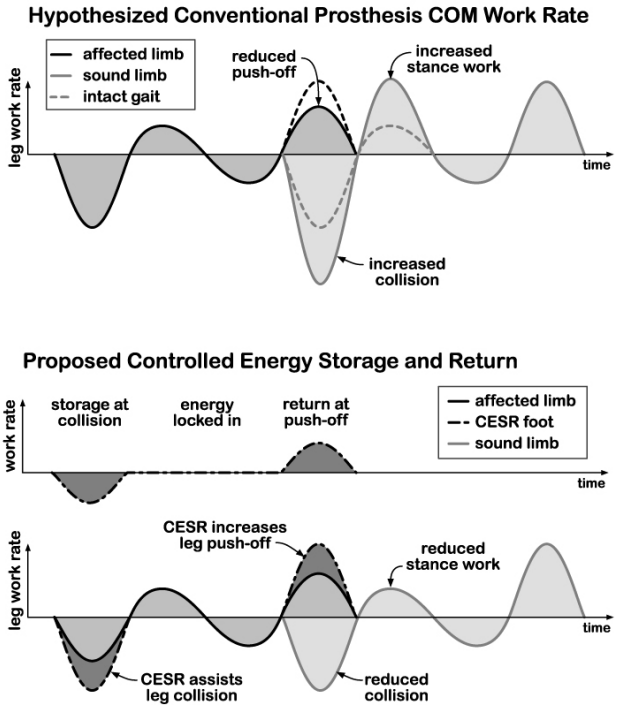

Figure 2.3: Hypothesized Center of Mass (COM) work rate in amputees (top) and proposed Controlled Energy Storage and Return pattern to reduce mechanical work requirements (bottom). **Top:** Dynamic walking models predict that a reduction in push-off work can cause a disproportionately larger increase in collision work (Figure 2.1b), increasing the total amount of positive mechanical work required from the leg. **Bottom:** Energy is stored by the CESR foot during collision, replacing negative work in the biological leg. The CESR then returns this energy during push-off, adding to the push-off work of the intact limb. This increased push-off is hypothesized to reduce collision losses and rebound work requirements in the contralateral leg. This design is unlike conventional prosthetic feet which absorb little energy during collision and return energy spontaneously during stance.

The purpose of this study was to examine whether a prosthetic foot performing Controlled Energy Storage and Return (CESR) could reduce mechanical work requirements as compared to conventional prosthetic feet, thereby reducing metabolic energy requirements. We developed a prototype CESR foot prosthesis and used it to

demonstrate that a foot prosthesis could store energy normally dissipated in Collision and use the energy to increase Push-off. We performed controlled human subject experiments to compare the CESR foot to a conventional foot prosthesis and to intact gait. We calculated COM work rate and joint work rates as subjects walked on an instrumented treadmill to examine whether the CESR foot could reduce mechanical work requirements compared to the conventional foot. We calculated metabolic rate to determine whether the CESR foot could reduce metabolic energy use compared to the conventional foot. We measured stride frequency to test whether subjects preferred longer steps with the CESR foot. We measured step width and step width variability to gain insight into possible effects of balance. Finally, we measured and examined effective roll-over shape in each condition.

2.2 Methods

To test the effects of Controlled Energy Storage and Return (CESR), we developed a prototype CESR foot prosthesis and performed controlled human subject experiments. We tested intact individuals as they walked normally (Normal) and while they walked using a prosthetic foot simulator boot with the CESR prototype (CESR) and with a conventional foot prosthesis (Conventional) attached. Subjects walked on an instrumented treadmill while we measured kinetics and kinematics, used to calculate center of mass work and joint work, as well as metabolic rate.

2.2.1 CESR foot prosthesis prototype

We developed a prototype foot prosthesis to perform Controlled Energy Storage and Return (CESR) in the proposed manner. The foot stored energy in a spring through negative work at the heel during Collision, locked it in place throughout stance, and returned the energy in the form of positive work at the toe during Push-off (Figure 2.4). The prototype was comprised of high-strength aluminum, steel, and carbon fiber mechanical components, small electric motors to actuate latches, and contactless potentiometers to sense foot movements. Collision and Push-off energy were stored in a large compression spring. A microcontroller running a state machine integrated sensory information and performed control actions to initiate push-off and reset. Electrical power

for the controller and latch actuation were provided by a small Nickel-metal hydride battery array or by a wall adaptor.

The CESR prototype was comprised of six component groups: the interface component, the toe assembly, the heel assembly, the primary compression spring, the heel clutch, and the toe latch (Figure 2.4). The interface component attached to the socket adaptor pylon or prosthesis simulator boot through a standard pyramid adaptor (Figure 2.5). The heel and toe assemblies rotated on ball bearings about a shaft which was rigidly attached to the interface component. The primary compression spring acted between the heel and toe assemblies. The one-way heel clutch acted between the heel assembly and the interface component, allowing the heel to rotate clockwise (compressing the spring) freely but locking when forced in the opposite direction (unless released by motor actuation). The toe latch acted between the toe assembly and the interface component, and prevented the toe assembly from rotating clockwise (plantar-flexing) unless unlatched.

During gait, the CESR prototype stored energy in the primary compression spring during Collision, locked it in place throughout stance, returned it during Push-off, then reset for the next step. On first ground contact (heel strike) the compression spring was in its relaxed position and the heel clutch and toe latch were in their locking positions. As the foot was loaded, the heel plate was forced proximally, compressing the primary spring and storing Collision energy. The heel was then locked in place by the one-way heel clutch. The compressed spring was held throughout mid-stance, locked in by the heel clutch and toe latch. During Pre-load, torque on the toe assembly built as the center of pressure advanced and ground reaction forces increased, eventually overcoming the torque of the primary compression spring and pushing against a limit stop. This relieved the toe latch of load, allowing a motor to move it out of the way, effectively releasing the toe assembly. During Push-off, the primary compression spring was then allowed to force the toe assembly through plantar-flexion, returning stored energy. Simultaneously, the carbon fiber toe spring returned energy that was stored during Pre-load. At the onset of swing, the foot then reset into the ready position by unlocking the heel clutch.

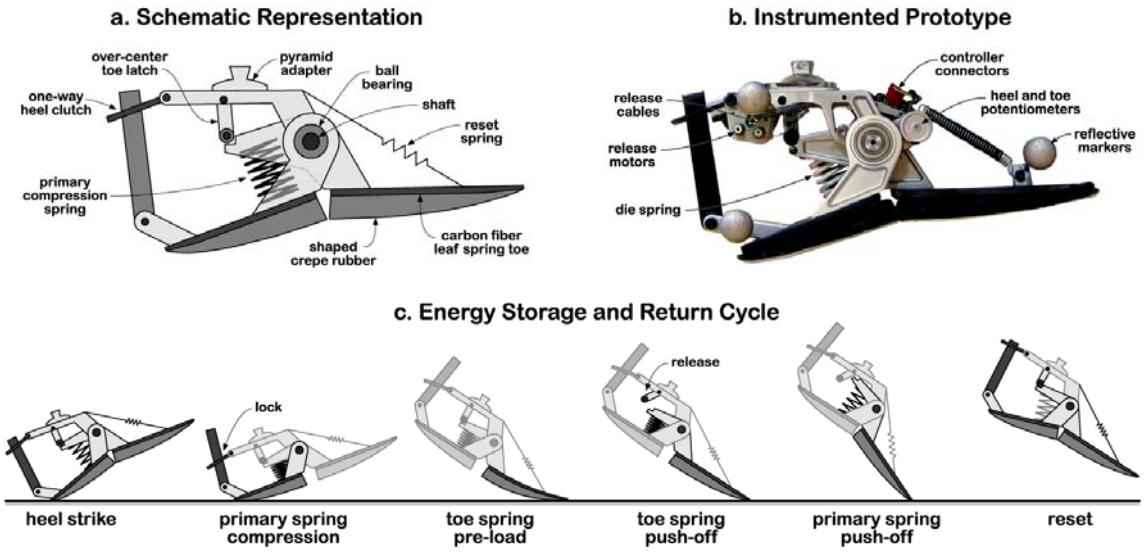

Figure 2.4: CESR prototype and mechanical function. **a.** Schematic representation of the mechanical elements of the CESR foot. The prosthesis was comprised of six component groups: the interface component, the toe assembly, the heel assembly, the primary compression spring, the heel clutch, and the toe latch. The interface component attached to the socket adaptor pylon or prosthesis simulator boot (see figure 2.5) through a standard pyramid adaptor. The heel and toe assemblies rotated on ball bearings about a shaft which was rigidly attached to the interface component. The primary compression spring acted between the heel and toe assemblies. The one-way heel clutch acted between the heel assembly and the interface component, and allowed the heel to rotate clockwise (compressing the spring) freely but locked when forced in the opposite direction (unless released by motor actuation). The toe latch acted between the toe assembly and the interface component, and prevented the toe assembly from rotating clockwise (plantar-flexing) unless unlatched. **b.** Photograph of the instrumented prototype used in these experiments. The prototype is constructed of high-strength aluminum and steel components with flexible carbon fiber leaf springs comprising the toe and heel. Motors and springs acting through a system of cables and capstans provide a means for releasing and re-engaging the heel clutch and toe latch. Potentiometers measure the rotation of the toe and heel assemblies with respect to the interface component. These electronic components connect to a small backpack with batteries and a microcontroller through a ribbon cable. Reflective markers were used to track the foot spatially. **c.** Energy storage and return cycle (highlighted components have just moved). When the foot first contacts the ground, heel strike, the compression spring is in its relaxed position. As the foot is loaded, the heel plate is forced proximally, compressing the primary compression spring and storing collision energy. The heel is then locked in place by the one-way heel clutch. The compressed spring is held throughout mid-stance, locked in by the heel clutch and the toe latch. During pre-load, the carbon fiber toe spring deforms under body weight, storing energy that is then returned during push-off. During push-off, the toe latch is released and the primary compression spring returns its energy. At the onset of swing, the heel clutch is unlocked and the return spring resets the foot into the ready position.

Prototype components were constructed of custom-machined 7075-T6 aluminum (interface component, toe and heel blocks), hardened O1 tool steel (latch surfaces), 416 stainless steel (shafts), and 0-90 carbon/fiberglass laminate (heel and toe leaf springs). The primary compression spring was a 2 inch long, 1.2 inch outer-diameter, chrome-vanadium steel die spring (9584K67; McMaster-Carr, Chicago, IL.). Two 10mm

coreless DC electro-motors with 64:1 gear reductions in planetary gear-heads (1016M012G+10/1K64:1; MicroMo, Clearwater, FL.) actuated the latches. Rotations of the toe and heel assemblies relative to the interface component were measured using contactless inductance-coil potentiometers (MP1545AS; P3 America Inc., San Diego, CA.). Sensory integration and control were performed by a robostix™ microcontroller board (Gumstix, Inc., Portola Valley, CA.) running an ATMega128 microcontroller chip (Atmel Co., San Jose, CA.). The CESR prototype weighed 1.37 kg.

2.2.2 Experimental Methods

We compared the mechanics and metabolics of able-bodied human subjects as they walked normally and wearing different prostheses mounted to simulator boots. We measured oxygen consumption to quantify metabolic energy expenditure and lower-body kinetics and kinematics to estimate center of mass work using the individual limbs method and joint work using inverse dynamics. Comparisons were all made for a single walking speed on an instrumented treadmill. Subjects trained in a separate session prior to collections.

A total of 11 able-bodied adult male subjects (aged 19–28 yrs) participated in the study. We tested intact individuals to allow for direct comparison with intact gait and to minimize risks associated with a novel mobility technology. All subjects ($N = 11$, body mass 79.6 ± 7.2 kg, leg length 0.973 ± 0.043 m, mean ± SD) provided informed consent. Walking trials were conducted at a speed of 1.25 m/s.

Three walking conditions were applied: walking with athletic shoes (Normal), with the CESR foot (CESR), and with a Conventional foot prosthesis (Conventional). During all trials, subjects were instructed to walk as naturally as possible. During CESR and Conventional trials, subjects wore a prosthesis simulator boot unilaterally on the right leg (Affected limb) and a lift shoe on the left foot (Contralateral limb), as shown in Figure 2.5. The prosthesis simulator boot weighed 1.30 kg, and the lift shoe weighed 1.42 kg, with each adding approximately 0.129 m in leg length. Simulator boots were modified AirCast© boots, described in Adamczyk et. al. (2007). During CESR trials, the CESR

foot prosthesis prototype was attached to the prosthesis simulator boot, while in Conventional trials a Seattle LightFoot 2™ was attached. The feet were weight-matched by adding 0.630 kg to the Conventional foot. In both conditions, subjects wore a backpack containing a microcontroller which was connected to the simulator boot through a ribbon cable and connected to an analog data acquisition system through coaxial cables.

Subjects participated in a training session prior to collections in order to allow for adaptation to occur. Subjects trained under each condition, Normal, CESR, and Conventional, for ten minutes each. Additionally, subjects were given an initial acclimation period of five to ten minutes of self-selected overground walking with each prosthetic foot. One day separated training and collection sessions to ensure complete recovery.

For energetics calculations, we measured the rate of oxygen consumption ($\dot{V}_{O2}$ in ml O_2/sec) and carbon dioxide production ($\dot{V}_{CO2}$ in ml CO_2/sec) using an open-circuit respirometry system (Physio-Dyne Instrument, Quogue, NY). Each trial lasted at least ten minutes, including at least six minutes to allow subjects to adapt and reach steady state, followed by three minutes of data recording for average $\dot{V}_{O2}$ and $\dot{V}_{CO2}$ during steady state. Metabolic rates $\dot{E}$ (in Watts) were estimated with the formula (modified from Brockway, 1987)

$$\dot{E} = 16.48\dot{V}_{O2} + 4.48\dot{V}_{CO2}.$$

We also measured each subject's metabolic rate for quiet standing in a separate trial and subtracted it from the rate for walking to yield a net metabolic rate. All conditions, including quiet standing, were conducted in random order. Respiratory exchange ratios were less than unity for all subjects and conditions, indicating that energy was supplied primarily by oxidative metabolism in all test conditions.

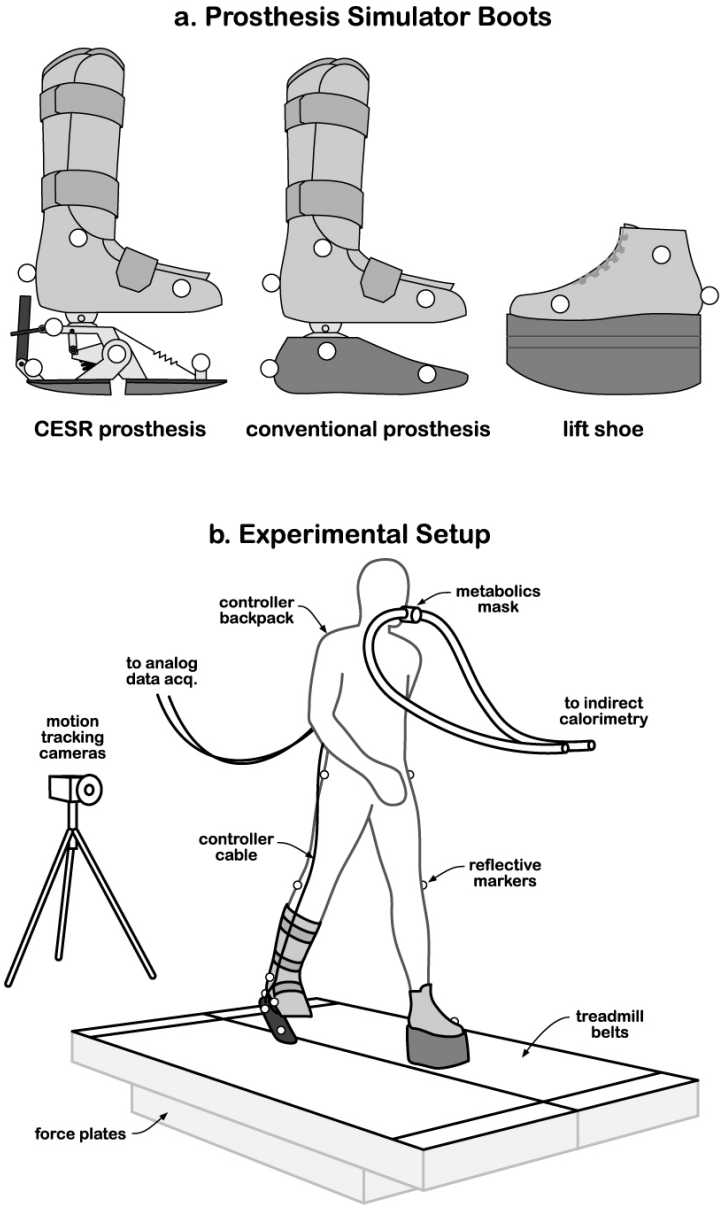

Figure 2.5: Experimental setup. **a.** Intact individuals wore prosthesis simulator boots fitted with the CESR foot and with a conventional foot prosthesis. The simulator boots were worn unilaterally, with a height-matched lift shoe on the contralateral foot. The simulator boots were comprised of AirCast© pneumatic boots augmented with a pyramid adaptor to allow for attachment of the prostheses (similar to Adamczyk et. al., 2007). **b.** Mechanics and metabolics were collected simultaneously using an instrumented split-belt treadmill (described in detail in Collins et. al., 2008) while subjects walked at 1.25 $m \cdot s^{-1}$. A camera system and reflective markers measured body and prosthesis segment locations, force plates measured center of pressure locations and ground reaction forces, and potentiometers measured prosthesis toe and heel plate rotations. A metabolics cart measured the volumes of oxygen consumed and carbon dioxide produced to estimate metabolic rate through indirect respirometry.

For mechanics calculations, we measured kinematics and ground reaction forces as subjects walked on an instrumented treadmill. Kinematic data were recorded with an 8-

camera motion capture system (Motion Analysis Corporation, Santa Rosa, CA) at 120 Hz. Force data were recorded at 1200 Hz using an instrumented split-belt treadmill (Collins et. al., 2008). Treadmill belt speed was maintained at 1.25 m/s. We recorded at least 40 consecutive strides per condition for each subject. For inverse dynamics analysis, a set of motion capture markers were placed bilaterally on the lower extremities according to a modified Helen Hayes marker set. In conditions where subjects wore a prosthesis simulator boot, markers were placed on the simulator boot in locations approximating the same bony landmarks. In Conventional trials, markers were placed on the heel, fifth metatarsal, and lateral malleolli equivalents of the prosthesis, as is common practice (e.g. Geil et. al., 2000). In CESR trials, markers were rigidly attached to the foot on both ends of the shaft, on the interface component, on the tip of the heel and on the tip of the toe.

2.2.3 Analysis

We calculated joint work rates and work performed on the COM for all conditions. We estimated joint work rates using standard inverse dynamics analysis (e.g. Winter, 1990; Siegler 1997). Distal link endpoint forces were measured using force plates during ground contact and were known to be zero during swing phases. Anthropometric data were estimated from the equations of Winter (1979), and were augmented to include the mass properties of the prosthesis simulator and lift shoes, which were measured by hand. Velocities and torques were low-pass filtered at 25 Hz. Joint rotations, torques, and work rates were calculated within the sagittal plane. We similarly calculated the work rates of the prosthetic feet using inverse dynamics. Inertial properties were estimated using the component CAD models (Solidworks, Concord MA). Prosthesis rotations were calculated using markers. Additionally, potentiometer data was used to measure compression spring motion in the CESR foot. Prosthesis work rates were calculated in three dimensions. We estimated the rate of work performed on the COM by each leg using the individual limbs method (Donelan 2002), defined as the vector dot product of each leg's ground reaction force against the COM velocity. We calculated step width and step width variability to infer balance ability. We tracked center of pressure in the shank reference frame to estimate effective roll-over shape of the feet during gait.

Each stride was normalized to percent stride and averaged for each subject and condition. All quantities were analyzed in dimensionless form, to help account for variations in subject size. Torque and work quantities were normalized by each subject's body weight and leg length (MgL, where M is body mass, g is gravitational acceleration, and L is leg length), with the additional factor of $g^{0.5}L^{-0.5}$ (the leg's pendulum frequency) for work rate quantities. Averages, standard deviations, and statistics were computed in dimensionless quantities. We report variables in the familiar dimensional units such as W kg^{-1}, converted using average normalization factors. The average normalization factors used were: 873 kg m^2 s^{-2} for torque and mechanical work, $2.63 \cdot 10^3$ kg m^2 s^{-3} for mechanical work rate and metabolic rate, and 3.02 s^{-1} for frequency.

We compared average work rate in four component phases of COM work rate and nine component phases of joint work rate. For each limb, COM work was divided into Collision, Rebound, Preload, and Push-off, with boundaries determined by successive zero-crossings of the work rate (Figure 2.2). For each joint, work rates were divided into phases typical to clinical gait analysis (e.g. Whittle, 1996; Figure 2.10). Ankle work was divided into an A1 phase beginning at initial contact and ending at the zero-crossing at ankle push-off, and an A2 phase comprised of ankle push-off. Knee work was divided into a K1 phase beginning at initial contact and ending at the zero-crossing near the end of double support, a K2 phase ending at the zero-crossing at the end of single-support, a K3 phase ending at the zero-crossing of knee torque during mid-swing, and a K4 phase comprised of terminal swing. Hip work was divided into an H1 phase beginning at initial contact and ending at the zero-crossing near the end of double-support, an H2 phase ending at the zero-crossing during the subsequent double-support, and an H3 phase including swing. Joint work phases were non-overlapping and together comprised an entire stride. Each phase of joint and COM work were considered in terms of average work rate, with positive and negative contributions considered separately. Average work rate was calculated as the total positive or negative work performed during the phase divided by the stride time. Thus, contributions of each phase of COM or joint work rate

can be correlated to changes in metabolic rate and can be compared across conditions with differing stride frequency.

We compared step width variability and mean step width in order to gain insight into possible effects of the feet on balance during gait. Individual step widths were calculated as the lateral component of the difference between the positions of calcaneus markers during the middle of the double-support period. Step width variability was calculated as the standard deviation of the first eighty consecutive step widths over the course of the trial.

We statistically compared outcome variables that captured the primary energetics and mechanics results. We compared net metabolic rate, stride frequency, mean step width, step width variability, average work rate during COM phases, average work rate during joint phases, and average work rate of the prosthetic feet. Statistical comparisons were made with repeated measures ANOVA for each variable, with a significance level of 0.05. Where differences were significant, post hoc comparisons were performed using paired t-tests.

2.3 Results

We found that the Conventional foot prosthesis condition led to an increase in metabolic cost similar to that observed in the amputee population, while the CESR foot only caused about half the energetic penalty. Subjects selected to walk with faster strides with the Conventional foot than with the CESR foot, even though the feet were weight-matched. The CESR foot produced more than twice as much push-off as the Conventional foot, increasing Push-off of the Affected limb and decreasing Contralateral Collision and Rebound. Energy to increase push-off was harvested during Collision of the Affected limb, reducing negative work requirements for the biological limb. Joint work in the hip and knee were greater with the Conventional foot than with the CESR. Indicators of balance ability were mixed, with subjects preferring wider but less variable steps with the CESR than with the Conventional foot. Electrical power consumed by the CESR prototype was an order of magnitude less than its average mechanical work rate.

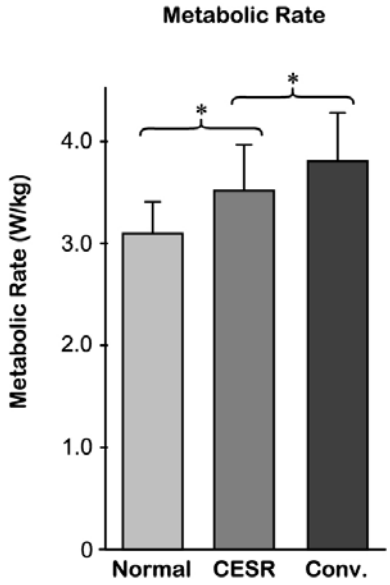

Figure 2.6: Metabolic rate was significantly reduced when wearing the CESR foot as compared to the Conventional foot prosthesis. Metabolic cost increased by 23.1% ($p = 4 \cdot 10^{-5}$) when subjects wore the Conventional foot, but this penalty was only 13.8% ($p = 3 \cdot 10^{-4}$) when subjects wore the CESR foot, an improvement of 9.4% ($p = 3 \cdot 10^{-5}$). Error bars are standard deviation, asterisks denote statistical significance at a level of $p < 0.05$, and statistical comparisons of non-sequential conditions are not displayed.

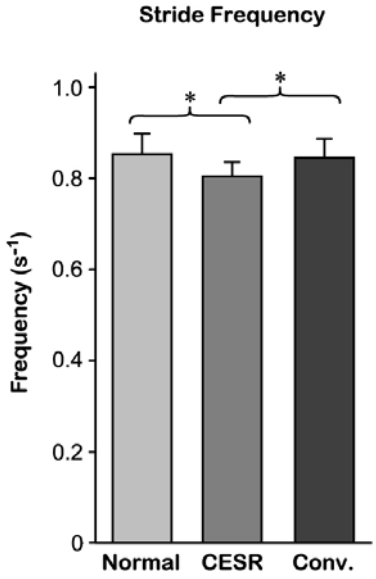

Figure 2.7: Subjects walked with a higher stride frequency in the Conventional condition than in the CESR condition. Subjects walked with 6% slower strides in the CESR condition than Normal ($p = 7 \cdot 10^{-5}$), which may be expected due to increased distal limb mass. However, with matched distal limb mass, subjects walked with 5% faster strides with the Conventional foot than with the CESR foot ($p = 6 \cdot 10^{-6}$), which may result from collision avoidance. Error bars are standard deviation, asterisks denote statistical significance at a level of $p < 0.05$, and statistical comparisons of non-sequential conditions are not displayed.

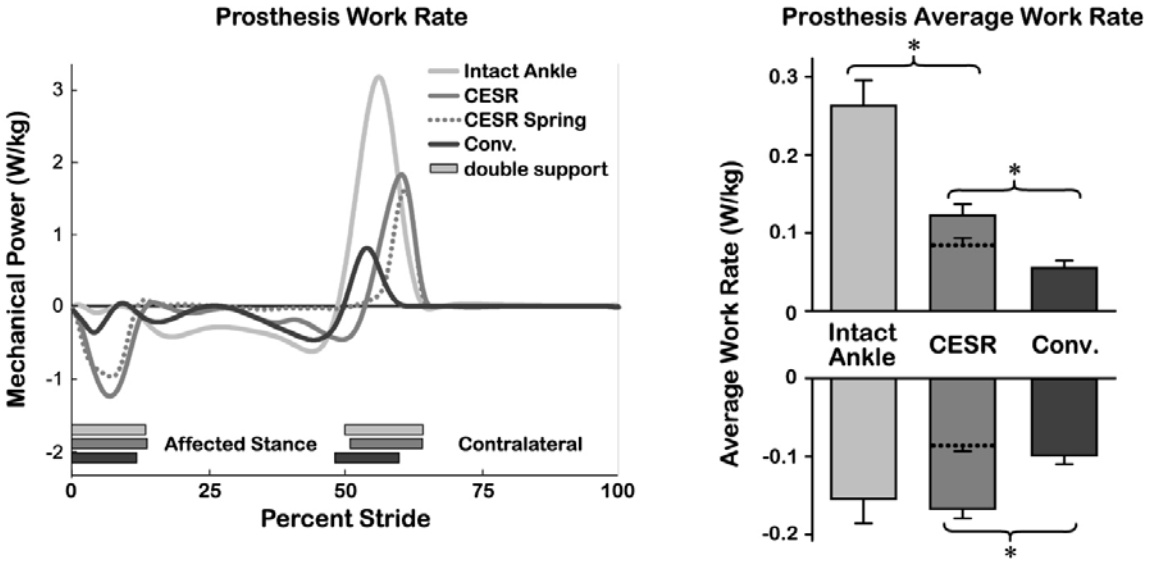

Figure 2.8: Prosthesis work rate comparison. The CESR foot provided more positive mechanical work during push-off than the Conventional foot. Both feet absorbed energy during Preload, but the CESR foot absorbed significantly more during Collision. Mechanical work rate of an intact ankle during normal gait is included as a reference. **Left:** Mechanical work rate trajectories. The component of CESR work rate due to the primary compression spring alone, where velocities were measured using potentiometers, is shown dotted. Double support periods for each condition, which significantly varied between conditions and were asymmetric in the prosthesis conditions, are indicated by shaded rectangles. **Right:** Stride-averaged work rate comparison. Spring component of CESR average work rate shown dotted. The CESR foot provided 122% more push-off work than the Conventional foot ($p = 4 \cdot 10^{-9}$), but still provided less than half the push-off work of the intact ankle during normal gait ($p = 1 \cdot 10^{-7}$).

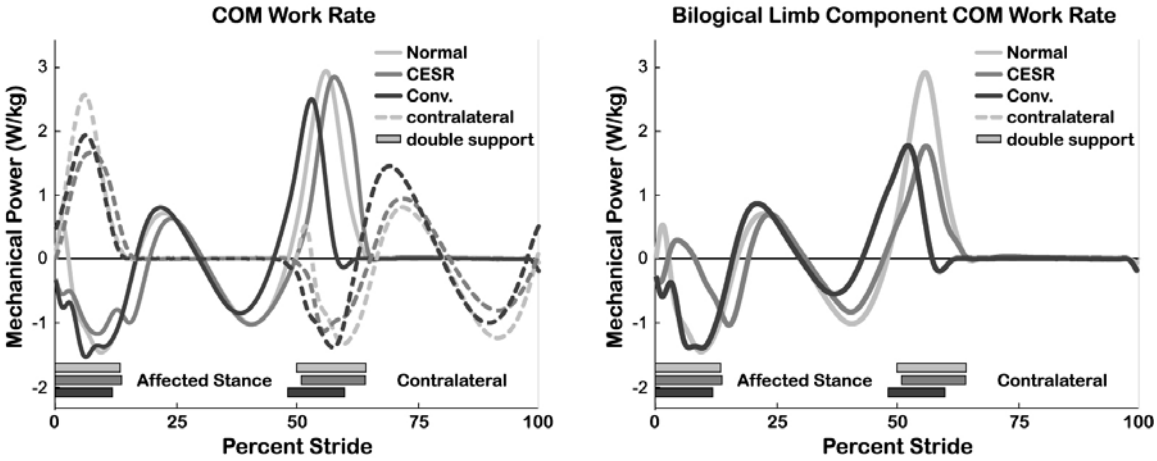

Figure 2.9: Center of Mass (COM) work rates as estimated using the individual limbs method. **Left:** total limb work rate. **Right:** Biological component of limb work rate, i.e. with prosthesis contribution removed. Solid lines correspond to the limb on which the prosthesis simulator was worn (Affected limb), dashed lines correspond to the opposite limb (Contralateral limb). Percent stride begins at heel strike of the Affected limb. Double support periods for each condition are denoted by shaded rectangles at bottom.

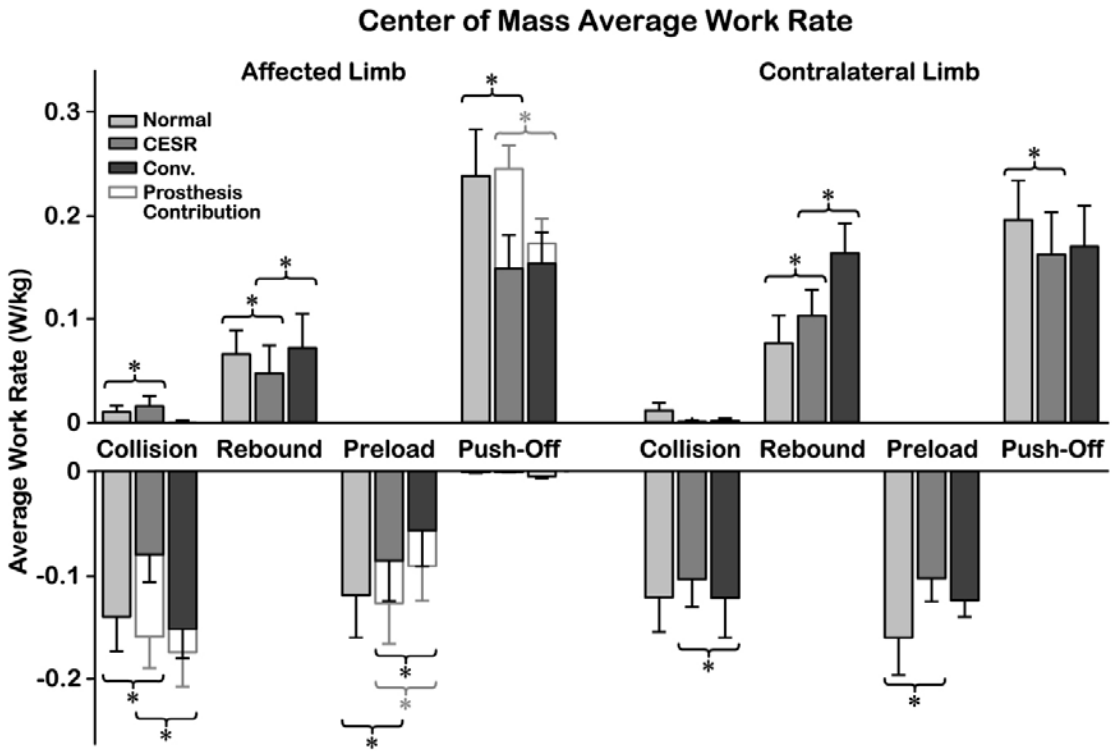

Figure 2.10: Average work rate during Collision, Rebound, Preload, and Push-Off phases of COM work as estimated using the individual limbs method. The separate contributions of the biological limb and the prostheses are distinguished by line shading. Total Affected limb Push-off work was 42% greater with the CESR foot than the Conventional foot prosthesis ($p = 2 \cdot 10^{-8}$). Contralateral Collision losses were 17% greater with the Conventional foot than the CESR foot ($p = 0.005$), even though subjects walked with shorter strides. Contralateral Rebound work was 58% greater with the Conventional foot than the CESR foot ($p = 3 \cdot 10^{-8}$). Statistical significance between biological components shown in black, between total shown in gray. See Figure 2.2 for definitions and Figure 2.8 for trajectories. Error bars are standard deviation, asterisks denote statistical significance at a level of $p < 0.05$, and statistical comparisons of non-sequential conditions are not displayed.

Both the CESR foot and the Conventional foot prosthesis led to significant increases in metabolic cost, but the CESR foot only caused about half as much of an energetic penalty. The net metabolic rate in Normal trials was 3.09 ± 0.30 W kg^{-1}. In Conventional trials, the net metabolic rate was 3.81 ± 0.47 W kg^{-1}, an increase of 0.72 W kg^{-1} or 23.1% ($p = 4 \cdot 10^{-5}$). For CESR trials, net metabolic rate was 3.52 ± 0.47 W kg^{-1}, an increase of 0.42 W kg^{-1} or 13.8% ($p = 3 \cdot 10^{-4}$), but still 0.29 W kg^{-1} less than Conventional (9.4% reduction, $p = 3 \cdot 10^{-5}$).

Subjects selected to walk with faster strides with the Conventional foot than with the CESR foot, even though the feet were weight matched. Self-selected stride frequency

was 0.854 ± 0.044 s^{-1} in Normal walking. In the CESR condition, stride frequency was 0.854 ± 0.044 s^{-1}, a reduction of 0.050 s^{-1} or 6% ($p = 7 \cdot 10^{-5}$), likely due to the increased leg length and distal foot mass of the prosthesis simulator and lift shoe. By contrast, stride frequency in Conventional trials was 0.846 ± 0.041 s^{-1}, not significantly different from Normal ($p = 0.4$), but 5% faster than with the CESR ($p = 6 \cdot 10^{-6}$).

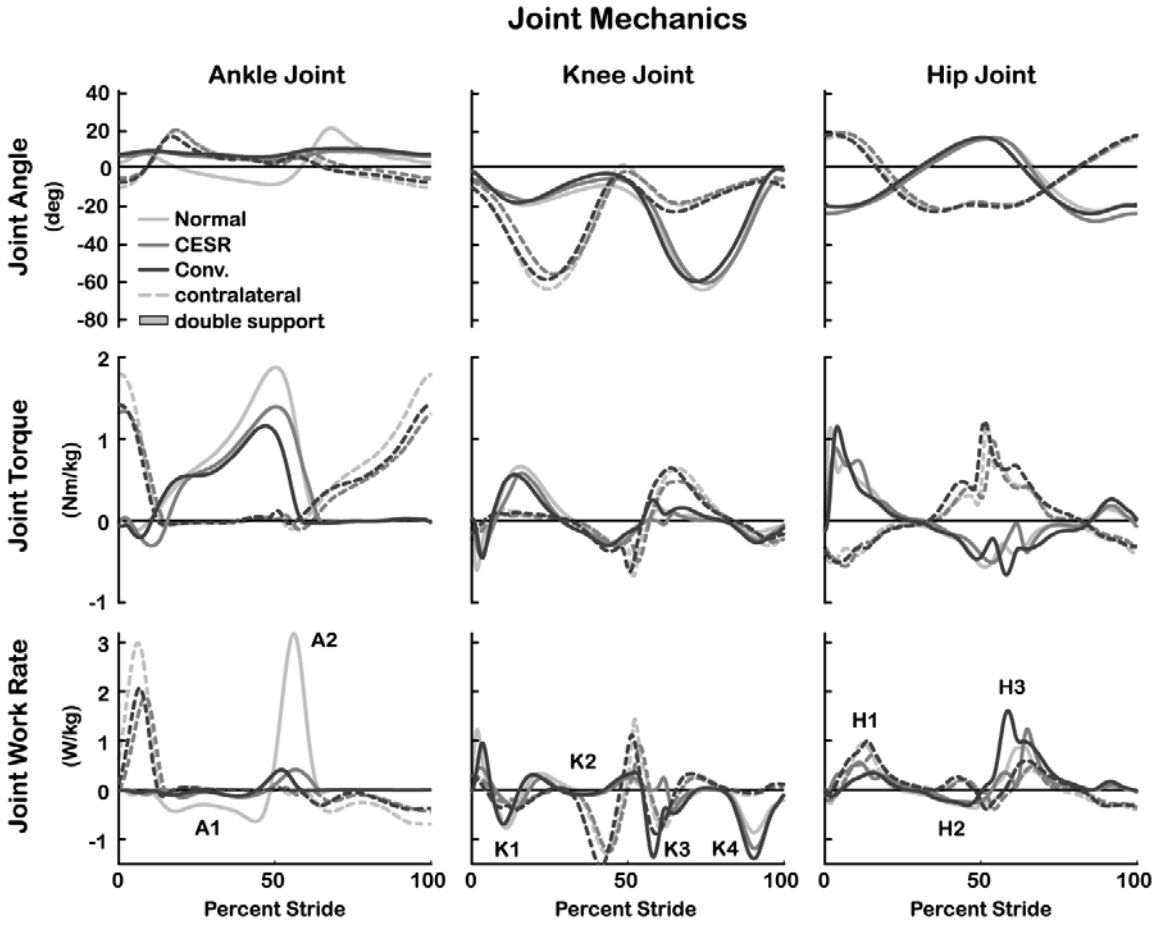

Figure 2.11: Biological joint angles (top row), torques (middle row), and work rates (bottom row) as estimated using inverse dynamics. Clinical phases of joint work for the Affected side are marked as A1, A2, etc. Solid lines correspond to the limb on which the prosthesis simulator was worn (Affected limb), dashed lines correspond to the opposite limb (Contralateral limb). Percent stride begins at heel strike of the Affected limb. In the Affected limb, the biological ankle joint was fixed in the prosthesis simulator boot, resulting in only minor displacement and work.

The CESR foot produced more than twice as much push-off as the Conventional foot while consuming very little electricity. The Conventional foot prosthesis absorbed an average of -0.100 ± 0.011 W kg^{-1} and returned an average of 0.055 ± 0.009 W kg^{-1} over

the course of a stride, consistent with previously reported values (e.g. Prince, 1998). The CESR foot absorbed an average of -0.168 ± 0.012 W kg^{-1} and returned an average of 0.122 ± 0.014 W kg^{-1} over the course of a stride, an increase of 0.067 W kg^{-1} or 122% ($p = 4 \cdot 10^{-9}$). The intact ankle produced an average of 0.263 ± 0.034 W kg^{-1} by comparison. The electrical power used by the CESR foot was on average 0.844 W (0.010 W kg^{-1}), of which 0.471 W (0.006 W kg^{-1}) was consumed by the microcontroller and 0.374 W (0.004 W kg^{-1}) was consumed by motors to operate the latches.

Push-off in the Affected limb was greater when subjects used the CESR foot than the Conventional foot, leading to decreased Contralateral Collision and Rebound despite shorter step length. Push-off average work rate in the Affected limb under the Conventional condition was 0.173 ± 0.024 W kg^{-1}. Push-off average work rate in the Affected limb during CESR trials was 0.245 ± 0.023 W kg^{-1}, an increase of 0.072 W kg^{-1} or 42% ($p = 2 \cdot 10^{-8}$). Contralateral Collision average work rates were -0.122 ± 0.038 W kg^{-1} with the Conventional foot and -0.104 ± 0.027 W kg^{-1} with the CESR foot, a reduction of -0.018 W kg^{-1} or 17% ($p = 5 \cdot 10^{-3}$). Contralateral Rebound average work rates were 0.164 ± 0.029 W kg^{-1} with the Conventional foot and 0.103 ± 0.025 W kg^{-1} with the CESR foot, a reduction of 0.061 W kg^{-1} or 58% ($p = 3 \cdot 10^{-8}$).

Greater push-off in the CESR foot resulted from increased energy storage during Collision of the Affected limb, resulting in a reduction in negative work performed by the biological limb. Collision average negative work rate in the Affected limb during Conventional trials was -0.174 ± 0.032 W kg^{-1}, of which -0.152 ± 0.028 W kg^{-1} was performed by the biological limb (as opposed to the prosthesis). Collision average negative work rate in the Affected limb during CESR trials was -0.159 ± 0.030 W kg^{-1}, of which -0.080 ± 0.027 W kg^{-1} was performed by the biological limb, not a significant reduction in total Collision ($p = 0.2$), but a 0.072 W kg^{-1} or 47% reduction in the biological component ($p = 2 \cdot 10^{-6}$).

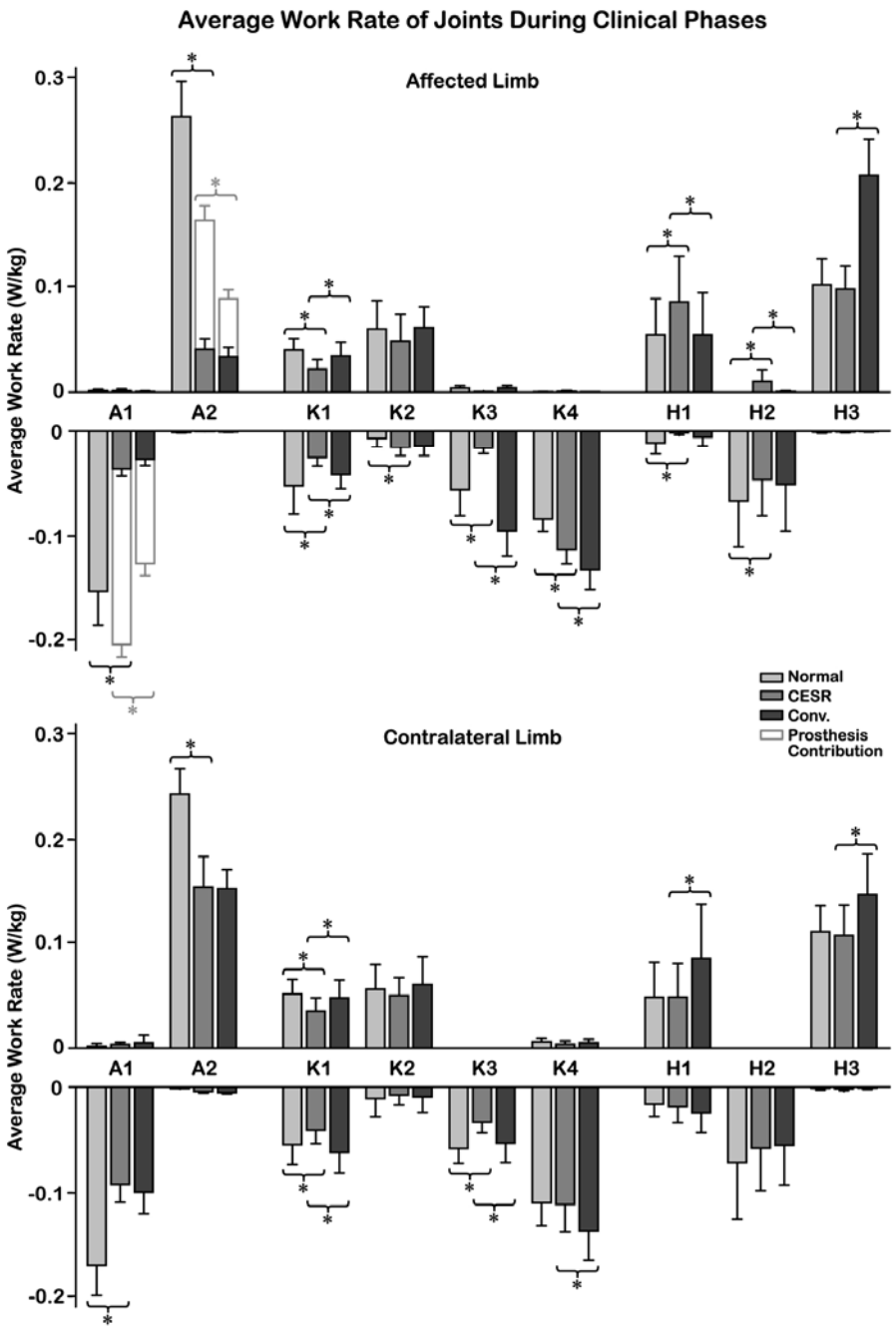

Figure 2.12: Average work rates of the joints during clinical phases of gait, as estimated using inverse dynamics. Affected limb H3 was 110% greater in Conventional trials than in CESR trials ($p = 2 \cdot 10^{-7}$), with K3 and K4 also increasing significantly (470% and 17%, $p = 6 \cdot 10^{-7}$ and $p = 7 \cdot 10^{-4}$, respectively), possibly due to faster leg swing. A similar effect was observed in Contralateral H3, K3, and K4. Conversely, Affected limb H1 was 58% greater in the CESR condition than in the Conventional condition ($p = 4 \cdot 10^{-6}$), with the opposite effect in Contralateral H1 (Conventional 76% greater, $p = 3 \cdot 10^{-4}$). In the bar graph, separate contributions of the biological limb and the prostheses are distinguished by line shading. Likewise, statistical significance between biological components are shown in black, between totals shown in gray. See text for definitions and Figure 2.10 for trajectories. Error bars are standard deviation, asterisks denote statistical significance at a level of $p < 0.05$, and statistical comparisons of non-sequential conditions are not displayed.

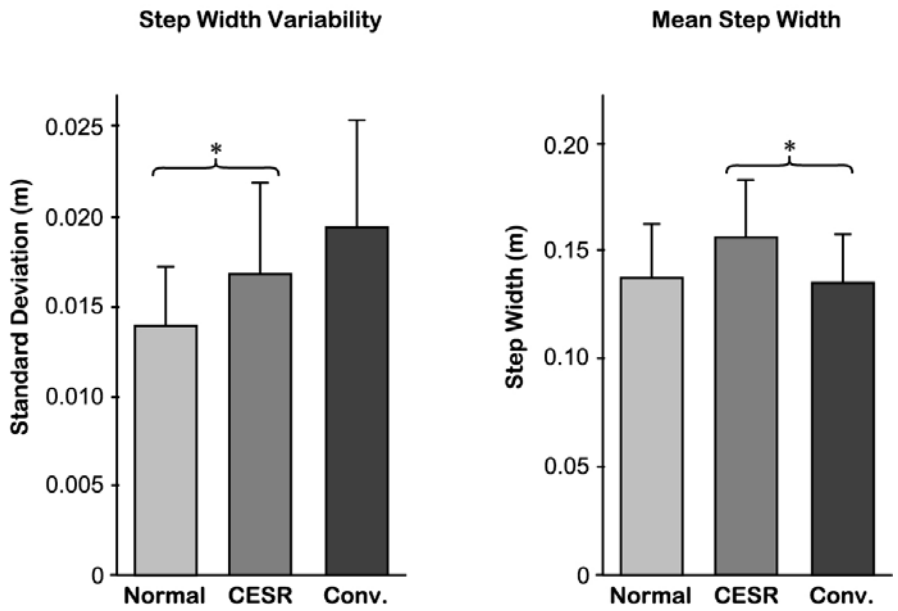

Figure 2.13: Lateral foot placement variability was greater in both simulated prosthesis conditions, while step width was greater with the CESR than with the Conventional foot. Step width variability was 21% greater than normal in the CESR condition ($p = 0.04$) and 40% greater in the Conventional condition ($p = 0.002$). Step width variability was also 16% greater with the Conventional foot than with the CESR foot, though this result meet our statistical significance criteria ($p = 0.06$). Step width in the CESR condition was 16% greater than in the Conventional condition ($p = 0.006$), and appeared to be 14% greater than in Normal gait, though this result did not meet our significance criteria ($p = 0.07$). Error bars are standard deviation, asterisks denote statistical significance at a level of $p < 0.05$, and statistical comparisons of non-sequential conditions are not displayed.

Joint average work rates in the hip and knee were greater with the Conventional foot than with the CESR. In the Affected knee joint, K3 average work rates were -0.096 ± 0.024 W kg^{-1} with the Conventional foot and -0.017 ± 0.006 W kg^{-1} with the CESR foot, a reduction of -0.079 W kg^{-1} ($p = 6 \cdot 10^{-7}$), while K4 average work rates were -0.133 ± 0.019 W kg^{-1} with the Conventional foot and -0.115 ± 0.013 W kg^{-1} with the CESR foot, a reduction of -0.018 W kg^{-1} ($p = 7 \cdot 10^{-4}$). A similar but less pronounced trend was observed on the Contralateral side. In the Affected hip joint, H1 average work rates were 0.054 ± 0.040 W kg^{-1} with the Conventional foot and 0.086 ± 0.043 W kg^{-1} with the CESR foot, an increase of 0.032 W kg^{-1} ($p = 4 \cdot 10^{-6}$), with the opposite effect observed on the Contralateral side where H1 average work rates were 0.086 ± 0.052 W kg^{-1} with the Conventional foot and 0.049 ± 0.032 W kg^{-1} with the CESR foot, a decrease of 0.037 W kg^{-1} ($p = 3 \cdot 10^{-4}$). On the Affected side, H3 average work rates were 0.207 ± 0.035 W kg^{-1} with the Conventional foot and 0.098 ± 0.022 W kg^{-1} with the CESR foot, a sharp decrease of 0.108 W kg^{-1} ($p = 2 \cdot 10^{-7}$), with a similar but less pronounced effect observed

on the Contralateral side. Ankle joint work rate did not significantly change with foot prosthesis and was not very meaningful because the prosthesis simulator boots severely restricted motion of the biological ankle joint on the Affected side.

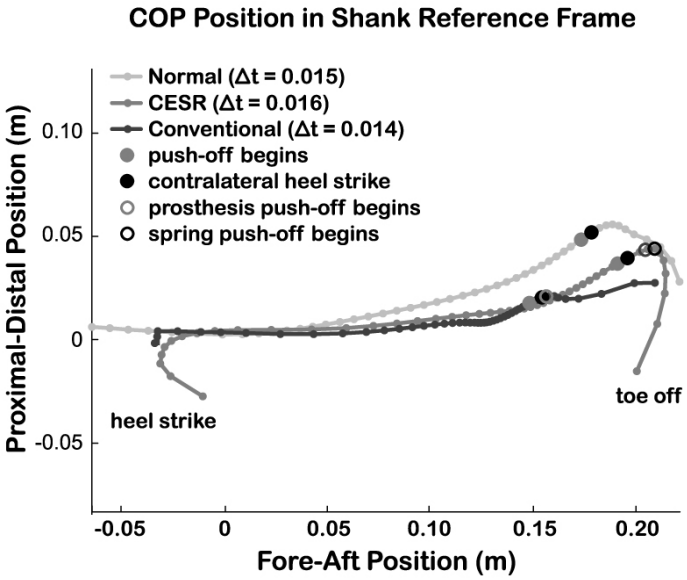

Figure 2.14: Center of Pressure (COP) trajectories in the shank reference frame. Push-off in the CESR foot produced significant plantar-flexion motion of the COP towards toe-off, similar to that found in Normal gait, while the Conventional foot prosthesis did not. However, Collision of the CESR foot also produced a significant dorsi-flexion motion in the COP starting at heel strike, unlike the relatively flat trajectory in Normal and Conventional conditions.

Mean step width was greater with the CESR foot, while step width variability appeared to be greater with the Conventional foot. In Normal walking, mean step width was 0.137 ± 0.025 m and step width variability was 0.0138 ± 0.0033 m. Mean step widths were 0.135 ± 0.023 m with the Conventional foot and 0.156 ± 0.027 m with the CESR, an increase of 0.021 m or 16% ($p = 0.006$). Mean step width variabilities were 0.0193 ± 0.0060 m with the Conventional foot and 0.0167 ± 0.0050 m with the CESR foot, an apparent decrease of 0.0026 m, though this result did not meet our criteria for statistical significance ($p = 0.06$). Weak statistical comparisons within these measures were due to high intra-subject variability.

The center of pressure (COP) trajectory in the shank reference frame of the CESR foot more closely resembled that of Normal gait during Push-off, but included a sharp dissimilarity during Collision (Figure 2.14).

2.4 Discussion

We developed a prototype foot prosthesis and conducted human subject experiments to compare Controlled Energy Storage and Return to conventional foot prosthesis function. We proposed that a CESR foot could store energy during Collision by replacing negative work typically performed by the intact limb. We found that the biological component of Collision work was reduced with the CESR foot, while the total Collision work did not change significantly. We proposed that stored energy could be returned so as to increase Push-off of the Affected limb compared to a Conventional foot. We found no differences in the biological component of Push-off between prosthesis conditions, but found the total Push-off of the Affected limb to be greatly increased due to CESR foot push-off work. We hypothesized that increased Affected Push-off could lead to reduced Contralateral Collision and Rebound. We found Contralateral Collision and Rebound average work rates to be significantly reduced with the CESR foot compared to the Conventional foot. Finally, we hypothesized that by reducing the mechanical work rate of the limbs, metabolic rate could be reduced. We found that metabolic rate was significantly lower with the CESR foot than with the Conventional foot; subjects incurred only about half of the energetic penalty as compared to Normal.

Use of the CESR foot significantly reduced metabolic cost as compared to the Conventional foot prosthesis. Subjects experienced an increase in metabolic cost similar to that observed in the amputee population when wearing simulator boots with the Conventional foot prosthesis attached. A metabolic equivalent would be to walk wearing a 19 kg backpack. Metabolic rate in subjects using the CESR foot was reduced by 9.4%, a greater improvement than has been observed in prior comparisons of prosthetic feet. This reduction may be attributed to improved gait mechanics as a result of increased Push-off by the CESR foot.

The CESR foot prosthesis prototype produced more than twice the Push-off work of the Conventional foot by storing Collision energy that would have otherwise been dissipated. Both foot prostheses performed dramatically less Push-off work than the intact ankle did

during the A2 phase of Normal gait. However, with the assistance of the CESR prosthesis and with additional work from the knee and hip, subjects were able to perform Push-off in the Affected limb that equaled that observed in Normal gait. Storing and returning more energy with the CESR foot did not lead to increased losses during other parts of the gait cycle, but rather reduced negative work performed by the biological limb during Collision. The CESR foot may have reduced muscle energy use not only by reducing work production, but also by reducing active work absorption, which is performed at negative efficiency in human muscle. By contrast, the Conventional prosthesis provided dramatically less push-off work, and even with additional knee and hip work Push-off in the Affected limb was significantly reduced compared to the CESR condition. Interestingly, subjects did not make up this difference by further increasing knee and hip work. It may be that such increases would be more costly to produce than the mechanical benefits of increased Push-off. Alternatively, the knee and hip could be ill disposed to produce more work in this limb configuration, placing a limit on the amount of Push-off that can be performed without use of the ankle. The Conventional foot prosthesis may have also directly interfered with increased Push-off by the biological limb since it continued to absorb energy well after the biological limb began producing positive work during Push-off (Figures 2.8 and 2.9). Forefoot compliance in the Conventional foot may hinder as well as help.

Electric power consumed by the CESR prototype was less than one Watt, or less than one tenth the average positive work rate of the prosthesis. If similar push-off were to be produced directly by electric motor with a typical conversion efficiency of about 50%, such a motor would require twenty times the electric power of the CESR prototype, on average, and so would require twenty times the batteries or would discharge the same batteries twenty times faster.

Subjects chose to walk with a faster stride frequency when using the Conventional foot than the CESR foot, likely trading increased leg swing costs for reduced collision losses. Dynamic walking models and human subject experiments suggest that the energy use associated with leg swinging rises quickly with increasing stride frequency (Doke, 2005).

Leg swinging costs have also been shown to greatly increase with increasing distal limb mass (e.g. Martin, 1997). We expected subjects to select a slightly slower stride frequency than Normal in both the CESR and Conventional foot conditions due to increased distal mass and leg length. This held true for the CESR condition. In Conventional trials, however, it appears that subjects incurred greater leg swing costs by taking shorter, faster steps. Joint work in the K3 and K4 phases of the knee and the H3 phase of the hip are often associated with swinging the leg, and these were all significantly greater with the Conventional foot than with the CESR. Dynamic walking models predict that walking with shorter, faster steps can reduce the energy required to redirect the COM during the step-to-step transition (Kuo, 2001). Subjects may have chosen to walk with higher stride frequency so as to mitigate step-to-step transition costs that were exacerbated by a lack of Push-off in the Affected limb during Conventional trials.

Center of mass mechanical work rates were significantly lower with the CESR foot than with the Conventional foot prosthesis, especially in terms of work associated with the step-to-step transition. Even though subjects took shorter steps with the Conventional foot than with the CESR foot, Contralateral Collision losses were still greater in the Conventional condition. This is consistent with our hypothesis that reduced Push-off of the trailing leg during the step-to-step transition could lead to increased in energy dissipated in the Collision of the leading leg. Likewise, our finding that Contralateral Rebound work was greater when using the Conventional foot is consistent with the hypothesis that increased collision losses could lead to greater work mid-stance. These increased mechanical work requirements for the lower limbs likely significantly contributed to the greater metabolic rate observed in the Conventional condition than the CESR condition.

Although the COM work rate analysis presented here provides useful insight into the mechanical basis for the observed metabolic results, the individual limbs method is susceptible to errors that could have impacted our results. Although we have attributed COM work to the lower limbs and, by implication, the muscles in those limbs, COM

work may also occur in other ways, such as by the deformation and/or restitution of soft tissues. Careful examination of Figures 2.10 and 2.12 will reveal that while significant COM work is done during Collision and Rebound, far less work is attributed to the joints during corresponding phases. Thus, some of the negative work replaced by the CESR during Collision may have otherwise been dissipated by soft tissues rather than actively dissipated by muscle. Alternatively, some of this work may have otherwise been immediately restored during Rebound, and indeed we observed a slightly reduced Rebound on the Affected side in the CESR condition. Some tuning of the spring stiffness of the CESR might allow for optimal collection of this energy. Another potentially confounding factor for COM work analysis is that contributions to leg swing and center of mass redirection are not easily separated. Thus, some of the Push-off work that we have theorized assists in the step-to-step transition may actually be contributing to leg swing by pushing the foot on the Affected side forward during terminal stance. In CESR trials, the Push-off peak on the Affected side was skewed towards terminal stance (Figure 2.9), and the push-off work of the CESR foot was mostly performed during the latter portion of double-support (Figure 2.8). Although some body mass lies in the swing foot, propelling this foot forward would do little to redirect the COM towards the ensuing pendulum phase. This may indicate that less true Push-off was achieved in the CESR condition than it might at first appear. Finally, we have previously found it difficult to interpret COM work rate results in which substantially differing mechanical interventions are performed in different conditions (Vanderpool et. al., 2007). In this case, comparisons between Normal and CESR or between Normal and Conventional conditions may be confounded by a number of factors including alteration of the elastic propertied of the distal links and the addition of a rocker-bottom shape on both the Affected and Contralateral sides. We have therefore avoided making overt comparisons of COM work rate between Normal and CESR or Conventional gaits.

Similarly, although our inverse dynamics analysis proved useful in identifying possible joint-level explanations for the observed metabolic trends, the analysis has shortcomings. We used a simplified marker set to identify joint and segment positions. This may have led to errors in absolute results, but likely did not reduce the utility of inter-condition

comparisons. However, we also performed the analysis within the sagittal plane, which prevented observation of transverse and/or coronal plane joint work. This is especially limiting with respect to the hip joint, where transverse rotations of the pelvis may be used to provide Push-off when the ankle is unable to do so. This limitation may explain why we were not able to identify increases in hip and/or knee work that must have occurred between Normal and prosthesis conditions to allow for substantial biological limb Push-off in spite of drastically reduced biological ankle A2 work.

Indicators of balance ability were mixed, with subjects preferring wider steps but exhibiting less variability with the CESR than with the Conventional foot. We anticipated that the CESR foot could put subjects off balance because it pushes off without direct control by the user and presents a complex coordination task. Therefore, we expected that lateral foot placement variability and mean step width might be greater in the CESR condition. The result that step width was greater with the CESR foot while lateral foot placement variability was greater with the Conventional foot is inconclusive. Subjects may have walked with wider steps to improve their margin of stability (Donelan, 2004) in the CESR condition due to a perception of greater fall risks. Mean step width may also have been influenced by the mechanics of the foot; subjects may have chosen lateral foot placements that allowed optimal Push-off or Collision work. Given the differing step widths between conditions, it is difficult to subsequently interpret foot placement variability, since expected variability decreases with increasing step width (Bauby, 2000). Both deviations from Normal gait are likely to include a metabolic penalty, either for additional control costs related to increased lateral foot placement variability (Donelan, 2004) or for additional step-to-step transition costs related to increased mean step width (Donelan, 2001).

Foot prostheses compared in this study were weight-matched. This allowed for a controlled comparison of the feet on the basis of mechanical function, but likely penalized the Conventional foot to some degree in terms of gross metabolic energy requirements. In theory, a foot performing the same CESR function could weigh much less than this experimental prototype and our results clearly suggest that such a foot could

result in lower energy use. However, it is possible that the differences observed here would be reduced for this prototype without weight matching.

We chose to compare the CESR foot and Conventional foot on able-bodied subjects wearing prosthesis simulator boots rather than on amputees. Testing able-bodied subjects allowed us to compare prosthesis conditions with normal gait within each subject. Able-bodied subjects were also at lesser risk of falls or injury while using a novel and possibly unreliable prosthesis prototype. With most of these issues resolved, we plan to conduct experiments with this prototype on amputee subjects so as to obtain the most pertinent metabolic comparisons in the near future. Nonetheless, the results seem to indicate that our prosthesis simulator boots provided a useful platform for testing the Conventional and CESR feet. Metabolic cost in Conventional trials was increased by an amount similar to that typically observed in the literature, and the mechanical work rate of the Conventional foot was highly consistent with previously reported data. However, a portion of the higher metabolic cost in the prosthesis conditions is likely due to the increased distal limb mass. It seems likely that the metabolic energy penalty for wearing the CESR foot for an amputee could be even lower than estimated here.

These findings are consistent with the hypothesis that increasing push-off work in the affected limb of amputees may reduce mechanical work requirements in gait, thereby reducing metabolic cost. Increased push-off in the trailing leg during the step-to-step transition appeared to reduce collision work in the contralateral limb and lead to reduced limb work mid-stance. The success of the prototype examined here suggests that controlled energy storage and return is an effective way to provide this extra push-off.

Acknowledgments

This work was supported by an NSF Small business Technology Transfer Research grant. Arthur Kuo helped develop the CESR concept and assisted with experimental design. Peter Adamczyk helped develop the CESR prototype and Karl Zelik assisted with data collections. Glenn Klute, Michael Orendurff, Joseph Czerniecki, and the staff of the Seattle VA Center of Excellence for Limb Loss Prevention and Prosthetic Engineering helped to develop the CESR foot concept for amputee populations.

Chapter 3
Swinging the arms makes walking easier

Abstract

Humans swing their arms while they walk, a result of both passive tendencies and muscular forces. However, biomechanists have been able to agree on neither the function of this motion nor the relative contributions of muscular and pendular effects in its generation. To better understand the role of arms swinging in gait, we developed a simple dynamic walking model with free-swinging arms and performed human subject experiments. Our model demonstrated several passive modes of oscillation, including the normal mode exhibited by humans and an anti-phase mode in which arms swing in phase with the ipsilateral leg. We also simulated a mode in which the arms were kept stationary at the model's sides. We then performed experiments in which mechanics and metabolics were recorded while human subjects walked with normal arm swinging, arms held at their sides, arms bound to their sides, and with arms swung in the anti-phase mode. Our model results and experimental data both support the proposition that the primary function of the arms during gait is to reduce fluctuations in vertical angular momentum without significant effort, thus keeping muscular requirements and metabolic energy use low. In simulations and experiments, we found that fluctuations in vertical angular momentum and peak vertical ground reaction moments significantly increased in held, bound, and anti-phase conditions. In human subjects, these changes were accompanied by significant (7–26%) increases in metabolic cost. Although the net effect of arm swinging was significant, achieving it seemed to require little effort under normal conditions. Over a range of model speeds and parameter values, both the normal and anti-phase simulated modes were passive, requiring no direct control. Likewise, human subjects exhibited functionally low joint torques and powers in normal and anti-phase conditions. Taken together, these results suggest that arm swinging is easy to achieve,

yet significantly reduces fluctuations in vertical angular momentum and external moment requirements, thereby significantly reducing metabolic energy use.

3.1 Introduction

Humans swing their arms as they walk, a result of both passive tendencies and muscular forces. However, biomechanists have disagreed as to the function of this motion. Further, the relative contribution of muscular and pendular effects in the generation of arm swinging has remained contentious. We seek to apply a dynamic modeling approach and modern experimental techniques to help resolve the function of arm swinging and the mechanisms behind its generation during gait.

Both passive tendencies and muscular forces contribute to the motion of the arms during gait, but their relative contributions have remained unclear. Early biomechanists speculated that the arms might swing purely as a result of the movements of the shoulders during gait, behaving as passive pendulums (Gerdy, 1829; Weber, 1836), a notion that persisted until the mid 20th century (e.g. Morton, 1952). It has since been shown that joint torques (Elftman, 1939; Hinrichs, 1990), including those arising from muscle contraction (Fernandez-Ballesteros, 1965; Jackson, 1978; Hinrichs, 1990), play a role in the generation of the motion of the arms. However, the importance of muscular contributions has remained unclear. Dynamic analyses have resulted in a wide range of resultant joint moments at the shoulder, from 3.8 Nm (Jackson, 1978) to 7.5 Nm (Elftman, 1939) to 12 Nm (Hinrichs, 1990). These disparities may reflect the relatively high uncertainty and low sample sizes consequent to the laborious photographic analysis techniques used in previous studies. Technological advances may now allow for more accurate calculations of upper limb joint torques during gait.

Electromyographic studies of the muscles of the upper limbs have shown that shoulder musculature exhibits some activity during gait (while elbow muscles are generally quiet), but interpretations of this activity have varied widely. Fernandez-Ballesteros (1965) found peak muscle activations in the posterior deltoid of the shoulder to be at most 10% of the activation at maximum voluntary contraction. However, the authors concluded

muscular forces dominated the arms' motion. Jackson (1983) also observed low peak activations, but concluded that the muscles were only needed to keep arm motions from becoming "ragged". Hinrichs (1990) found slightly lower peak shoulder activations, ranging from 4-9% across a variety of gait speeds, but concluded that the relative contributions of passive tendencies and muscle forcing remained unresolved, and suggested better models were needed.

Mathematical models might be useful in establishing the role of upper limb musculature in generating the movements of the arms. Jackson (1983) presented a sagittal model of the upper limb that used shoulder movements and muscle torques as inputs in generating arm motions, and found that cyclical muscle activation patterns were required to generate rhythmic motion. However, Jackson did not search for motions systematically, meaning motions requiring little or no muscle activation could have been missed. Kubo (2004) presented a similar model in three dimensions, but found that arm motions observed in human gait could be produced without any contribution from active muscle contraction. We suggest that a dynamic walking model incorporating three-dimensional whole-body motions and systematic searching for different modes of oscillation could provide more understanding of possible passive motions. Before attempting to control the motions of the arms, it may be useful to see what they are capable without any control at all. Additionally, such a model might help us to better understand the function of the arms during gait.

Descriptions of the function of arm swinging during human walking vary widely in the literature. The main possible functions that have been suggested include reduction of angular momentum fluctuations about a vertical axis (Elftman, 1939; Hinrichs, 1990; Li, 2001), stabilization/reduced rotation of the trunk (Fernandez-Ballesteros, 1965; Murray, 1967), reduced vertical center of mass displacement (Murray, 1967; Hinrichs, 1990), and prevention of "jerky" motions (Jackson, 1983). It has even been proposed that arm swinging may be an evolutionary relic from quadrupedalism that serves little or no purpose (e.g. Murray, 1967; Jackson, 1983).

Notably, minimization of energy expenditure has been rejected as a primary function of arm swinging. This is surprising, since humans tend to select neuromuscular coordination strategies that minimize energy use in locomotion (e.g. Zarugh). However, an early examination of the contributions of the arms to metabolic cost by Ralston (1964) apparently revealed no significant increase in energy consumption when subjects' arms were both bound to their sides, although no data was published for this finding. A later study (Hanada, 2001) found a statistically insignificant increase in metabolic energy expenditure when subjects walked with one arm bound to their torso. A more complete study of the metabolic consequences of swinging the arms seems warranted given these surprising results.

We hypothesized that the primary function of the arms during walking is to minimize energy expenditure by reducing fluctuations in angular momentum about a vertical axis without significant effort. As Elftman (1939) first demonstrated, the arms' contribution to vertical-axis angular momentum opposes the legs' contribution, such that these two components partially cancel and therefore reduce the angular momentum fluctuations of the body as a whole. We propose that these fluctuations are important because they require muscle action that consumes metabolic energy. In order to change the angular momentum of the body as a whole, an external moment must be applied by the legs equal to the rate of change. As fluctuations in angular momentum increase, these external moments must also increase, requiring greater muscular force production under normal walking conditions. Larger fluctuations in angular momentum also imply greater angular velocities of the body as a whole, which could lead to greater mechanical power requirements for the legs. These two factors strongly imply that, considered in isolation, metabolic energy use should increase with increasing fluctuations in vertical angular momentum. However, there may also be a cost to producing motions that result in lower vertical angular momentum. Forcing the legs, torso, or arms to move in strange ways might exact a metabolic penalty due to increased muscular force or work. Therefore, arm swinging would achieve a net reduction in metabolic energy use only if the cost of producing arm motions were less than the benefit from reduced ground reaction torques produced by the legs.

We further hypothesized that beneficial arm motions could use very little metabolic energy, requiring muscular activity only to start the arms in motion, correct large disturbances, and provide increased shoulder stiffness at fast cadences. Prior simple dynamic walking models (e.g. McGeer) have demonstrated that walking gaits can be almost entirely passive, requiring energy input only to redirect the center of mass velocity during the step-to-step transition and provide small control inputs for stabilization. We hypothesized that similar passive motions might exist for the arms.

We tested these hypotheses using a simple dynamic model of human walking and in human subject experiments. We systematically searched for passive cyclic arm motions in simulation to test the hypothesis that arm swinging may have no fundamental actuation requirements. We also used the model to test the hypothesis that the normal phasing of arm and leg swinging reduce fluctuations in vertical angular momentum as compared to stationary arms or opposite-phase arm swinging, and that vertical ground reaction moments were directly related to changes in vertical angular momentum. We performed human subject experiments in which subjects walked at constant speed with four different arm motions: normal arm swinging, arms bound to the sides of the torso, arms voluntarily held at the sides of the torso, and opposite-phase arm swinging. We used inverse dynamics analysis of the joint torques required for these motions to test the hypothesis that normal arm swinging may require little muscular activity. We also measured vertical angular momentum of the whole body using both kinematic and kinetic analyses, testing the hypothesis that normal arm swinging reduced fluctuations in vertical angular momentum. We measured metabolic energy use during these gaits using indirect calorimetry to test the hypothesis that the normal arm motion minimized metabolic energy requirements. Finally, we used inverse dynamics and individual limbs analyses of the lower limbs to examine possible mechanisms that could explain how changes in vertical angular momentum translate into changes in metabolic energy use.

3.2 Methods

To better understand the arms' role in gait, we developed a simple dynamic walking model with free-swinging arms and performed controlled human subject experiments. We examined gaits with arms swinging as typically seen in humans (Normal), with the arms bound to the torso (Bound), and with arms swinging with opposite phasing from normal (Anti-Phase). We calculated model angular momentum and ground reaction moments in simulation and measured subjects' vertical angular momentum, ground reaction moments, joint torques, center of mass work (estimated using the individual limbs method), and metabolic energy use experimentally.

3.2.1 Model

We developed a simple walking model with free-swinging arms. The model (Figure 2.1a) was based on the simple three-dimensional dynamic walking model described in Kuo (1999), modified to include free-swinging arms. The model consisted of two cylindrical feet, two straight legs, a pelvis, and two arms, with a single degree of freedom at the line of ground contact (rolling), each ankle joint (inversion-eversion), each hip joint (flexion-extension), and each shoulder joint (flexion-extension). The arms were attached at the hip so as to minimize additional parameters and degrees of freedom and to keep closed-form equations of motion easily executable. Model proportions and mass properties were selected so as to be roughly anthropomorphic (e.g. Winter, 1990), with each arm comprising 4% of body weight, each leg comprising 16% of body weight, and the pelvis/torso comprising 60% of body weight.

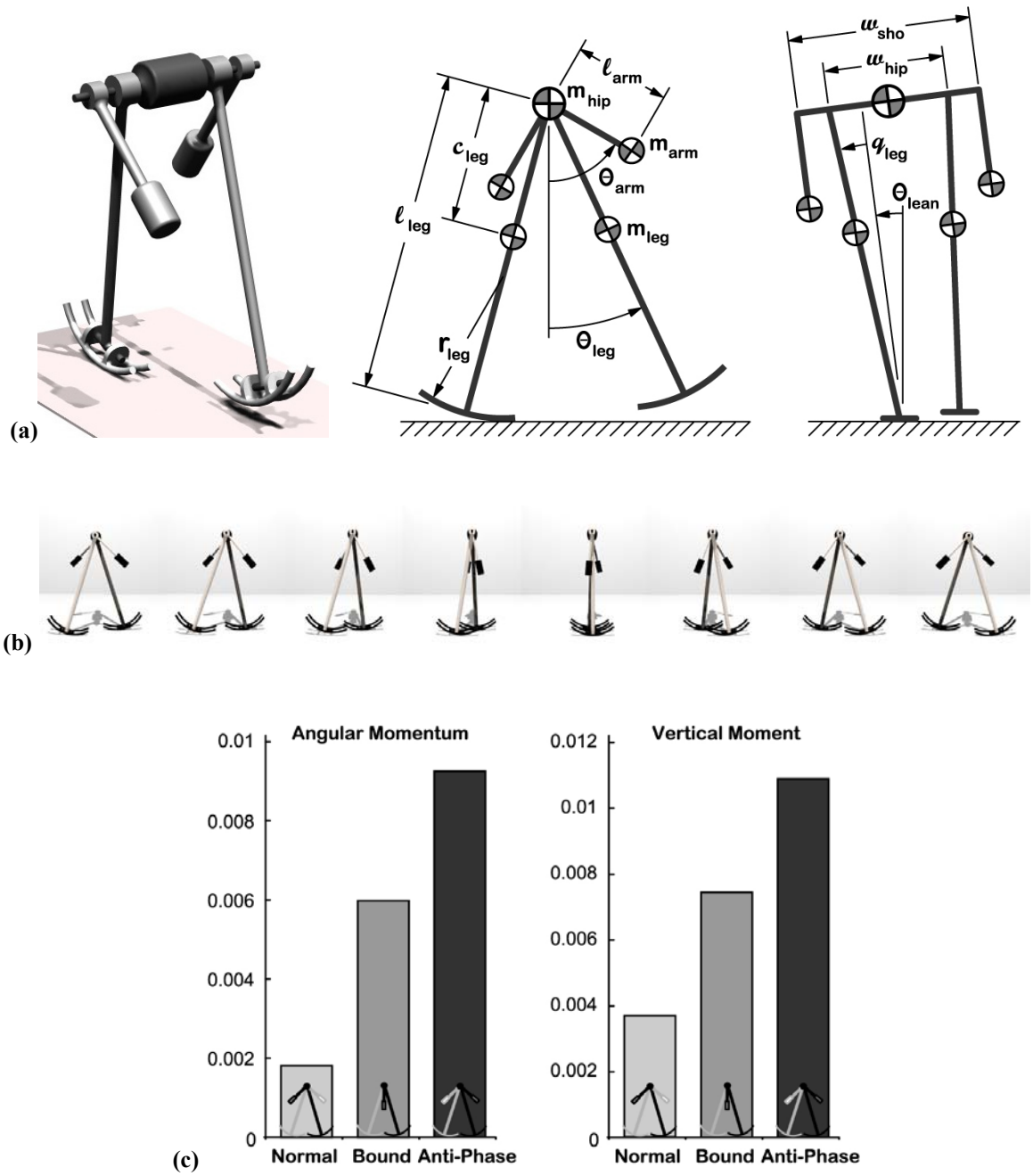

Figure 3.1: (a) Illustration of the simple dynamic walking model with arms. **(b)** Frame-by-frame rendering of the Normal gait, where the ipsilateral arm and leg have the same shading. **(c)** Simulation results for selected arm swinging modes.

We then used a gradient search method (e.g. Kuo, 1999) to find limit-cycle walking motions with different modes of arm swinging. We searched for specific modes of arm swinging using a technique wherein the modes were first enforced, then the enforcing constraints were gradually relaxed and finally removed altogether (using a differential

damped-spring and inertia in a manner similar to that described by Gomes 2005). We used this method to find several different modes of oscillation of the arms including a motion similar to that observed in normal human gait (Normal, Figure 3.1b), a motion with opposite phasing from normal (Anti-Phase), a mode in which the arms were constrained to remain vertical at the sides (Bound), a mode in which the arms and legs were 90 degrees out of phase (Mid-Phase), and a period-2 oscillation in which both arms swing in parallel (Parallel). All of the motions were found with the same model parameters and walked with the same slope (speed varied slightly between models). Additionally, we searched for a mode in which the arms remained nearly still and oscillated at twice the frequency of the legs (Double), which was found at slower gait speeds. Animations of these arm swinging modes, mode characteristics, and dynamic walking model parameters may be found in supplementary materials. The whole-body motions were all unstable, tending to fall over sideways, as found in the precursor model. Eigenvalues associated with arm motions indicated neutral stability, i.e. the arms did not tend to move toward or away from their fixed points when perturbed by small disturbances.

Arm swinging mode significantly affected vertical angular momentum and ground reaction moments in our simulations. As the phasing of arm swinging went from Normal to Bound to Anti-Phase, peak vertical angular momentum and peak vertical ground reaction moments increased (Figure 3.1c).

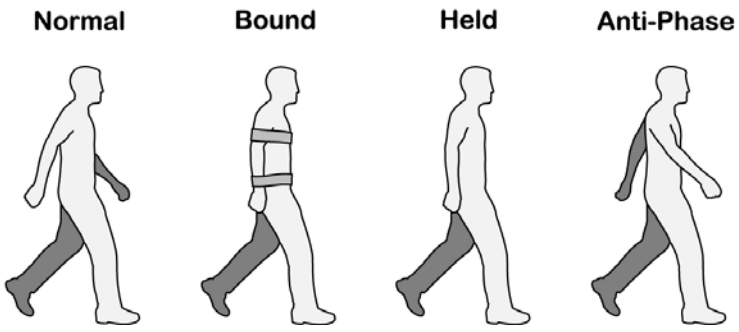

Figure 3.2: Illustration of the walking conditions tested experimentally.

3.2.2 Experimental Methods

We compared the mechanics and metabolics of able-bodied human subjects as they walked with their arms swinging in various ways. We measured oxygen consumption to quantify metabolic energy expenditure, and vertical angular momentum, vertical ground reaction moment, joint powers, and work performed on the COM to quantify gait mechanics. Comparisons were all made for a single walking speed, with metabolic data recorded during treadmill walking and mechanics measurements conducted during overground walking.

A total of 7 adult male and 3 adult female subjects (aged 23–47 yrs) participated in the study. All subjects provided informed consent. All subjects (N = 10, body mass 70.5 ± 11.3 kg, leg length 0.902 ± 0.074 m, mean ± SD) participated in energetics trials, and all male subjects (N = 7, body mass 75.0 ± 10.2 kg, leg length 0.931 ± 0.073 m) participated in the mechanics trials. All walking trials were conducted at a speed of 1.25 m/s.

Four walking conditions were applied: walking with arms swinging normally (Normal), bound to the sides with elastic straps (Bound), held at the sides voluntarily (Held), or swung in the opposite phasing from normal (Anti-Phase), depicted in Figure 3.2. During Normal walking trials, subjects were instructed to walk as naturally as possible. During Held walking trials, subjects were instructed to hold their arms loosely at their sides such that their wrists remained slightly posterior to the greater trochanter at the hip, an arm posture that was enforced during Bound trials through the use of two wide elastic sports bandages. This posture was chosen so as to minimize the interference of the hands with body motions and prevent the arms from obscuring motion tracking markers at the greater trochanter. During Anti-Phase conditions, subjects were instructed to swing their arms in phase with the ipsilateral leg and with swing amplitude approximately equal to normal. Subjects typically required an adaptation period of a few minutes to become comfortable with this condition, after which all subjects reported no difficulties.

For energetics trials, we measured the rate of oxygen consumption ($\dot{V}_{O2}$ in ml O_2/sec) and carbon dioxide production ($\dot{V}_{CO2}$ in ml CO_2/sec) using an open-circuit respirometry

system (Physio-Dyne Instrument, Quogue, NY). Each trial lasted at least seven minutes, including at least three minutes to allow subjects to reach steady state, followed by three minutes of data recording for average $\dot{V}_{O2}$ and $\dot{V}_{CO2}$ during steady state. Metabolic rates $\dot{E}$ (in Watts) were estimated with the formula (modified from Brockway 1987)

$$\dot{E} = 16.48\dot{V}_{O2} + 4.48\dot{V}_{CO2}.$$

We also measured each subject's metabolic rate for quiet standing in a separate trial of the same duration and subtracted it from the rate for walking to yield a net metabolic rate. All conditions, including quiet standing, were conducted in random order. Respiratory exchange ratios were less than unity for all subjects and conditions, indicating that energy was supplied primarily by oxidative metabolism in all test conditions. No metabolic data were collected during overground walking. Energetic trials were always collected immediately preceding mechanics trials so that subjects would have maximum training before mechanics data were collected.

For mechanics trials, we measured kinematics and ground reaction forces as subjects walked over ground-embedded force plates. Kinematic data were recorded with an 8-camera motion capture system (Motion Analysis Corporation, Santa Rosa, CA) at 120 Hz. Force data were recorded at 1200 Hz with two force plates (AMTI, Watertown, MA). Speed was measured with two photogates, positioned 2.5m apart and trials were discarded if actual walking speed was not within 5% of the desired speed of 1.25 m/s. We recorded at least 10 successful trials per condition for each subject. For inverse dynamics and angular momentum analyses, a set of motion capture markers were placed bilaterally on the upper and lower extremities. Marker locations included the fifth metatarsal of the foot, the heel at the calcaneus, the medial and lateral malleolli, the medial and lateral epicondyles of the knee, the greater trochanter at the hip, the anterior superior iliac spine, the sacrum, the acromion of the shoulder, the lateral epicondyle of the elbow, the posterior aspect of the wrist (i.e. proximal to the back of the hand), and a three-marker cluster on each thigh and shank.

We measured vertical ground reaction moments and calculated vertical angular momentum for all conditions. Vertical ground reaction moment was defined as the

moment between the foot and the ground about a vertical axis, as measured by force plates (e.g. Li, 2001). During all times of foot contact, including double support, each foot had a non-zero vertical ground reaction moment. Vertical angular momentum was calculated from segment kinematics and defined with respect to the body center of mass (e.g. Elftman, 1939) and was dominated by segment center of mass terms for the upper extremities. Anthropometric data were estimated from the equations of Winter (1979). Velocities and torques were low-pass filtered at 25 Hz as part of this analysis. Whole body angular momentum based on segmental analysis was verified using kinetics-based angular momentum measures, obtained by integrating moments about the body center of mass due to ground reaction forces and moments.

We also calculated joint powers and work performed on the COM for all conditions. To obtain joint powers, standard inverse dynamics analyses were performed in three dimensions (e.g. Winter, 1990; Siegler, 1997). For the lower limbs, distal link endpoint forces were measured using force plates, while for the upper limbs distal link endpoint forces were known to be zero. Anthropometric data were estimated from the equations of Winter (1979) and velocities and torques were low-pass filtered at 25 Hz. Joint torques were defined with respect to the primary axis of interest, which typically lay near the perpendicular to the sagittal plane. The glenohumeral shoulder joint axis was defined to lie along a straight line across the shoulders, while the humeroulnar elbow joint was defined as an axis passing through the elbow joint and lying perpendicular to the plane defined by the upper and lower arm segments. We used ground reaction forces to estimate the rate of work performed on the COM by each leg using the individual limbs method (Donelan, 2002), defined as the vector dot product of each leg's ground reaction force against the COM velocity.

Each trial was normalized to percent gait cycle and averaged for each subject and condition. All torque, power, and work quantities were analyzed in dimensionless form, to help account for variations in subject size. Torque and work quantities were normalized by each subject's body weight and leg length (MgL, where M is body mass, g is gravitational acceleration, and L is leg length), with the additional factor of $g^{0.5}L^{-0.5}$

(the leg's pendulum frequency) for power quantities and its inverse, $L^{0.5}g^{-0.5}$ (the leg's pendulum period) for momentum quantities. Averages, standard deviations, and statistics were computed in dimensionless quantities. We report variables in the familiar dimensional units such as W kg^{-1}, converted using average normalization factors. The average normalization factors used were: 685 kg m^2 s^{-2} for torque and mechanical work, $2.22 \cdot 10^3$ kg m^2 s^{-3} for mechanical power, $2.06 \cdot 10^3$ kg m^2 s^{-3} for metabolic rate, and $2.11 \cdot 10^3$ kg m^2 s^{-1} for angular momentum.

We statistically compared outcome variables that captured the primary energetics and mechanics results. We compared net metabolic rate, peak vertical angular momentum, peak vertical ground reaction moment, and peak upper limb joint torques. Net metabolic rate was calculated as the average metabolic rate during steady state with the average metabolic rate for quiet standing removed. Peak vertical angular momentum, peak vertical ground reaction moments, and peak upper limb joint torques were each calculated as the maximum absolute value during a single stride. Statistical comparisons were made with repeated measures ANOVA for each variable, with a significance level of 0.05. Where differences were significant, post hoc comparisons were performed using paired t-tests.

3.3 Results

We found that Bound, Held, and Anti-Phase modes of arm swinging significantly increased fluctuations in vertical angular momentum and ground reaction moments as compared to Normal, without reductions in upper limb joint torques or power, which resulted in a significant net increase in metabolic rate in human subjects. Normal and Anti-Phase modes of arm swinging required only functionally low torques in human subjects, while the Held condition required significantly larger peak shoulder joint torque. Metabolic rate was also significantly greater in the Held condition than the Bound condition.

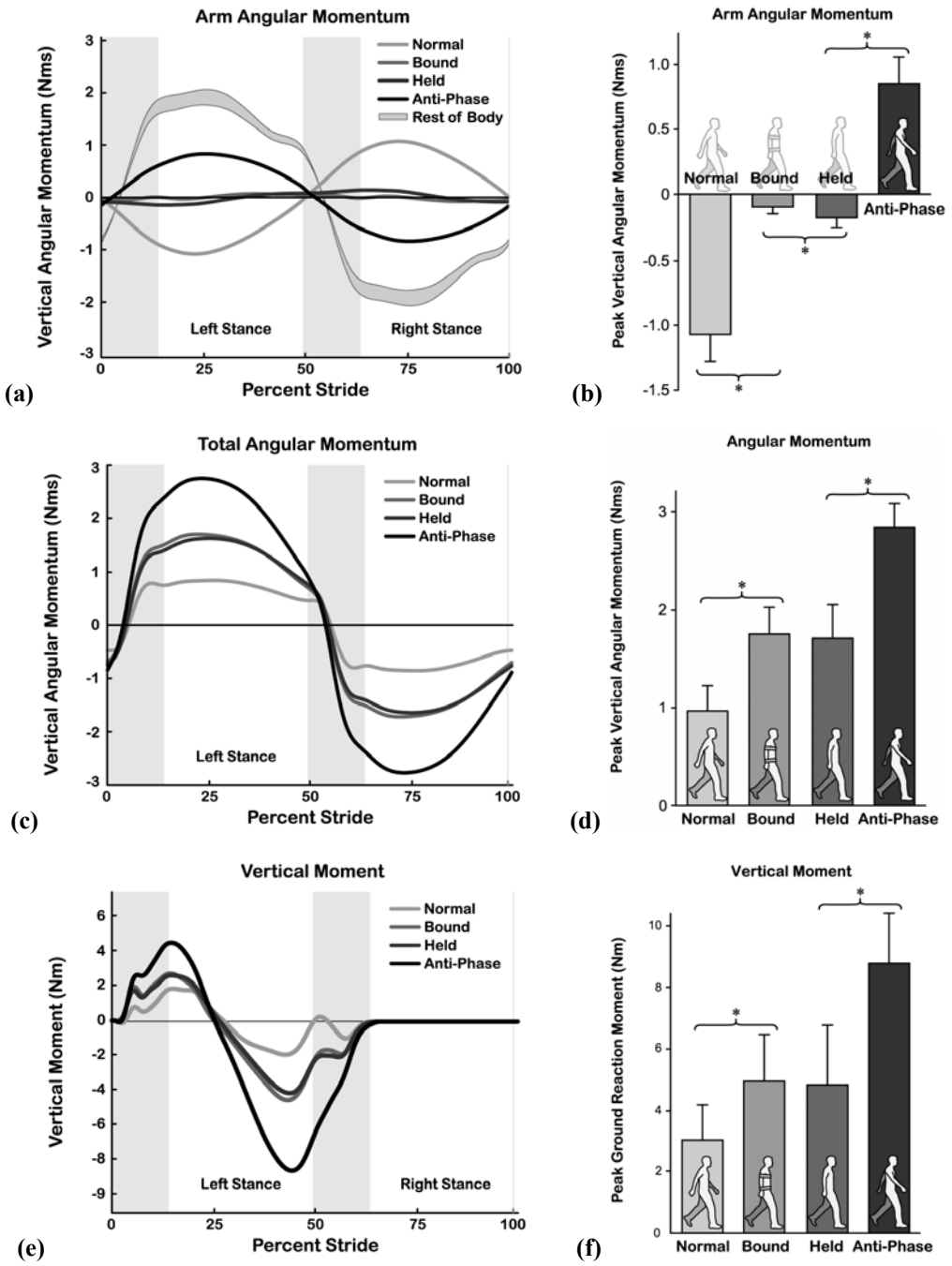

Figure 3.3: Arm component of vertical angular momentum (**(a)** & **(b)**), total body angular momentum (**(c)** & **(d)**), and vertical moment at the stance foot (**(e)** & **(f)**). Double support is denoted by a shaded region in plots. In **(a),** the grey band represents the span across conditions of the mean trajectories of the sums of the other components of vertical angular momentum, which were dominated by the leg component. Bar graphs compare peak angular momentum during the stance phase of the left foot and peak absolute value of vertical moment. Error bars show one standard deviation, and asterisks indicate statistical significance with a significance level of $p = 0.05$. Arm angular momentum changed as expected across conditions while angular momentum of the rest of the body remained roughly constant, resulting in significant changes in whole body angular momentum as a function of arm condition. Increased fluctuations in vertical angular momentum corresponded to significant increases in peak vertical moments.

Whole-body angular momentum about a vertical axis was strongly affected by arm swinging mode. In the Normal condition the angular momentum of the arms was of opposite phase to that of the legs, while in both Bound and Held conditions the arms had negligible angular momentum and in the Anti-Phase condition the arms' angular momentum was in phase with that of the legs (Figures 3.3a and 3.3b). However, the angular momentum of the rest of the body, dominated by leg angular momentum, remained nearly constant across conditions (Figure 3.3a). The net effect was that total body angular momentum significantly increased in Bound and Held conditions (an increase of 0.010 Nms kg^{-1} or 80% over Normal, p = 0.0002), and further increased in the Anti-Phase condition (an increase of 0.015 Nms kg^{-1} or 118% over Held, p = 2e-5), as shown in Figures 3.3c and 3.3d. Peak vertical ground reaction moments similarly increased from

Normal to Bound (0.025 Nm kg^{-1} or 65% greater than Normal, p = 0.0003) and Held to Anti-Phase (0.053 Nm kg^{-1} or 134% greater than Held, p = 0.001), as shown in Figures 3.3e and 3.3f.

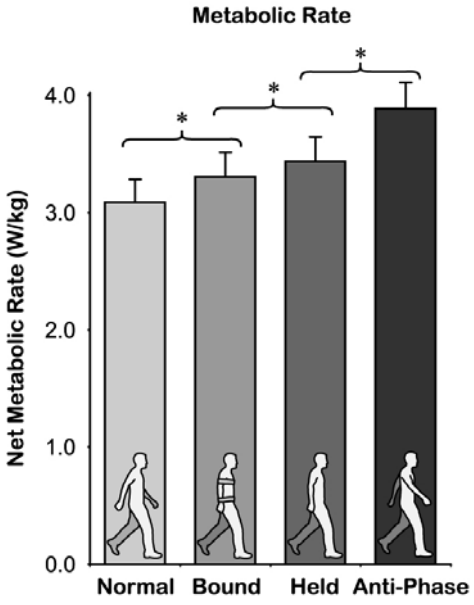

Figure 3.4: Net metabolic rate increased across conditions. Error bars represent standard deviations and asterisks indicate a statistically significant difference with a significance level of p = 0.05.

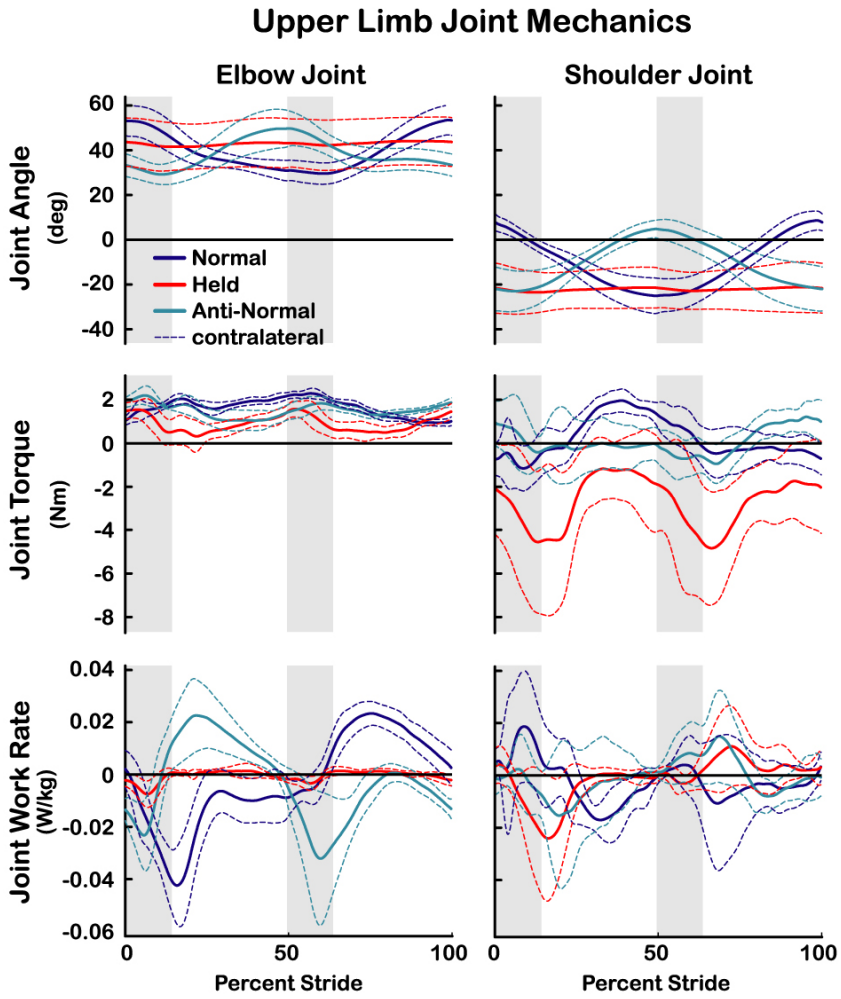

Figure 3.5: Upper limb joint angles, torques, and powers for the Normal, Held, and Anti-Phase conditions over one stride. Gray regions denote double support. Scale smaller than for lower limb trajectories (Figure 3.7) by a factor of 20 in torques and a factor of 50 in powers. Shoulder and elbow angles during Normal and Anti-Phase conditions were of similar magnitude and roughly 180° out of phase, while motions were small during Held trials. Shoulder torques had similar magnitude but opposite phasing in Normal and Anti-Phase conditions, while peak torques significantly increased in the Held condition. Shoulder powers had similarly small magnitudes across conditions. Elbow torques were always in flexion and did not change across conditions, consistent with the observations by Murray (1967) and Hinrichs (1990) that during gait the elbow joint may be mostly passive with spring-like ligaments preventing full elbow extension. Elbow powers in Normal and Anti-Phase conditions were spring-like and of equal magnitude and opposite phase, while little elbow joint power was observed in the Held condition.

Metabolic energy use also significantly increased over Normal in Bound, Held, and Anti-Phase conditions. Metabolic rate in the Normal condition was 3.09 ± 0.12 W kg^{-1}, in the Bound condition was 3.31 ± 0.20 W kg^{-1} (7% greater than Normal), in the Held condition was 3.44 ± 0.21 W kg^{-1} (11% greater than Normal), and in the Anti-Phase condition was 3.89 ± 0.21 W kg^{-1} (26% greater than Normal, Figure 3.4). Increases between each

condition were statistically significant, with $p = 0.0007$ for comparisons of Bound to Normal, $p = 0.004$ for comparisons of Held to Bound, and $p = 0.00001$ for comparisons of Anti-Phase to Held.

Upper limb joint torques remained functionally low across conditions, though peak shoulder torque during the Held condition increased significantly. Peak shoulder joint torques were low in Normal and Anti-Phase conditions, measuring only 25% of the torque required to hold the arm in a motionless horizontal posture (Figures 3.5 and 3.6). In the Held condition, peak shoulder torque increased by 0.035 Nm kg^{-1} (139%, $p = 0.01$). There were no significant differences in peak shoulder torques between Normal and Anti-Phase conditions ($p = 0.2$). No significant differences were observed for peak elbow torques, which were consistently approximately 0.03 Nm kg^{-1}. Joint torques were not calculated for the Bound condition because the elastic restraints were largely responsible for upper limb segment accelerations.

There were no significant changes in the vertical excursion of the center of mass as a function of arm condition. Vertical excursions were 0.050 ± 0.010 m for Normal, 0.054 ± 0.008 m for Bound, 0.052 ± 0.008 m for Held, and 0.054 ± 0.009 m for Anti-Phase. In simulation, the dimensionless vertical excursions were 0.046 for the Normal mode, 0.053 for the Bound mode, and 0.045 for the Anti-Phase mode, with differences primarily due to changes in step length.

Lower limb joint angles, joint torques, and joint powers were not significantly different across conditions (Figure 3.7). Positive work performed on the center of mass as estimated using the individual limbs method was 0.32 ± 0.045 J/kg for Normal, 0.36 ± 0.030 J/kg for Bound, 0.35 ± 0.029 for Held, and 0.36 ± 0.038 for Anti-Phase These were statistically significant increases over Normal in each of the other conditions, Bound ($p = 0.004$), Held ($p = 0.04$), and Anti-Phase ($p = 0.001$), while none of the other differences between conditions were statistically significant ($p > 0.3$).

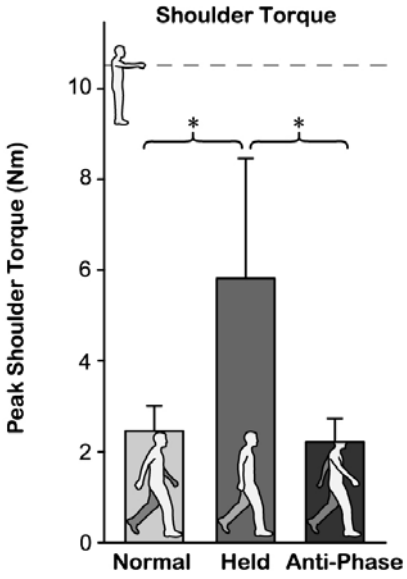

Figure 3.6: Peak shoulder joint torques were always low, but increased in the Held condition. Error bars represent standard deviations and asterisks indicate a statistically significant difference with a significance level of p = 0.05. The shoulder torque required to hold the arm in a horizontal posture without motion is indicated by a gray dashed line.

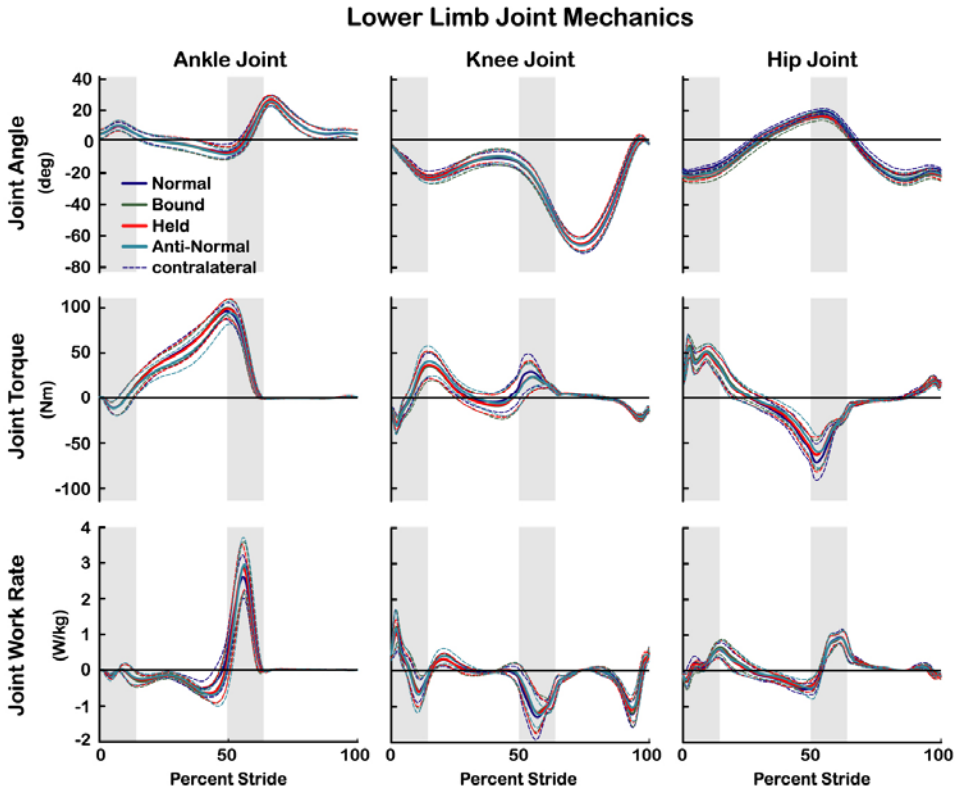

Figure 3.7: Lower limb joint angles, torques, and powers for each of the conditions tested. No statistically significant differences due to arm swinging condition were observed within these measurements.

3.4 Discussion

We performed simulations and human subject experiments aimed at determining the function of arm swinging and the mechanisms controlling it in human gait. We proposed that normal arm swinging is easy to perform and offsets the motions of the legs so as to reduce changes in angular momentum of the whole body about a vertical axis, keeping metabolic energy use low. We found that holding the arms at one's sides, binding the arms in a similar position, or swinging the arms with opposite phasing from normal all resulted in increased angular momentum, increased peak ground reaction moments, and increased metabolic cost. We proposed that arm motions might primarily be the result of passive dynamics, rather than muscular activity. We found fully passive gaits in simulation exhibiting an array of modes of arm swinging, including a mode similar to that typical of human gait. We also calculated upper limb joint torques and found them to be functionally small during normal gait. These findings are consistent with the hypotheses that arm swinging takes little effort to achieve, but significantly contributes to economy of gait.

Increases in the change in vertical angular momentum over the course of a stride corresponded with increases in metabolic energy use as expected, but our experimental results give limited insight as to the precise muscular mechanisms behind this interaction. During single support, vertical ground reaction moments were the primary cause of changes in vertical angular momentum of the body. Presumably, these internal/external rotation torques must be supported by the musculature of the leg, e.g. at the hip joint, incurring a cost due to the production of force. Since the hip typically also rotates during stance, increased forces may also lead to increased muscular work. However, we were not able to usefully quantify such changes in this experiment due to limitations in the power of our inverse dynamics analysis. Further, a significant portion of the change in whole body angular momentum occurred during double-support. As vertical angular momentum fluctuations increased, subjects increased their double-support rotational impulse in a variety of ways, including taking wider steps, taking longer steps, and increasing horizontal ground reaction forces. Individual subjects exhibited increased center of mass work during the step-to-step transition, increased peak joint torques, and

increased joint work. However, no consistent strategy emerged across subjects. We are left with the same understanding with which we started: greater reaction force and moment requirements generally imply greater muscular force and power requirements, both of which imply increases in metabolic energy use. One way or another, changing the body's vertical angular momentum seems likely to require metabolic energy, and indeed did in this experiment.

Our simulation and experimental results both strongly suggest that swinging the arms can require little effort. In simulation, both Normal and Anti-Phase gaits were fully passive, requiring no muscle activation to generate the motion. However, they were only neutrally stable, meaning that some amount of control would be required to maintain the motion in the face of disturbances. This suggests that the primary role of upper limb muscles at this gait speed may be to initiate arm motions and recover them from perturbations, but not to provide substantial forcing. Our experimental results support this notion. Peak shoulder torques were consistently less than 30% of the torque required to hold the arm horizontally in both Normal and Anti-Phase conditions. Positive shoulder joint work was a mere 0.04 J kg^{-1} per stride, less than 0.5% of the total joint work. As Murray (1967) and Jackson (1983) suggested, a significant portion of the upper limb joint torques and powers may be due to passive tissues, implying even less of a role for muscle in generating arm swinging. In fact, at this speed, it required more muscular effort to prevent the arms from moving in the Held condition than to allow them to swing normally. A comparison of the Held and Bound conditions suggests that holding the arms in place requires a small but measurable amount of metabolic energy, presumably related to muscular torque production at the shoulder. Since this increase in metabolic cost was rather small (about 4%) and peak shoulder torques were greatest in the Held condition, we might speculate that shoulder torque production during normal gait likely constitutes on the order of 2% of metabolic energy use. The result that shoulder torques were roughly equal in the Normal and Anti-Phase conditions further underlines the fact that the energetic impact of arm swinging has little to do with the cost associated with driving the arms and much to do with the effects of the arms' motions on the rest of the body.

Interestingly, subjects did not choose to minimize whole body angular momentum. In the Normal condition, subjects could have moved their arms in such a way that the angular momentum of the arms completely balanced the angular momentum of the legs at all times. Likewise, subjects could have used their torsos to offset the angular momentum of the legs when their arms were prevented from playing this role. However, subjects chose to do neither. The reasons for this choice probably lie with the trade-off between the ease of the motion and its benefit. Perhaps swinging the arms naturally is easy enough to warrant its use for obtaining a beneficial reduction of angular momentum, while strictly controlling arm motions or moving the torso in an exaggerated manner is not.

The model used in this study has some obvious limitations due to its simplicity, but still seems to be a useful tool. Arms were represented in a simplified form, with no elbows and an attachment point at the hip. It is possible that an intervening torso or a two-link arm could change some of the arm-swing dynamics. The model does not provide a direct means for estimating increases in metabolic energy use in human subjects, but rather predicts trends in angular momentum and ground reaction moment. Metabolic consequences of these changes must be inferred from a separate understanding of physiology. However, simple models can be powerful. Indeed, simulated results show a strikingly similar trend in angular momentum and ground reaction moment as a result of arm swinging condition.

We seem to have arrived at useful results despite certain limitations to our experimental procedure. During both Held and Bound conditions, subjects' hands were held in a position slightly posterior to the position where they would hang naturally. This posture was chosen to prevent the hands from interfering with leg motions and to prevent markers from being obscured, but may have had the unintended effect of increasing metabolic cost slightly in the Held condition. Fortunately, the Bound condition is available for comparison and the similarities suggest that this effect was likely minor. If anything, it would lead us to over-estimate the effect of shoulder torque production on metabolic energy use, which we already consider to be a minor contributor to the total energy cost

of gait. Another limitation is that metabolics trials were collected on a treadmill, while mechanics were collected overground, which may cause differences in gait. Without the use of an instrumented treadmill (e.g. Collins, 2007) we were unfortunately unable to avoid these confounding effects while performing the long steady-state metabolic collections.

Speed has been shown to have a strong effect on arm swinging during gait (e.g. Murray 1967), and we did not directly study its effects in our human subject experiments. However, our results may lend insight into the impact of speed on the role of arm swinging during gait. With increasing gait speed, the arms may swing higher and faster to partially cancel the effects of longer, quicker steps by the legs. In simulation, we found the Normal mode of arm swinging to persist passively over a wide range of gait speeds, but at high speeds or with fast leg swing frequencies actuation was needed to maintain sufficiently rapid arm motions. We found this could be provided in the form of a spring. So, the importance of arm swinging to maintaining economy and the role of the muscles in generating arm swinging will likely both increase with speed. By contrast, at very low speeds, the angular momentum of the legs fluctuates little, and so requires little or no counter-motion from the arms. In simulation, we found qualitatively different modes of oscillation at very low speeds, including a mode resembling "double-swing" as observed by others (Webb, 1994; Wagenaar, 2000). However, there would appear to be little motivation for choosing or maintaining any particular low-amplitude arm motion at slow speeds, which may explain why there is a great deal of variation in arm motions for naïve subjects at these speeds (Donker, 2001).

It has been suggested that arm swinging may reduce metabolic energy use by reducing the vertical excursion of the body center of mass (e.g. Murray, 1967). The phasing of normal arm swinging is such that the arms are at their highest point at the same time that the rest of the body is lowest due to the pendular arcs of the legs, which occurs at double support. However, the same is true of the Anti-Phase condition tested here. Our results would indicate that any possible energetic effects of using the arms to modulate vertical

excursion of the center of mass are vastly outweighed by the energetic effects of allowing arm swinging to reduce vertical angular momentum.

The results of our simulations and experiments support the proposition that arm motions during gait may be primarily the result of natural dynamical tendencies, with muscles used mostly to initiate motion and correct errors as they arise. Although arm swinging may be easy to achieve, its effect on energy use during gait is significant. Arm swinging can reduce fluctuations in vertical angular momentum and ground reaction moments without additional muscular effort, thus reducing energy expenditure. Rather than a facultative relic of the locomotion needs of our quadrupedal ancestors, arm swinging appears to be an integral part of economical human gait.

Acknowledgments

This research was supported by an NIH grant. Arthur Kuo and Peter Adamczyk assisted with experimental design and interpretation of results. Matthew Vanderpool assisted in data collection.

Chapter 4

Age-related changes in balance-related step kinematics during overground walking

Abstract

We compared step kinematics from younger (N = 10, age <40 yrs) and older adults (N = 12, age 60+) over hundreds of steps of overground walking. Previous studies have reported age-related changes in gait parameters such as mean step width and length and their respective variabilities, but with conflicting results. Robust age-related differences could potentially be identified using model-driven hypotheses and measurements of many steps. Computational models of walking dynamics suggest that walking is passively stable in the fore-aft direction, but unstable laterally. Stability could be provided through active control of lateral foot placement. Imperfect control, subject to age-related changes in sensory and motor precision, would be expected to result in changes in step width variability, more so than other parameters that maybe less directly related to balance control. Walking with eyes closed would also be expected to affect step width variability more than other parameters. We used a mobile measurement system to accurately record many contiguous steps. Step width variability (defined as standard deviation of steps) was 69% greater than length variability for all subjects and conditions (0.0310 m vs. 0.0179 m, $p = 1 \cdot 10^{-16}$). Total step width variability was 20% greater in older vs. younger adults with eyes open (0.0292 m vs. 0.0242 m, p = 0.002). Closing the eyes caused width variability to increase by 34% ($p = 3 \cdot 10^{-9}$), twice the change in length variability (p = 0.005). The widths vs. length variability differences were accentuated by filtering out slow fluctuations in walking speed that occur over 20 steps or more. Older adults walked with 18% greater mean step width, but with marginal statistical significance (p = 0.02). Our results agree with other studies performed with treadmill walking (Owings and Grabiner, 2004a), indicating that the accuracy and quantity of steps measured on a

treadmill can predict the trends observed in overground step kinematics.

4.1 Introduction

Aging is accompanied by a variety of changes in gait, some with major functional consequences. Older persons have greater unsteadiness and less mobility, and experience a vastly higher rate of falls than young adults (Alexander et. al., 1992; Center for Disease Control and Prevention, 2005). Some gait changes may be directly related to physiological factors affecting balance, for example increased sensory thresholds for proprioception, reduced visual acuity, and poorer motor function (Horak et. al., 1989; Manchester, 1989). Other changes may have more indirect relation to balance and depend on psychological or other age-related factors, such as fear of falling. For example, preference for a wider base of support may reflect compensations or conservative strategies selected as a consequence of poorer balance (Gabell and Nayak, 1984; Brach et. al., 2005). Slower preferred walking speeds could be a complex function of cardiovascular capacity, muscle strength, and cognitive function (Inzitari et. al., 2006). Because these various factors are often intertwined, it may be difficult to separate one from the other. However, some changes to gait may be more mechanistic and more directly related to balance than others. It is helpful to identify balance-related gait measures, because they might be detected and then addressed differently than those that are less mechanistic. Balance-related gait measures might also be especially sensitive to gradual changes that occur with age, making them well-suited to assessing the gait of healthy older adults, as opposed to only those who are frail or have pathologies.

Many age-related changes occur in step kinematics. For example, older adults tend to self-select a slower mean walking speed than younger adults (Himann et. al., 1988). Even at the same speed, older adults tend to select a slightly shorter step length and a higher step frequency. There are conflicting reports regarding mean step width, but some show significantly wider steps with age (Heitmann et. al., 1989; Maki, 1997; Moe-Nilssen and Helbostad, 2005). We suspect that these various changes often reflect conscious or unconscious preferences, because a healthy older adult is often capable of walking faster or with narrower steps than usually preferred. The particular preference is

certainly of scientific interest, but it also appears to be only indirectly related to physiological balance capabilities (Chamberlin et. al., 2005). Other changes occur in variability of steps rather than averages. For example, age-related increases have been reported (Stolze et. al., 2000; Owings and Grabiner, 2004a) in the variability of step length, width, and period, although again with some conflicting results (Gabell and Nayak, 1984; Moe-Nilssem and Helbostad, 2005). Step variabilities appear superficially to have more direct relation to balance during walking, because they may reflect step-by-step adjustments made to maintain balance. However, the conflicting results make it unclear which variables are most sensitive, and whether they are indeed related to balance.

The identification of balance-related gait variables can benefit from a modeling approach. We previously devised a simple computational model of walking dynamics. This model suggests that the motion of the legs within the sagittal plane is passively stable, requiring no active control of foot placement (Kuo, 1999).

However, the same model indicates that lateral motion is unstable, requiring active feedback control such as through lateral foot placement. Given imperfect sensors and muscles, active foot placement control would be expected to exhibit variability, especially in the lateral direction. Reduction of sensory input, such as through removal of vision, should also adversely affect lateral balance more so than fore-aft, and result in increased lateral foot placement variability. Subsequent measurements of young adult subjects walking overground support these hypotheses (Bauby and Kuo, 2000). Defining variability as the standard deviation of foot placements, our measurements showed 79% greater variability laterally than fore-aft. When subjects walked with their eyes closed, lateral variability increased by 53%, far more than the 21% increase in fore-aft variability. Lateral foot placement variability therefore appears to be a good indicator of balance during walking. The same modeling approach can also be applied to aging, where sensory thresholds increase, motor precision decreases, and overall motor performance is reduced. The imprecision introduced by these factors would be expected to affect lateral foot placement control more so than the passively stable fore-aft motion.

The same model therefore predicts that lateral foot placement variability will exceed fore-aft variability to a greater degree in older adults compared to younger ones (Dean et. al., 2007).

The measurement of foot placement variability, however, presents practical difficulties. Variability is best measured over many steps, but a typical laboratory-mounted motion capture system can only record a few contiguous steps at a time. Instrumented walkways can record several steps, but their resolution, of approximately ± 1cm (e.g., GaitRite, CIR Systems Inc., Havertown, PA), is poor compared to a typical foot placement variability of only about 3cm (Bauby and Kuo, 2000). Treadmills enable recordings of many steps with an accurate motion capture system, but humans may walk slightly differently on treadmills than overground, due to the different visual flow or the artificial constraint on speed. It is therefore preferable to measure step variability during natural, overground gait for many steps. This, however, presents a separate difficulty. Our subjective observations indicate that pedestrians do not maintain a very steady speed in overground gait, especially compared to the controlled speed of a treadmill. Because step length varies consistently with speed, naturally-occurring speed fluctuations could contribute to foot placement variability while having little to do with balance control. It may therefore be helpful to filter out the effect of speed fluctuations from measurements of overground gait over long distances, in order to highlight other effects that are hypothetically most related to balance.

The purpose of the present study was to examine balance-related gait differences between older and younger adults. If aging leads to decreased precision of sensors and motor output, we would expect greater lateral foot placement variability with age. As with our previous results with younger adults, we would also expect removal of vision to disproportionately affect lateral foot placement. We also hypothesize that total foot placement variability may include some variability that is associated primarily with slow fluctuations in speed, as opposed to step-by-step adjustments made for balance. We performed measurements of overground gait in younger and older adult human subjects to test these hypotheses.

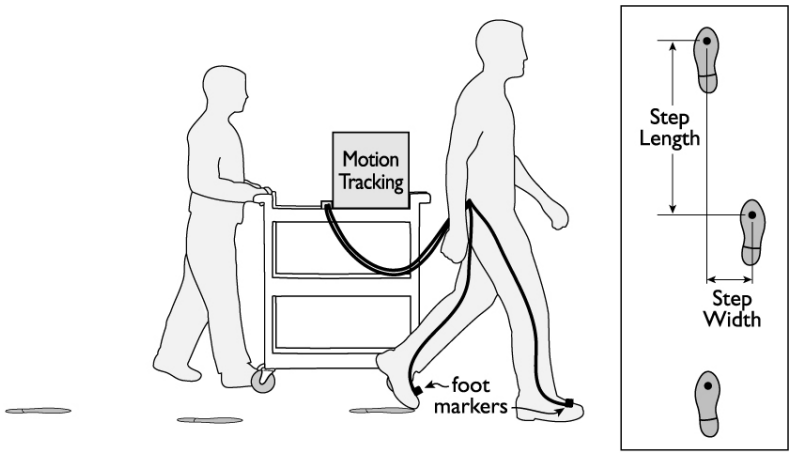

Figure 4.1: Method of data collection (left) and definition of step length and step width (box at right). Subjects wore a magnetic marker on each foot, placed above the third metatarsal (depicted as squares), as well as a marker near the sacrum (not pictured). A magnetics-based motion tracking system (MotionStar, Ascension Technology) was wheeled alongside subjects as they walked overground. Steps were described by step length (along the direction of travel) and step width (perpendicular to the direction of travel).

4.2 Methods

We measured gait of Young and Elderly adult subjects as they walked overground over hundreds of steps, with eyes either open or closed. We recorded mean gait parameters such as walking speed, step length, and step width, as well as step variabilities. Total foot placement with each step was also decomposed into components that vary quickly or slowly with time, to separate possible balance-related variations in foot placement from those associated with slow fluctuations in speed. We compared differences in these parameters as a function of age and of eyes open/closed condition. Finally, we quantified the contributions of the two types of variations to total step variability and their association with walking speed.

4.2.1 Experimental Methods

We conducted measurements in two subject age groups, labeled Young and Elderly (figure 4.1). We defined subjects 20-40 yrs as Young, and 60+ yrs as Elderly. 14 Young (10 male, 4 female, 21-37 yrs, leg length 0.95 ± 0.06 m) and 12 Elderly (9 male, 3 female, 64-82 yrs, leg length 0.94 ± 0.06 m) healthy adults walked overground at self-selected speeds (1.44 ± 0.15 ms^{-1}). During the recruitment process, subjects were screened against any neurological, orthopaedic, or other conditions that might affect their

gait. Recruited subjects gave informed consent to participate in this study. The experimental conditions tested were eyes-open, wherein subjects walked normally and in a straight line marked by traffic cones, and eyes-closed, wherein subjects walked with their eyes closed and followed the sound of a portable radio carried about three meters ahead of them. Subjects walked in 4 to 6 independent trials per condition for at least 100 consecutive steps each. Thus, we were able to collect data on at least 400 consecutive steps for each subject in each condition, a sufficient quantity to calculate statistics reliably (Owings and Grabiner, 2003).

We measured step kinematics using a magnetics-based tracking system (MotionStar, Ascension Technology, Milton, VT), mounted on a portable cart that was rolled alongside subjects as they walked. Markers were placed on the forefoot above the third metatarsal and at the sacrum. Marker positions were collected at 100 Hz, and then filtered using a 3rd order butterworth low-pass digital filter with a cut-off frequency of 6 Hz. Step parameters were computed from marker positions with an algorithm developed previously (details in Bauby and Kuo, 2000). We assumed that subjects' feet did not move during stance, using successive steps to track the motion of the ground relative to the mobile tracking system. Subtracting out this motion yielded absolute marker trajectories. We then separated marker motion into fore-aft and lateral components, based on an instantaneous walking direction computed from a moving average of the heading of the sacral marker over two strides. Subjects changed direction very little; the largest average variation observed was $\pm 0.8^{\circ}$ occurring for Elderly subjects walking with eyes closed. Instantaneous walking speed was computed from each step length divided by the corresponding step period.

4.2.2 Analysis

We decomposed step-by-step foot placements into long-and short-term components (figure 4.2). We observed long-term or slowly-varying trends in step-by-step gait parameters, over the course of many steps, similar to other reports in the literature (Hausdorff et. al., 1995). In order to consider these long-term fluctuations independently from short-term deviations that may be more relevant to balance, we separated the two.

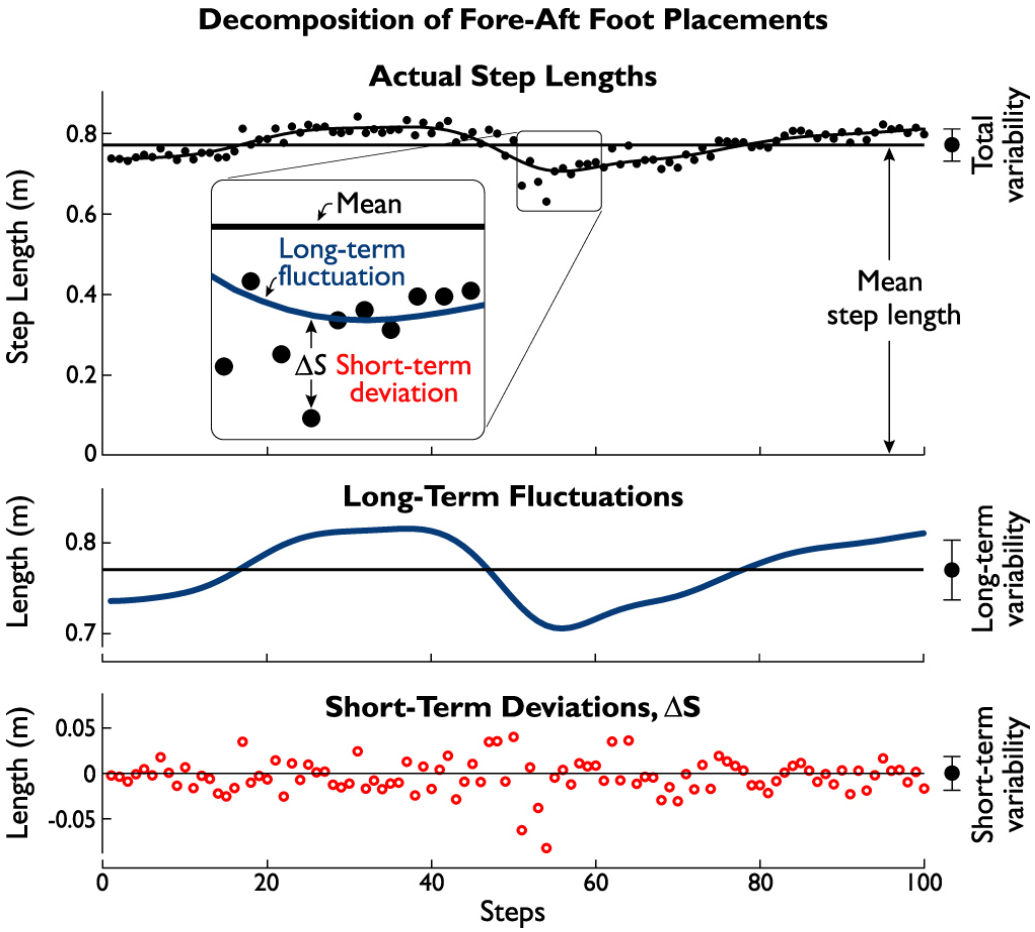

Figure 4.2: Decomposition of fore-aft foot placements, demonstrated with one sample trial. We decomposed step-by-step foot placements into two components: long-term fluctuations and short-term deviations. Total step lengths (top, black dots) were used to obtain mean step length, as well as total step variability, defined as the standard deviation of total step length. Long-term fluctuations (middle, blue line) were obtained from total step lengths using a low-pass filter with a cut-off frequency of 0.05 steps^{-1}. Long-term variability was defined as the standard deviation of long-term fluctuations. Short-term deviations (bottom, red circles) were measured with respect to long-term fluctuations (see inset). Short-term variability was defined as the standard deviation of the short-term deviations. This example plot shows a Young subject walking with slowly varying step length (and speed). Short-term variability can include active adjustments to foot placement made for maintaining balance.

Long-term fluctuations in gait parameters were calculated by passing total foot placements through a low-pass digital filter with a cut-off frequency of 0.05 steps^{-1} (inverse of 20 steps). We determined the cut-off frequency by testing a range of values and selecting one for which gait parameters showed low sensitivity. Cut-off frequencies based on 15–25 steps yielded identical trends in short-and long-term variability. This is consistent with the observation by Dingwell et. al. (2001) that the majority of the deviation of trajectories initially near each other in joint space occurs over 10 strides or

less. Left-to-right and right-to-left steps were considered separately to remove the effects of gait asymmetry and marker placement. We subtracted long-term fluctuations from total foot placements to find short-term deviations.

We then calculated the mean and long-term variability of gait parameters and the short-term variability of foot placements (Figure 4.2). Long-term gait parameter variability was calculated as the standard deviation of long-term step fluctuations over all of the trials for each subject and condition. Short-term foot placement variability was calculated as the standard deviation of the short-term foot placement deviations over all of the trials for each subject and condition. The total step variance (square of standard deviation) is equal to the sum of the short-and long-term variances.

Displacement measures were normalized by each subject's leg length, L, measured from the greater trochanter to the ground at the heel. Differences in leg length between populations were insignificant in this study (1.7% shorter in Elderly group, $p = 0.5$). Speed measures were calculated in dimensionless speed, obtained by dividing by $(gL)^{0.5}$, where g is gravitational acceleration. Time measures were calculated in dimensionless time, obtained by dividing by $L^{0.5}g^{-0.5}$. Data were then converted from dimensionless units to SI units for presentation using an average leg length of $L = 0.946$m, an average speed normalization factor of $(gL)^{0.5} = 3.04$ ms^{-1}, and an average time factor of $L^{0.5}g^{-0.5} = 0.311$s.

We tested for a relationship between fluctuations in long-term step length and speed. Mean step length has been reported to vary with walking speed through the equation $s = \alpha \cdot v^{\beta}$, where s = step length and v = speed (Grieve, 1968; Kuo, 2001). Taking the logarithm of this equation yields $\log s = \log\alpha + \beta \cdot \log v$, from which a linear regression yields estimates of α and β for each subject. Typical values for α are 0.95–1.42, and for β are 0.27–0.55 (Grieve, 1968). For each subject, all trials in a single condition were analyzed together.

We performed statistical tests comparing gait parameter means, long-term gait parameter

variabilities, and short-term foot placement variabilities across Young and Elderly groups and eyes-open and eyes-closed conditions. We first performed 2-way ANOVA, with age group and eyes open/closed as factors, the latter treated as a repeated measure. For those factors with significant differences, post-hoc tests were performed as follows. Eyes-open and eyes-closed conditions were compared with paired t-tests, and Young and Elderly groups with unpaired t-tests. Correlations between speed and step length were calculated using least-squares linear regression. We calculated individual experiment-wise probabilities for post-hoc comparisons as the total probability of false rejection, $p_{exp} = 1 - ((1 - p_1)(1 - p_2) \ldots (1 - p_n))$, where p_i are the relevant statistically significant probabilities.

4.3 Results

Although Young and Elderly subjects walked with very similar gaits, there were significant differences in several parameters. The overall walking speed was 1.44 ± 0.15 ms^{-1}. The major significant differences were as follows. All subjects walked with greater total lateral foot placement variability than fore-aft. This difference was accentuated in the Elderly group, and in both groups in the eyes closed trials. The Elderly group also walked with overall greater mean step width. Trends in step variability were enhanced when using short-term foot placement variabilities. Finally, long-term step length and speed were well correlated, indicating that long-term step fluctuations are not related to balancing during walking. Major results are presented below, first considering mean step parameters, then step variabilities, decomposed into short-and long-term components.

Mean step width was significantly greater in the Elderly group, while mean step length and walking speed were slightly reduced in the Elderly group and in eyes-closed trials (figure 4.3). Mean step widths during eyes-open trials were 0.167 m and 0.206 m for the Young and Elderly groups, respectively, and 0.178 m and 0.201 m during eyes-closed trials, an 18% greater mean step width for the Elderly group ($p = 0.02$). However, closing the eyes did not cause a significant increase in the Young or Elderly group ($p = 0.07$ and $p = 0.7$, respectively). Mean step length was correlated to mean walking speed ($r^2 = 0.6$, $p = 4 \cdot 10^{-12}$). During eyes-open trials, mean walking speeds were $1.50 ms^{-1}$ and

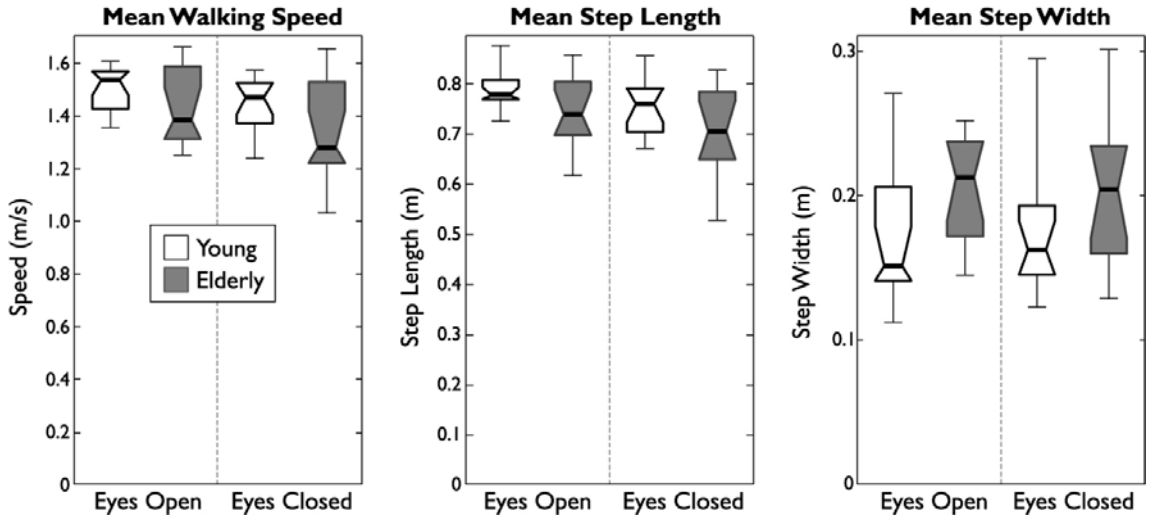

Figure 4.3: Box plots of mean walking speed, step length, and step width. For all box plots presented, the median is indicated by a black line in a notch that represents a robust estimate of uncertainty, the top and bottom of the box represent the upper and lower quartiles, respectively, and the whiskers show the entire data range. Means are reported in text. Elderly subjects walked with 18% greater mean step width than Young subjects ($p = 0.02$). Closing the eyes did not lead to significantly increased mean step width in Young or Elderly groups ($p = 0.07$ and $p = 0.7$, respectively). Mean step length was correlated to mean walking speed ($r^2 = 0.6$, $p = 4 \cdot 10^{-12}$). Young subjects preferred 6% longer steps than Elderly subjects ($p = 0.01$), but did not prefer to walk significantly faster ($p = 0.09$). With eyes closed, subjects selected 4% shorter steps ($p = 2 \cdot 10^{-6}$) and walked 5% slower ($p = 3 \cdot 10^{-5}$).

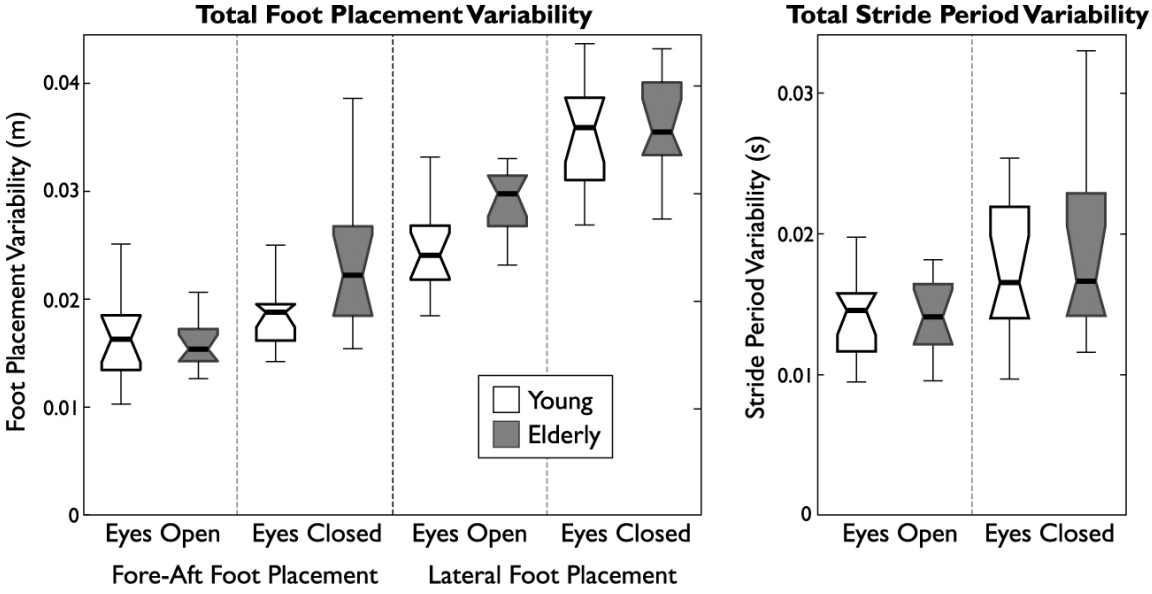

Figure 4.4: Box plots of total foot placement variability and total stride period variability. Total lateral foot placement variability was 69% greater than total fore-aft foot placement variability ($p = 1 \cdot 10^{-16}$). Total lateral variability increased by 34% when subjects closed their eyes ($p = 3 \cdot 10^{-9}$), twice as much as the increase in total fore-aft foot placement variability ($p = 0.005$). Elderly subjects walked with 20% greater total lateral foot placement variability than Young subjects with eyes open ($p = 0.002$), but with no significant difference with eyes closed ($p = 0.6$). Total stride period variability was not significantly different across age groups ($p = 0.3$) or eye conditions ($p = 0.2$). Variability was defined as standard deviation of foot placements.

1.45 ms^{-1} for Young and elderly groups, respectively, and 1.44 ms^{-1} and 1.36 ms^{-1}, respectively, during eyes-closed trials. Differences in mean speed between age groups were not significant ($p = 0.09$), but both groups preferred to walk 5% slower during eyes-closed trials ($p = 3 \cdot 10^{-5}$). Mean step lengths were 0.785 m and 0.742 m for Young and Elderly groups, respectively, during eyes-open trials and 0.755 m and 0.704 m, respectively, during eyes-closed trials. Elderly subjects preferred 6% shorter mean step length than Young subjects ($p = 0.01$), and both groups preferred 4% shorter mean step length in eyes-closed trials ($p = 2 \cdot 10^{-6}$). For comparisons of gait parameter means, $P_{exp} = 0.03$.

Total lateral foot placement variability was greater than fore-aft. This difference was accentuated in Elderly subjects, and for both subjects in the eyes-closed trials (figure 4.4). Total lateral variabilities during eyes-open trials were 0.0244 m and 0.0293 m for Young and Elderly groups, respectively, and 0.0351 m and 0.0361 m, respectively, during eyes-closed trials. Total fore-aft variabilities during eyes-open trials were 0.0163m and 0.0159m for Young and Elderly groups, respectively, and 0.0186 m and 0.233 m, respectively, during eyes-closed trials. Total lateral variability was 69% greater than total fore-aft variability across conditions ($p = 1 \cdot 10^{-16}$). Total lateral variability increased by 34%when subjects closed their eyes ($p = 3 \cdot 10^{-9}$), twice the change in total fore-aft variability ($p = 0.005$). Total lateral variability in the Elderly group was 20% greater than that for the Young group with eyes open ($p = 0.002$), but not with eyes closed ($p = 0.6$). Total stride period variability was not significantly different across age groups ($p = 0.3$) or conditions ($p = 0.2$).

Short-term lateral foot placement variability was consistently greater laterally than fore-aft. Similar to total variability, this difference was greater for Elderly subjects, and for both groups in the eyes-closed trials (figure 4.5). Short-term lateral variabilities during eyes-open trials were 0.0241 m and 0.0291 m for Young and Elderly groups, respectively, and 0.0348 m and 0.0359 m during eyes-closed trials. Short-term fore-aft variabilities during eyes-open trials were 0.0115 m and 0.0124 m for Young and Elderly

groups, respectively, and 0.0149 m and 0.0181 m, respectively, during eyes-closed trials. Short-term lateral variability was 118% greater than the short-term fore-aft variability across conditions ($p = 1 \cdot 10^{-16}$). Short-term lateral variability increased by 34% when subjects closed their eyes ($p = 4 \cdot 10^{-9}$), more than twice the change in short-term fore-aft variability ($p = 3 \cdot 10^{-4}$). Short-term lateral variability in the Elderly group was 21% greater than that for the Young group with eyes open ($p = 0.001$), but not with eyes closed ($p = 0.6$). Total variability was greater than short-term variability in the fore-aft direction, but not in the lateral direction (figures 4.4 and 4.5). Total fore-aft foot placement variabilities were 23% greater than short-term fore-aft foot-placement variability ($p = 9 \cdot 10^{-8}$). However, total lateral foot-placement variabilities were not different from short-term lateral variability (0.7% lower, $p = 0.9$). For the post-hoc comparisons of short-term variabilities $p_{exp} = 0.002$.

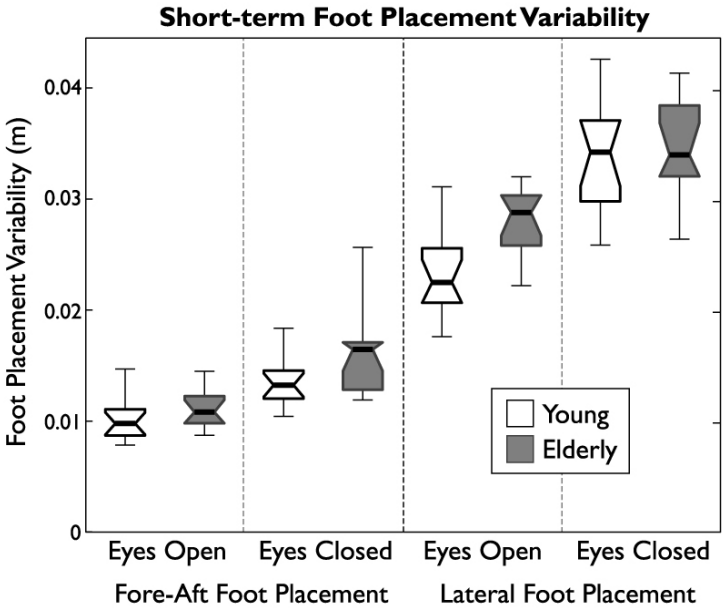

Figure 4.5: Box plot of short-term foot placement variability, defined as the standard deviation of short-term deviations (see figure 4.2). Lateral foot placement variability was greater than fore-aft foot placement variability for all conditions, 118% greater on average ($p = 1 \cdot 10^{-16}$). Lateral variability increased by 34% when subjects closed their eyes ($p = 4 \cdot 10^{-9}$), more than twice as much as fore-aft variability ($p = 3 \cdot 10^{-4}$). Elderly subjects walked with 21% greater lateral foot placement variability than Young subjects with eyes open ($p = 0.001$), but not with eyes closed ($p = 0.6$). Short-term fore-aft foot placement variability was significantly lower than total fore-aft variability due to the separation of long-term variability (on average 23% lower, $p = 9 \cdot 10^{-3}$). However, short-term lateral foot-placement variability was not significantly different from total lateral variability (on average 0.7% lower, $p = 0.9$).

In contrast to the short-term and total variabilities, long-term step width variabilities were much smaller than long-term step length variabilities (figure 4.6). They did not differ significantly for Young and Elderly subjects ($p = 0.7$), nor for eyes open/closed ($p = 0.2$). Long-term step width variabilities during eyes-open trials were 0.0029 m and 0.0029 m for Young and Elderly groups, respectively, and 0.0035 m and 0.0031 m, respectively, during eyes-closed trials. Long-term step width variance accounted for only about 1% of total lateral variance. Subjects walked with very consistent long-term heading, with a standard deviation increasing from 0.428° with eyes open to 0.771° (80%, $p = 7 \cdot 10^{-8}$) with eyes closed.

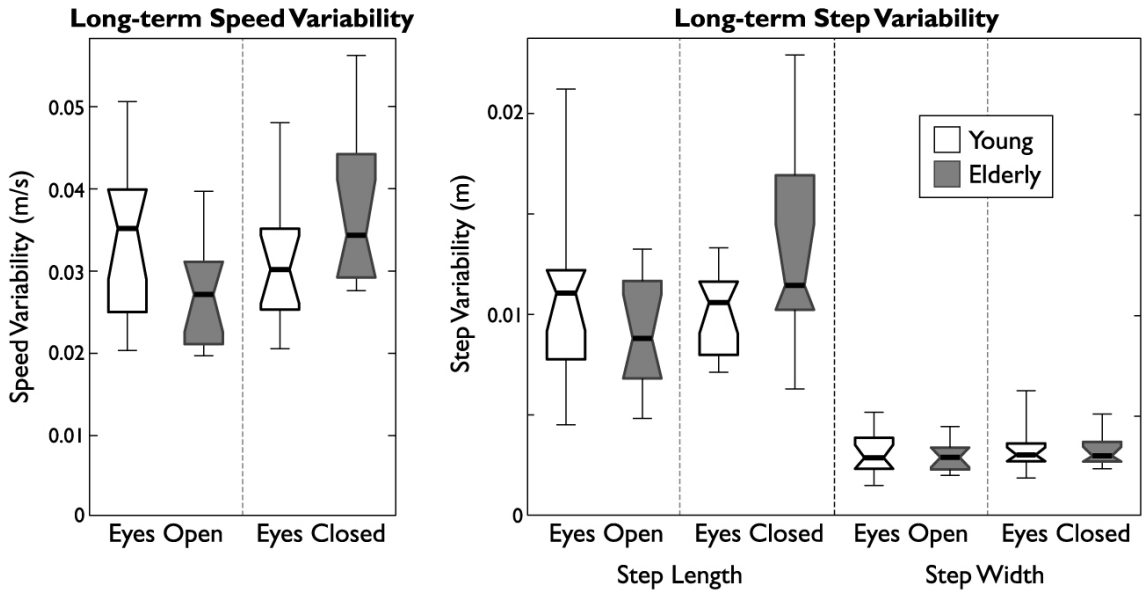

Figure 4.6: Box plots of long-term speed, step length, and step width variabilities, defined as the standard deviation of their respective long-term fluctuations (figure 4.2). Long-term speed and step length variability were strongly correlated ($r^2 = 0.7$, $p = 6 \cdot 10^{-15}$) and long-term step length variabilities were more than 2.5 times greater than corresponding step width variabilities ($p = 1 \cdot 10^{-16}$). Elderly subjects' long-term speed variability increased by 38% ($p = 0.006$) with eyes closed, and long-term step length variability increased by 49% ($p = 0.004$). Young subjects' long-term speed and step length variability changes were not significantly different in the eyes-closed condition ($p = 0.1$ and $p = 0.6$, respectively). There were no differences in long-term step width variability between Young and Elderly subjects ($p = 0.9$).

Long-term step length variabilities, however, were more than 2.5 times greater than step width variabilities ($p = 1 \cdot 10^{-16}$), and also followed similar trends to long-term speed variability (figure 4.6). Young subjects' long-term speed and step length variabilities were 0.0324 ms^{-1} and 0.0107 m, respectively, in eyes-open trials, with insignificant differences for eyes closed conditions ($p = 0.1$ and $p = 0.6$, respectively). However, the

Elderly group's long-term speed variability increased from 0.0244 ms^{-1} to 0.0338ms^{-1} (38%, p = 0.006) under the eyes-closed condition, with a corresponding increase in long-term step length variability from 0.0091m to 0.0135m (49%, p = 0.004). Long-term step length variability accounted for 40% of total fore-aft variance.

Long-term fluctuations in step length and speed were also strongly correlated to each other (figure 4.7). Long-term fluctuations did not occur at constant speed, step length, or step frequency, but rather along lines of the form $s = \alpha \cdot v^{\beta}$ (where s = step length and v = speed), similar to the trends for mean step length and speed reported by Grieve, 1968. Our data yielded values of $\alpha = 1.31 \pm 0.14$ and $\beta = 0.65 \pm 0.16$ for Young subjects ($r^2 = 0.85 \pm 0.12$, $p = 1 \cdot 10^{-16}$), and $\alpha = 1.28 \pm 0.14$ and $\beta = 0.66 \pm 0.13$ for Elderly subjects ($r^2 = 0.85 \pm 0.12$, $p = 1 \cdot 10^{-16}$).

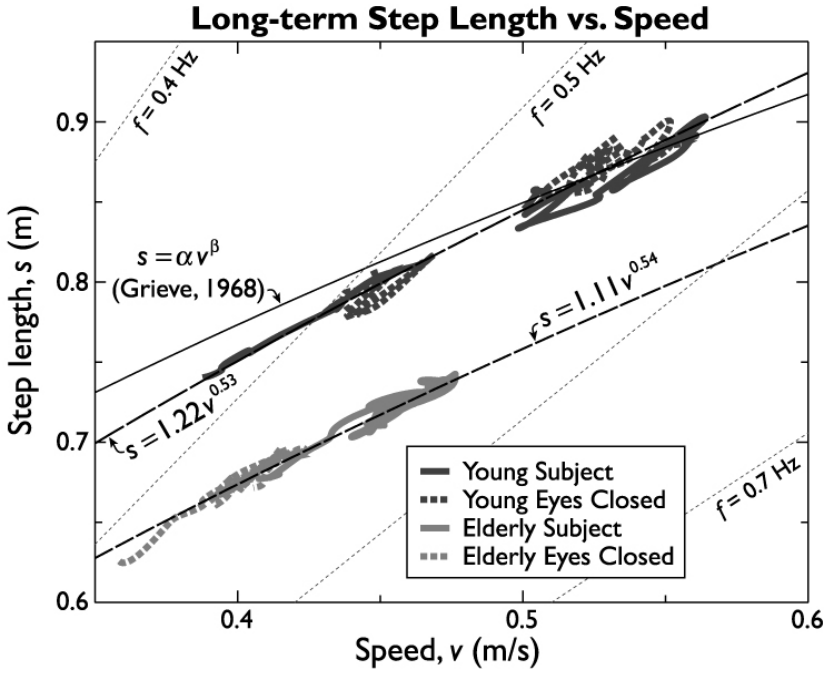

Figure 4.7: Long-term fluctuations in step length vs. speed, for two sample subjects. Data are shown for a typical Young subject and a typical Elderly subject, both with eyes open (thick gray lines) and closed (dashed thick gray lines). Long-term fluctuations refer to low-pass filtered step length and speed. Long-term speed fluctuated during the trial for each subject, but each always followed a consistent step length vs. speed relationship regardless of whether eyes were open or closed. The relationship was very similar to that reported by Grieve, 1968 for mean step lengths and speeds (adult average shown with thin black line). Each subject's data were fitted well by $s = \alpha v^{\beta}$, where s = step length and v = speed (fitted curves shown with thin dashed black lines).

4.4 Discussion

We hypothesized that lateral balance requires more control than fore-aft balance during walking, and thus is more sensitive to degradation of sensory and control channels. Because humans appear to use controlled lateral foot placement to stabilize lateral motions, we expected to find greater lateral than fore-aft foot placement variability across all conditions. We further expected greater lateral foot placement variability in the Elderly group and in subjects walking with eyes closed, due to decreased precision of sensory feedback. We tested these hypotheses by measuring step kinematics as Young and Elderly subjects walked overground with their eyes open or closed.

We found total foot placement variability to be consistently greater laterally than fore-aft, especially in eyes-closed trials and in the Elderly group (figure 4.4). The Young eyes open vs. closed results are similar to those reported previously by Bauby and Kuo (2000). The Young vs. Elderly results are similar to those reported by Owings and Grabinder (2004a) for treadmill walking. One inconsistent and unexplained result is the lack of significant difference in lateral variability between Young and Elderly with eyes closed. However, all of the significant differences are consistent with the hypothesis that foot placement, especially in the lateral direction, is actively controlled during gait. Active control is dependent on imperfect sensing and foot placement, both of which contribute to lateral foot placement variability. Closing the eyes and aging both appear to increase the imprecision, and therefore lateral variability. The lower variability of fore-aft foot placement may be due to lesser need for active control of foot placement, perhaps because of passive-dynamic stability in the sagittal plane (McGeer, 1990; Kuo, 1999).

Elderly subjects also walked with significantly wider steps than Young subjects. We observed an average difference of 18%, but with considerable intersubject variability ($p = 0.02$). Wider steps have the disadvantage of increasing the energetic cost of walking associated with step-to-step transitions, in which the body center of mass velocity is redirected laterally and vertically during double support (Donelan et. al., 2001). A competing advantage is that wider steps reduce the lateral instability of a dynamic walking model (Kuo, 1999), although this effect may be too small to explain the observed

difference. A potentially greater advantage is that wider steps increase the safety margin by which the lateral position of the body center of mass remains between the feet. Older adults may prefer a larger margin of safety as a consequence of greater step variability, irrespective of the effect on dynamic stability, but with a trade-off in energetic cost. Even so, step variability alone cannot explain the preference for wider steps, because neither subject group selected wider steps in the eyes closed condition, even when their step variability increased. Separate studies have shown that subjects do walk with narrower steps when they are externally stabilized in the lateral direction (Donelan et. al. 2004; Dean et. al., 2007). But the present results indicate that closing the eyes is insufficient to warrant wider steps. It is possible that older adults' preference for wider steps is only made gradually rather than instantaneously, or as a consequence of their confidence, fear of falling (Maki, 1997), or other factors not considered here.

Both Young and Elderly subjects walked with slowly fluctuating speed and step length. It is unsurprising that self-selected speed would fluctuate, as the overground walking condition did not enforce speed as on a treadmill. But this fluctuation is also reflected in step length (figure 4.2), accounting for about 40% of total step length variability. Both long-term step length variability and speed followed similar trends as a function of age and eyes open/closed (figure 4.6). Long-term step length also varied instantaneously with speed, in the same relationship that total step length varies with speed (figure 4.7) in order to minimize metabolic cost at a given speed (Elftman, 1966; Grieve, 1968; Zarrugh et. al., 1974; Kuo, 2001). The long term fluctuations occurring over 20 steps or more therefore appear to have much more to do with walking speed than with balance. In addition, long-term step width variability did not significantly differ as a function of age or eyes open/closed, and only accounted for 1% of total step width variability (figure 4.6). None of these trends were sensitive to the filter's cut-off frequency. For example, short-term lateral foot placement variability changed by less than 3% when altering the cut-off frequency by ± 50%.Dingwell et. al. (2001) also suggest that the vast majority of inter-step deviations occur within 10 strides. The key effect we observed was that speed and step length fluctuate slowly over many steps, while step width fluctuated from one step to the next.

The separation of speed-related fluctuations from short-term foot variations accentuates those effects related to balance. Examining short-term results, lateral foot placement variability was more than double that for the fore-aft direction (figure 4.5). Short-term fore-aft variability did not change significantly as a function of age or eyes open/closed, supporting the hypothesis that walking is passively stable in the sagittal plane and requires little active fore-aft foot placement control. The long- vs. short-term decomposition appears useful for reducing the effects of speed fluctuation that occur in overground walking. Speed does not fluctuate as spontaneously in treadmill walking, although we have observed subjects occasionally adjusting their fore-aft position on the treadmill with quick bursts of speed. These bursts would also be expected to contribute to fore-aft foot placement variability without being related to balance, but are likely more difficult to filter out than in overground walking.

Detection of age-related differences during walking is somewhat sensitive to instrumentation and walking conditions. Robust estimates are aided by high accuracy and a large number of steps (Owings and Grabiner, 2003). The accuracy of our mobile motion tracking system is slightly poorer than that of a laboratory-fixed optical tracking system. However, this disadvantage is offset by the ability to measure hundreds of contiguous, overground steps. A long walking distance ensures a relatively steady gait. Fixed optical tracking systems can only measure a small number of steps with high accuracy, and alternatives such as instrumented walkways have far poorer accuracy and/or limited length. Our instrumentation was sufficient to identify an age-related difference in step width of 18%, but with relatively weak statistical significance ($p = 0.02$). Others have also found small differences (Moe-Nilssen and Helbostad, 2005), but even so, step width does not appear to be a strong indicator of age-related changes to gait. It may be that increases in step width are only indirectly related to balance, and more directly to fear or fall risk (Maki, 1997; Chamberlin et. al., 2005; Heitmann et. al., 1989).

Step width variability appears to be a much more robust indicator of gait. We found statistically robust differences in step width variability between age groups ($p = 0.002$),

between eyes open and closed ($p = 3 \cdot 10^{-9}$), and between lateral and fore-aft variability for all subjects ($p = 1 \cdot 10^{-16}$). The age-related differences are consistent with previous reports (Owings and Grabiner, 2004a; Grabiner et. al., 2001; Bauby and Kuo, 2000). As discussed above and as supported by our previous study of external lateral stabilization (Donelan et. al., 2004), step width variability appears to be a good indicator of balance during walking. It may also be useful for indicating fall risk (Heitmann et. al., 1989), although with some conflicting evidence (Moe-Nilssen and Helbostad, 2005; Gabell and Nayak, 1984). The robustness of our results was likely associated with the large number of steps recorded at reasonable accuracy, as recommended by Owings and Grabiner (2003). The difference is also more apparent when normalizing standard deviation by leg length, as opposed to mean step width, as is used in a coefficient of variation (Stolze et. al., 2000; Gabell and Nayak, 1984). We prefer to normalize by leg length, because it accounts for expected differences due to subject height. Mean step width is not expected to affect step width variability in the same way. For example, subjects can walk at nearly zero (and theoretically zero or negative) mean step width with no difference in standard deviation (Donelan et. al., 2004), even though the coefficient of variation would approach infinity. Accurate measurements and appropriate normalization improve the robustness of step width variability as an indicator of balance during gait.

Step length and stride period variability, however, appear to change very little with age or with eyes open vs. closed. We detected no significant changes in these variables, consistent with the treadmill results of others (Owings and Grabiner, 2004a; Owings and Grabiner, 2004b; Grabiner et. al., 2001). The lack of sensitivity for these parameters may be due to the hypothesized passive stability of walking in the sagittal plane. Healthy individuals appear to exert much less active control of fore-aft foot placement than in the lateral direction. Stride period variability may, however, still be a useful indicator of fall risk in less healthy individuals (Hausdorff et. al., 2001), even if does not depend directly on age.

The observed changes in step width variability appear to be related to subtle changes that occur with age. Even though our subjects were healthy, they nonetheless displayed clear,

age-related increases in lateral foot placement variability. This variability increased still further with removal of vision. These differences were greater than those observed in other variables such as mean step width, step length, or stride period, that may differ more in subjects with greater fear or risk of falling. Step width variability, however, appears to be more sensitive to relatively small degradations in sensing and active foot placement that occur with age. These same trends have been observed in treadmill gait (Owings and Grabiner, 2004a; Owings and Grabiner, 2004b). Step width variability, when measured accurately over many steps and in either overground or treadmill conditions, may prove useful as a measure of balance-related gait function, or as an early indicator of fall risk.

Acknowledgments

Arthur Kuo assisted with experimental design and interpretation of results. Catherine Bauby and Sue Park assisted with data collection.

Appendices

Appendix A

Dynamic walking model of arm swinging

A.1 Simulation

A.1.1 Parameter Sets Studied

All of the simulations performed for the purposes of this study use the model described in figure 4.1a of the accompanying manuscript. In each case, a base anthropomorphic parameter set was used for most of the model parameters as follows. Throughout the model, all parameters are dimensionless:

gravitational acceleration $\boldsymbol{g} = 1$; leg length $\boldsymbol{L_{leg}} = 1$; leg center of mass position $\boldsymbol{C_{leg}} = 0.355$; leg rotational inertia $\boldsymbol{I_{leg}} = 0.016$; leg splay angle $\boldsymbol{q} = -0.075$ (feet 0.15 apart); foot radius $\boldsymbol{R} = 0.3$; hip width $\boldsymbol{W_h} = 0.3$; hip mass $\boldsymbol{m_{hip}} = 0.6$; arm length $\boldsymbol{L_{arm}} = 0.33$; shoulder width $\boldsymbol{W_{sho}} = 0.4$ (shoulders 0.2 from body center);

The remaining parameters were given three sets of values for three comparisons of interest: the Most Anthropomorphic set, the Demonstration set, and the Slow set. The Most Anthropomorphic set was used for comparisons to human gait, the results of which are displayed in figure 4.1b and 4.1c of the accompanying manuscript. In this set, the slope allows for a typical walking speed, the hip spring a typical cadence, the arms represent 4% of body mass, and the legs represent 16% of body mass such that the total body mass equals 1:

walking slope $\gamma = 0.03$; hip spring constant $\boldsymbol{k} = 0.0175$; arm mass $\boldsymbol{M_{arm}} = 0.04$; arm rotational inertia $\boldsymbol{I_{arm}} = 0.0015$; leg mass $\boldsymbol{M_{leg}} = 0.16$;

The Demonstration set was used to create more illustrative animations of the various secondary modes of oscillation that were discovered in the model. This set exhibits nearly identical Normal, Bound, and Anti-Phase behavior as the Most Anthropomorphic set, but exhibits more easily visually distinguishable Parallel and Third-Phase modes, animations of which are included in these supplementary materials. To better illustrate those modes of oscillation, the mass and rotational inertia of the arms were slightly reduced, the mass of the legs slightly increased (to maintain a constant body weight), and the hip stiffness slightly decreased:

walking slope $\gamma = 0.03$; hip spring constant $\boldsymbol{k} = 0.01$; arm mass $\boldsymbol{M_{arm}} = 0.03$; arm rotational inertia $\boldsymbol{I_{arm}} = 0.0012$; leg mass $\boldsymbol{M_{leg}} = 0.17$;

The Slow set was used to demonstrate the existence of a "double-swing" oscillation mode of the arms at relatively slow speeds, a phenomenon which has been previously observed in humans (cite). This parameter set is based on the Most Anthropomorphic set with the walking slope reduced to as to decrease gait speed:

walking slope $\gamma = 0.01$; hip spring constant $\boldsymbol{k} = 0.0175$; arm mass $\boldsymbol{M_{arm}} = 0.04$; arm rotational inertia $\boldsymbol{I_{arm}} = 0.0015$; leg mass $\boldsymbol{M_{leg}} = 0.16$;

A.1.2 Modes of Oscillation Observed

Each mode was different in quantifiable ways, some of which we report here as a reference. The primary difference between modes was in shoulder joint trajectory, and so these trajectories are presented graphically below. The economy of each mode was always equal to the walking slope, which was a pre-set parameter. We also defined hip stiffness a-priori for ease of comparison. Therefore, for each walking mode there were slightly different speeds and step lengths, reported below. As in prior 3-D models of this type (e.g. Kuo 1999) all simulated modes were unstable, primarily in side-to-side motions. Maximum eigenvalues for each mode are reported below.

Table of Mode Characteristics

	Slope	Speed	Step L	Max. λ
Most Anthropomorphic				
Normal	0.03	0.293	0.621	7.08
Bound	0.03	0.258	0.693	11.3
Anti-Phase	0.03	0.295	0.624	7.11
Demonstration				
Normal	0.03	0.285	0.632	7.82
Bound	0.03	0.257	0.676	12.3
Anti-Phase	0.03	0.287	0.634	7.83
Mid-Phase	0.03	0.281	0.622	7.68
Parallel	0.03	0.278	0.650	76.7*
Slow				
Double-Swing	0.01	0.157	0.451	15.1

* The parallel mode is a period 2 oscillation, leaving more time between repeatable states

Figures A.1 – A.9 show joint angle trajectories for each mode of oscillation. Arm segment angles are shown in light blue and pink, leg segment angles are shown in red and

green, and the side-to-side body angle is shown in dark blue. The arm and leg segment angles are based on the generalized coordinates used for simulation, but are approximately equal to their projections onto the sagittal plane due to the consistently small values of the lean angle. All angles are presented with respect to vertical, with positive values corresponding to positive rotations about an axis extending from the right side of the hip, i.e. with positive rotations corresponding to limb movements forwards in the direction of travel. For each mode, four consecutive steps are shown, so as to allow visualization of periodicity.

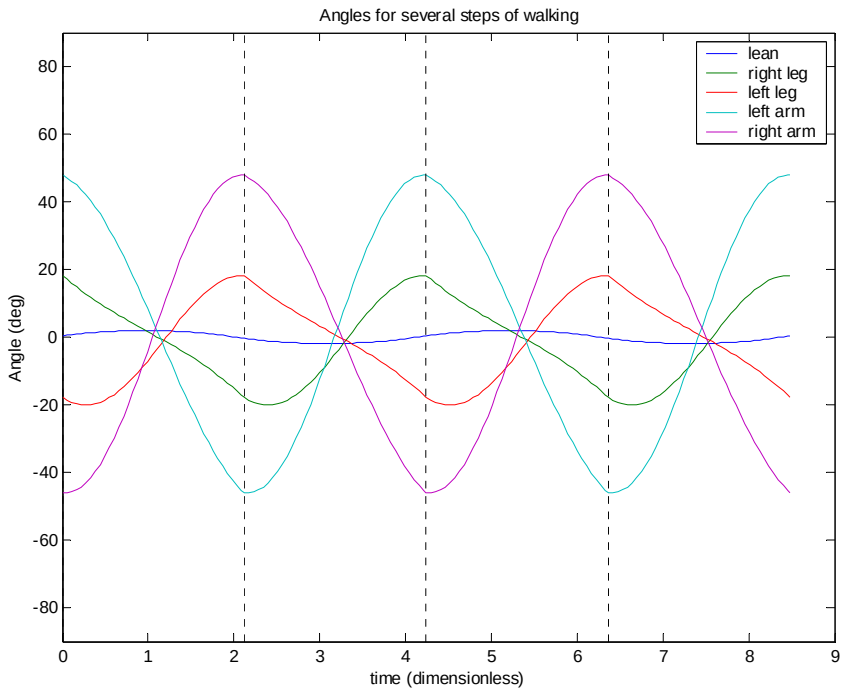

Figure A.1: Joint angle trajectories for the Most Anthropomorphic parameter set Normal mode of walking.

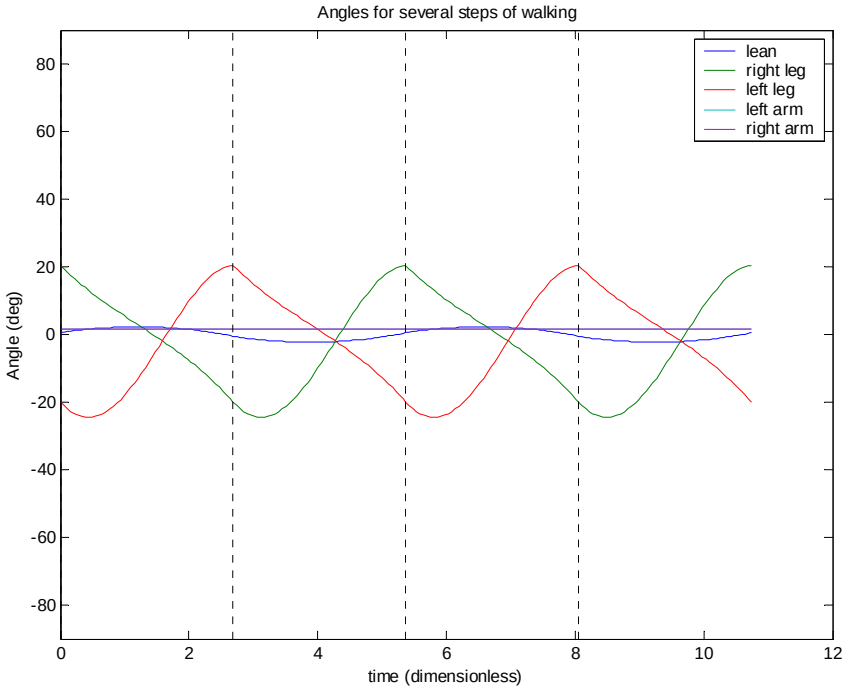

Figure A.2: Joint angle trajectories for the Most Anthropomorphic parameter set Bound mode of walking.

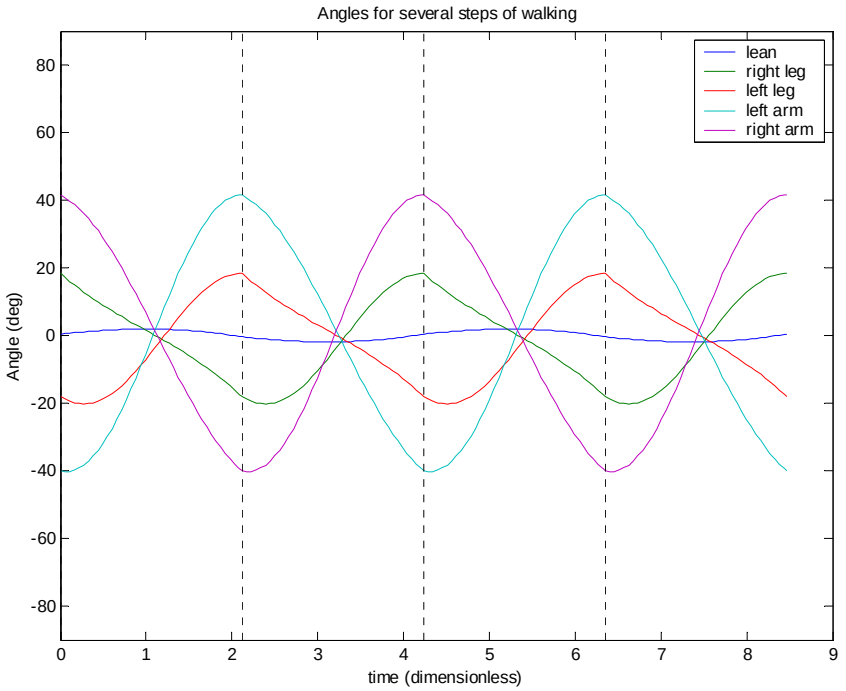

Figure A.3: Joint angle trajectories for the Most Anthropomorphic parameter set Anti-Phase mode.

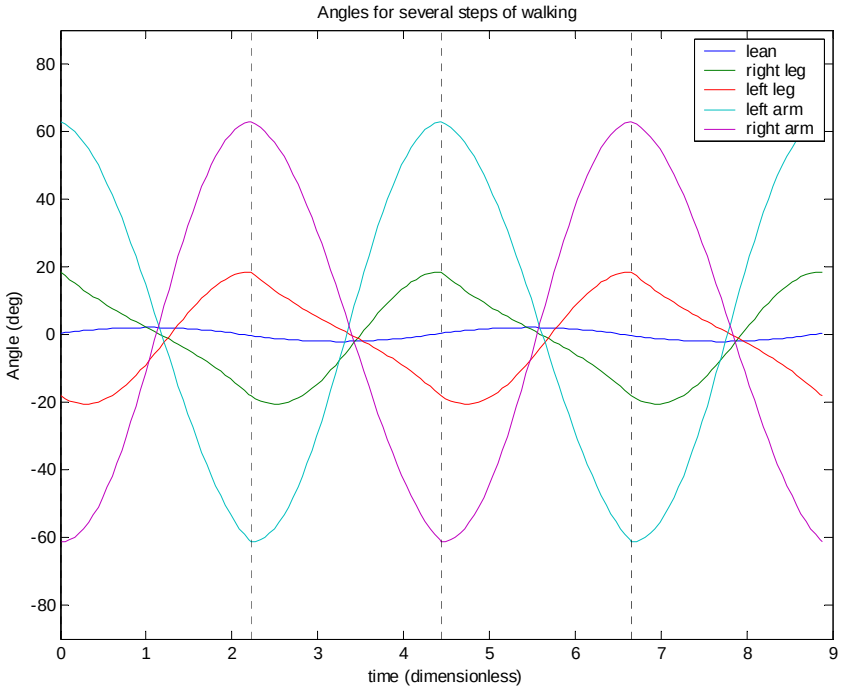

Figure A.4: Joint angle trajectories for the Demonstration parameter set Normal mode of walking.

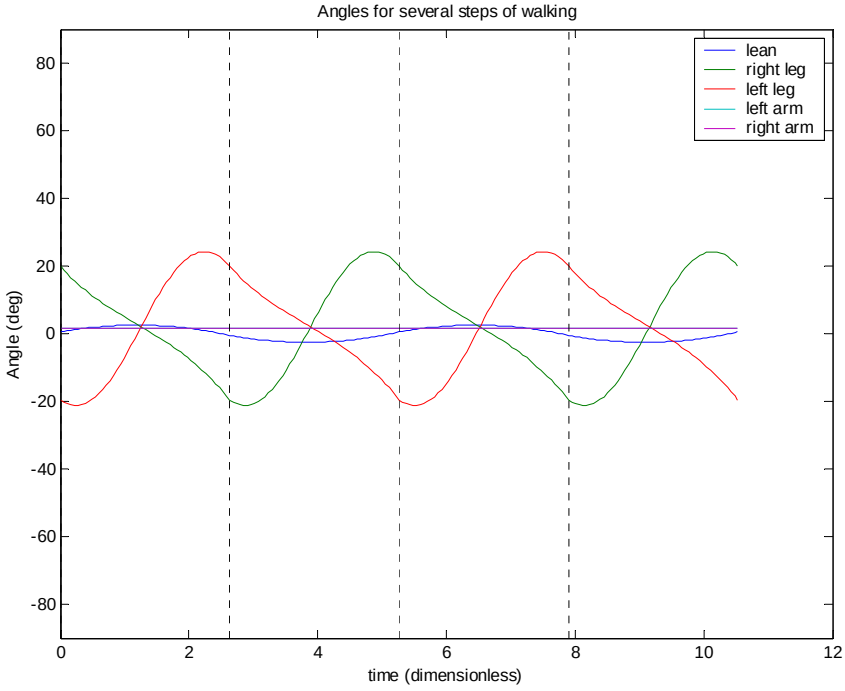

Figure A.5: Joint angle trajectories for the Demonstration parameter set Bound mode of walking.

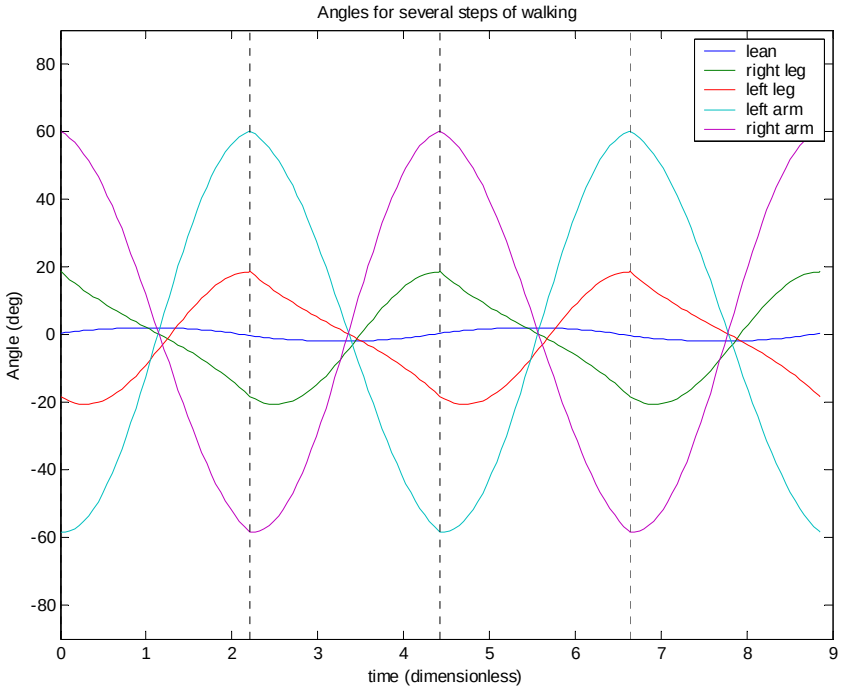

Figure A.6: Joint angle trajectories for the Demonstration parameter set Anti-Phase mode.

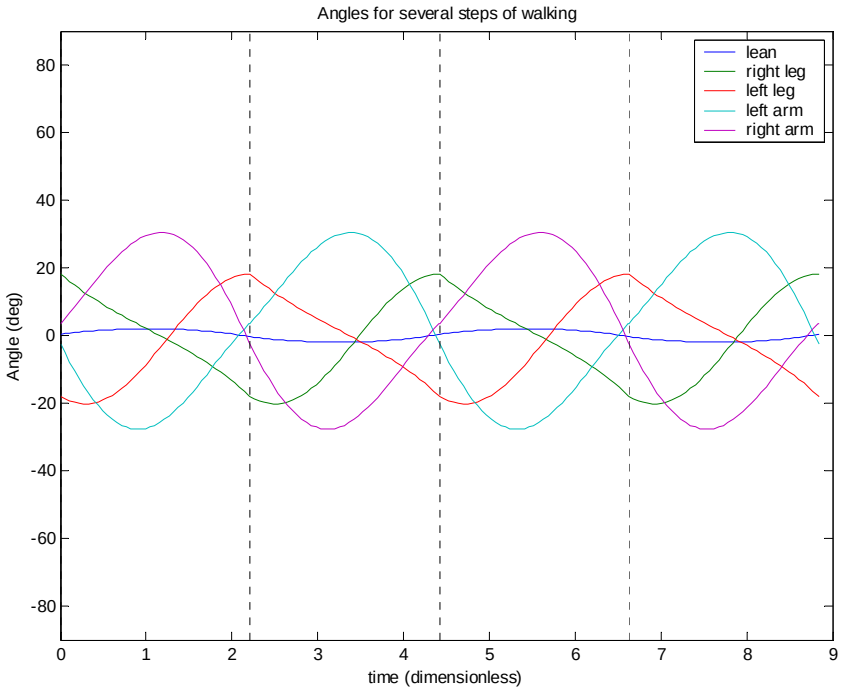

Figure A.7: Joint angle trajectories for the Demonstration parameter set Mid-Phase mode of walking.

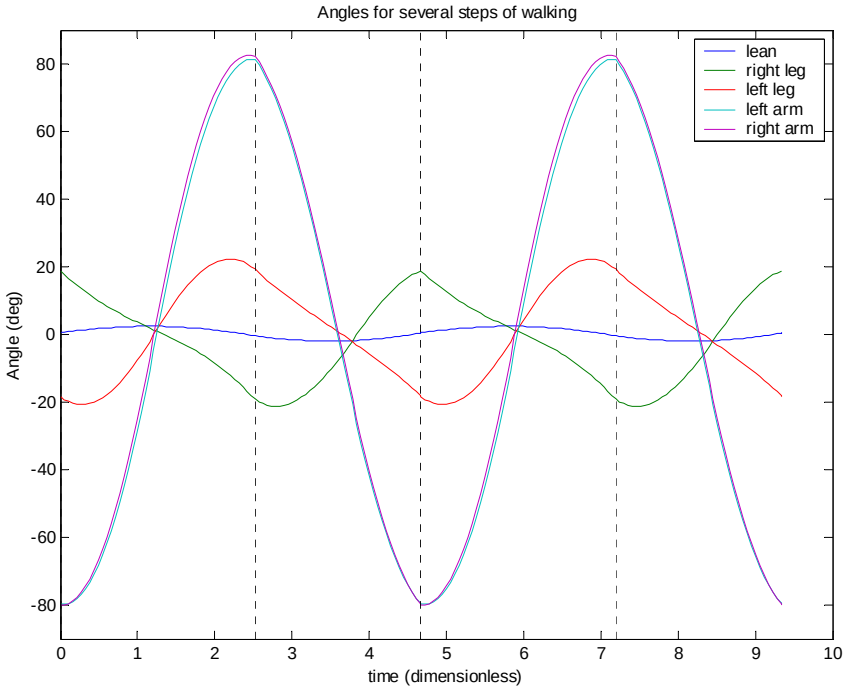

Figure A.8: Joint angle trajectories for the Demonstration parameter set Parallel mode of walking.

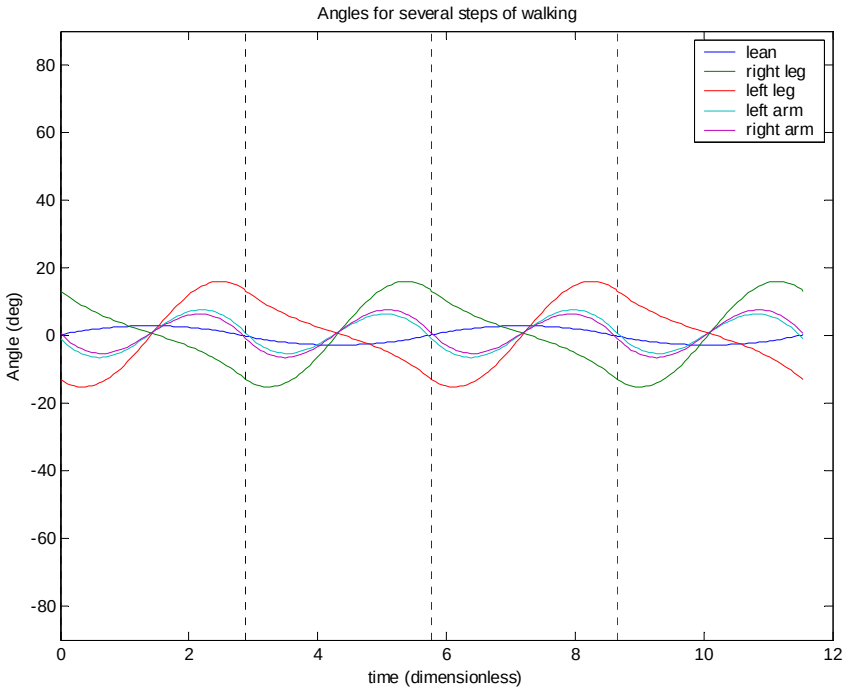

Figure A.9: Joint angle trajectories for the Slow parameter set Double-Swing mode.

References

Adamczyk, P. G., Collins, S. H., and Kuo, A. D. (2006) The advantages of a rolling foot in human walking. Journal of Experimental Biology, 209:3953-3963.

Adams, J. M. and Perry, J. (1992) Prosthetics. In: (Perry, J., ed.) Gait Analysis: Normal and Pathological Function. SLACK Inc.: Thorofare, NJ. pp. 165-200.

Alexander, B.H., Rivara, F.P., Wolf, M.E. (1992) The cost and frequency of hospitalization for fall-related injuries in older adults. American Journal of Public Health, 82(7): 1020-1023.

Alexander, R. M. (2003) Principles of Animal Locomotion. New Jersey: Princeton University Press.

Barth, D. G., Schumacher, L., Thomas, S. S. (1992) Gait analysis and energy cost of below knee amputees wearing six different prosthetic feet. J. Prosthet. Orthot. 4: 63-75.

Barr, A.E., Siegel, K.L., Danoff, J.V., McGarvey, C.L. 3rd, Tomasko, A., Sable, I., Stanhope, S.J. (1992) Biomechanical comparison of the energy-storing capabilities of SACH and Carbon Copy II prosthetic feet during the stance phase of gait in a person with below-knee amputation. Physical Therapy 72:344-54.

Bauby, C.E., Kuo, A.D. (2000) Active control of lateral balance in human walking. Journal of Biomechanics, 33: 1433-1440.

Bertram, J.A., Ruina, A. (2001) Multiple Walking Speed–frequency Relations are Predicted by Constrained Optimization. Journal of Theoretical Biology. 209(4): 445-453

Brach, J.S., Berlin, J.E., VanSwearingen, J.M., Newman, A.B., Studenski, S.A. (2005) Too much or too little step width variability is associated with a fall history in older persons who walk at or near normal speed. Journal of Neuroengineering and Rehabilitation, 26: 2-21.

Centers for Disease Control and Prevention. Web-based Injury Statistics Query and Reporting System (WISQARS) [Online]. (2005) National Center for Injury Prevention and Control, Centers for Disease Control and Prevention (producer). Available from: URL: www.cdc.gov/ncipc/wisqars. [Cited 23 Aug 2006].

Chamberlin, M.E., Fulwider, B.D., Sanders, S.L., Medeiros, J.M. (2005) Does fear of falling influence spatial and temporal gait parameters in elderly persons beyond changes associated with normal aging?. Journal of Gerontology: Medical Sciences, 60(9): 1163-1167.

Colborne, G.R., Naumann, S., Longmuir, P.E., and Berbrayer, D. (1992) Analysis of mechanical and metabolic factors in the gait of congenital below knee amputees. Am. J. Phys. Med. Rehabil. 92: 272 – 278.

Coleman, M, Ruina, A. (1998) An Uncontrolled Walking Toy That Cannot Stand Still. Physical Review Letters 80:16 3658 – 3661

Coleman, M.J., Garcia1, M., Mombaur, K., Ruina, A. (2001) Prediction of stable walking for a toy that cannot stand. Phys. Rev. E. 64:022901

Collins, S.H., Wisse, M., Ruina, A. (2001) A 3-D Passive Dynamic Walking Robot with Two Legs and Knees, International Journal of Robotics Research, 20 (7):607-615.

Collins, S., Ruina, A., Tedrake, R., Wisse, M. (2005) Efficient bipedal robots based on passive dynamic walkers. Science. 307(5712): 1082-1085.

Collins, S. H., Ruina, A. (2005) A bipedal walking robot with efficient and human-like gait. In Proc. IEEE International Conference on Robotics & Automation, Barcelona, Spain, 1983-1988.

Collins SH, Adamczyk PG, Kuo AD (2007) A simple method for calibrating force plates and force treadmills using an instrumented pole. Gait & Posture; in press.

Dean, J.D., Alexander, N. B., and Kuo, A. D. (2004) Age-related changes in maximal hip strength and movement speed. Journal of Gerontology: Medical Sciences, 59A: 286-292.

Dillingham, T.R., Pezzin, L.E., Mackenzie E.J. (2002) Limb Amputation and Limb Deficiency: Epidemiology and Recent Trends in the United States. Southern Medical Journal 95 (2002): 875-883

Dingwell, J.B., Cusumano, J.P., Cavanagh, P.R., Sternad, D. (2001) Local Dynamic Stability Versus Kinematic Variability of Continuous Overground and Treadmill Walking. Journal of Biomechanical Engineering, 123: 27-32.

Doke, J., Donelan, J. M., and Kuo, A. D. (2005) Mechanics and energetics of swinging the human leg. Journal of Experimental Biology. 208:439-445.

Donelan, J.M., Kram, R., and Kuo, A.D. (2001) Mechanical and metabolic determinants of the preferred step width in human walking. Proc. Royal Soc. Lond. B, 268: 1985-1992.

Donelan JM, Kram R, Kuo AD (2002a) Simultaneous positive and negative external mechanical work in human walking. J Biomechanics; 35(1):117-124

Donelan, J. M., Kram, R., and Kuo, A.D. (2002b) Mechanical work for step-to-step transitions is a major determinant of the metabolic cost of human walking. Journal of Experimental Biology, 205: 3717-3727.

Donelan, J. M., Shipman, D. W., Kram, R., and Kuo, A. D. (2004) Mechanical and metabolic requirements for active lateral stabilization in human walking. J. of Biomechanics, 37: 827-835.

Donker SF, Beek PJ, Wagenaar RC, Mulder T. (2001) Coordination between arm and leg movements during locomotion. J Motor Behavior; 33(1):86-102

Elftman, H. (1939) The function of arms in walking. Human Biology; 11:529-535.

Elftman, H., (1966) Biomechanics of Muscle. Journal of Bone and Joint Surgery, 48-A: 363-377.

Fernandez-Ballesteros ML, Buchthal F, Rosenfalck P. (1965) The pattern of muscular activity during the arm swing of natural walking. ACTA Physiol Scand; 63:296-310

Gabell, A., Nayak, U.S. (1984) The Effect of Age on Variability in Gait. Journal of Gerontology, 39(6): 662-6.

Gailey, R.S., Wenger, M.A., Raya, M., Kirk, N., Erbs, K., Spryopoulos, P., and Nash, M.S. (1994) Energy expenditure of trans-tibial amputees during ambulation at self-selected pace. Prosthet. Orthot. Int. 18: 84-91.

Gailey, R.S., Nash, M.S., Atchley, T.A., Zilmer, R.M., Moline-Little, G.R., Morris-Cresswell, N., Siebert, L.I. (1997) The effects of prosthesis mass on metabolic cost of ambulation in nonvascular trans-tibial amputees. Prosthet. Orthot. Intl. 21: 9-16.

Garcia, M., Chatterjee, A., Ruina, A., Coleman, M. (1998) The Simplest Walking Model: Stability, Complexity, and Scaling. J. Biomech. Eng. 120(2): 281-288

Garcia, M. (1998) Stability, scaling, and chaos in passive-dynamic gait models. Ph.D. Thesis, Cornell University, Ithaca, NY USA.

Geil, M.D., Parnianpour, M., Quesada, P., Berme, N., Simon, S. (2000) Comparison of methods for the calculation of energy storage and return in a dynamic elastic response prosthesis. Journal of Biomechanics 33: 1745-50.

Gerdy PN. (1829) Memoires sur le mecanisme de la marche le l'homme. J. Pysiol. Exp. Path. (Magendie); 9:1-28

Gomes, M.W., Ruina, A.L. (2005) A five-link 2D brachiating ape model with life-like zero-energy-cost motions. Journal of Theoretical Biology 237(3): 265-278

Grabiner, P.C., Biswas, S.T., Grabiner, M.D., 2001. Age-related changes in spatial and temporal gait variables. Archives of Physical Medicine and Rehabilitation, 82(1): 31-35.

Grieve, D.W., 1968. Gait Patterns and the Speed of Walking. Biomedical Engineering, 3: 119-122.

Hanada E. Kerrigan C. (2001) Energy consumption during level walking with arm and knee immobilized. Arch Phys Med Rehab; 82:1251-1254

Hausdorff, J.M., Peng, C.K., Ladin, Z., Wei, J.Y., Goldberger, A.L. (1995) Is walking a random walk? Evidence for long-range correlations in stride interval of human gait. Journal of Applied Physiology, 78: 349-358.

Hausdorff, J.M., Rios, D.A., Edelberg, H.K. (2001) Gait Variability and Fall Risk in Community-Living Older Adults: A 1-Year Prospective Study. Archives of Physical Medicine and Rehabilitation, 82: 1050-1056.

Heitmann, D.K., Gossman, M.R., Shaddeau, S.A., Jackson J.R., 1989. Balance performance and step width in noninstitutionalized, elderly, female fallers and nonfallers. Physical Therapy, 69(11): 923-31.

Herbert, L. M., Engsberg, J.R., Tedford, K.G., Grimston, S.K. (1994)A comparison of oxygen consumption during walking between children with and without below-knee amputations.Physical Therapy 74: 943.

Himann J.E., Cunningham D.A., Rechnitzer P.A., Paterson D.H., 1988. Age-related changes in speed of walking. Medicine and Science in Sports and Exercise, 20(2): 161-166.

Hinrichs RN. (1990) Whole body movement: Coordination of arms and legs in walking and running: In J. Winters & S.LY Woo (Eds.), Multiple Muscle Systems: .Biomechanics and Movement Organization (pp. 694-705), New York: Springer-Verlag.

Hirai, K., Hirose, M., Haikawa, Y., and Takenaka, T. (1998) The development of the Honda Humanoid robot. IEEE International Conference on Robotics and Automation Proceedings, Leuven, Belgium, May, pp. 1321–1326.

Horak, F.B., Shupert, C.L., Mirka, A. (1989) Components of postural dyscontrol in the elderly: A review. Neurobiology of Aging, 10(6): 727-738.

Inzitari, M., Carlo, A., Baldereschi, M., Pracucci, G., Maggi, S., Gandolfo, C., Bonaiuto, S., Farchi, G., Scafato E., Carbonin, P., Inzitari, D.; ILSA Working Group, (2006) Risk and predictors of motor-performance decline in a normally functioning population-based sample of elderly subjects: the Italian Longitudinal Study on Aging. Journal of the American Geriatric Society, 54(2): 318-324.

Jackson KM, Joseph J, Wyard SJ. (1978) A mathematical model of arm swing during human locomotion. J. Biomechanics; 11:277-289

Jackson KM, Joseph J, Wyard SJ. (1983) The upper limbs during human walking part 2: function. Electromyography and Clinical Neurophysiology; 23:435-446

James, U. (1973) Oxygen uptake and heart rate during prosthetic walking in healthy male unilateral above-knee amputees. Scand. J. Rehabil. Med. 5: 71-80.

Kubo M, Wagenaar RC, Saltzman E, Holt KG. (2004) Biomechanical mechanism for transitions in phase and frequency of arm and leg swing during walking. Biological Cybernetics; 91:91-98

Kuo, A.D. (1999) Stabilization of lateral motion in passive dynamic walking, International Journal of Robotics Research, 18 (9): 917-930.

Kuo, A.D. (2001) A simple model of bipedal walking predicts the preferred speed-step length relationship, Journal of Biomechanical Engineering, 123: 264-269.

Kuo, A.D. (2002) Energetics of actively powered locomotion using the simplest walking model, Journal of Biomechanical Engineering, 124: 113-120.

Lehmann, J.F., Price, R., Boswell-Bessette, S., Dralle, A., Questad, K., deLateur, B.J. (1993) Comprehensive analysis of energy storing prosthetic feet: Flex Foot and Seattle Foot Versus Standard SACH foot. Arch. Phys. Med. Rehabil. 74: 1225-1231.

Lehmann, J.F., Price, R., Boswell-Bessette, S., Dralle, A., Questad, K. (1993) Comprehensive analysis of dynamic elastic response feet: Seattle Ankle/Lite Foot versus SACH foot. Arch. Phys. Med. Rehabil. 74: 853 - 861.

Lemaire, E.D., Nielen, D., and Paquin, M.A. (2000) Gait evaluation of a transfemoral prosthetic simulator. Arch.Phys. Med. Rehabil. 81: 840-843.

Li Y, Wang W, Crompton RH, Gunther MM. (2001) Free vertical moments and transverse forces in human walking and their role in relation to arm-swing. J Experimental Biology; 204:47-58

Manchester, D., Woollacott, M., Zederbauer-Hylton, N., Marin, O. (1989) Visual, vestibular, and somatosensory contributions to balance control in the older adult. Journal of Gerontology: Medical Sciences, 44, M118-127.

Maki, B.E., 1997. Gait changes in older adults: predictors of falls or indicators of fear. Journal of the American Geriatrics Society, 45(3): 313-320.

Martin, P. E., Royer, T. D. and Mattes, S. J. (1997). Effect of symmetrical and asymmetrical lower extremity inertia changes on walking economy. Med. Sci. Sports Exerc. 29, 86.

McGeer, T. (1989) Powered flight, child's play, silly wheels, and walking machines. In: Proc. IEEE Robotics and Automation Conference, Piscataway, NJ : pp. 1592-1597.

McGeer, T. (1990) Passive dynamic walking. International Journal of Robotics Research. 9(2): 68-82.

McGeer, T. (1991) Passive dynamic biped catalogue. In: Proc. 2nd Int. Symp. of Experimental Robotics, Toulouse, France: pp. 465-490.

Moe-Nilssen, R., Helbostad J.L., 2005. Interstride trunk acceleration variability but not step width variability can differentiate between fit and frail older adults. Gait and Posture, 21(2): 164-170.

Molen, N.H. (1973) Energy/speed relation of below-knee amputees walking on motor-driven treadmill. Int. Z. Angew. Physiol. 31: 173.

Morton DJ, Fuller DD. (1952) Human Locomotion and Body Form: A Study of Gravity and Man. Williams & Wilkins

Murray MP, Sepic SP, Bernard EJ. (1967) Patterns of sagittal rotations of the upper limbs in walking, a study of normal men during free and fast walking. Physical Therapy; 47(4):272-84

Nielsen, D.H., Shurr, D.G., Golden, J.C., Meier, K. (1988) Comparison of energy cost and gait efficiency during ambulation in below-knee amputees using different prosthetic feet: a preliminary report. J. Prosthet. Orthot. 1: 24-31.

Owings, T.M., Grabiner,M.D., 2003. Measuring step kinematic variability on an instrumented treadmill: how many steps are enough? Journal of Biomechanics, 36(8): 1215-1218.

Owings, T.M., Grabiner, M.D., 2004a. Step width variability, but not step length variability or step time variability, discriminates gait of healthy young and older adults during treadmill locomotion. Journal of Biomechanics, 37(6): 935-938.

Owings, T.M., Grabiner, M.D., 2004b. Variability of step kinematics in young and older adults. Gait and Posture 20: 26-29.

Powers, C.M., Boyd, L.A., Fontaine, C., Perry, J. (1996) The influence of lower extremity muscle force on gait characteristics in individuals with below-knee amputations secondary to vascular disease. Phys. Ther. 76: 369-377.

Pratt, J. E., Krupp, B. T., Morse, C. J., and Collins, S. H. (2004) The RoboKnee: An exoskeleton for enhancing strength and endurance during walking. In Proc. IEEE International Conference on Robotics and Automation, New Orleans, LA, 2430-2435.

Prince, F., Winter, D.A., Sjonnensen, G., Powell, C., Wheeldon, R.K. (1998) Mechanical efficiency during gait of adults with transtibial amputation: a pilot study comparing the SACH, Seattle, and Golden-Ankle prosthetic feet. Journal of Rehabilitation Research and Development 35:177-85.

Ralston HJ. (1965) Effects of immobilization of various body segments on the energy cost of human locomotion. Proc. Int'l Congress on Ergonomics; 53-60

Saunders, J. B., Inman, V. T., and Eberhart, H. D. (1953) The major determinants in normal and pathological gait. J. Bone Jt. Surg., Am. 35(A):544–553.

Siegler S, Liu W. (1997) Inverse dynamics in human locomotion. In: Allard P, Cappozzo A, Lundberg A, Vaughan CL, editors. Three-dimensional analysis of human locomotion. New York: John Wiley & Sons, p:191–209

Srinivasan, M. & Ruina, A. 2005 Computer optimization of a minimal biped model discovers walking and running. Nature 439, 72–75

Strogatz, S.H. (1994) Nonlinear Dynamics and Chaos. Addison Wesley

Stolze, H., Friedrich, H.J., Steinauer, K., Vieregge, P., 2000. Stride Parameters in Healthy Young and Old Women - Measurement Variability on a Simple Walkway. Experimental Aging Research, 26(2): 159-168.

Thomas, S.S., Buckon, C.E., Helper, D., Turner, N., Moor, M., Krajbich, J.I. (2000) Comparison of the Seattle Lite Foot and Genesis II Prosthetic Foot during walking and running. Journal of Prosthetics and Orthotics 12:9-14.

Torburn, L., Powers, C.M., Guiterrez, R., Perry, J. (1995) Energy expenditure during ambulation in dysvascular and traumatic below-knee amputees: a comparison of five prosthetic feet. Journal of Rehabilitation Research and Development 32:111-9.

Tucker, V. A. (1975) The energetic cost of moving about. American Scientist. 63(4): 413-419.

Vanderpool, M.T., Collins, S.H., Kuo, A.D. (2008) Ankle Fixation Need Not Increase the Energetic Cost of Human Walking. Gait & Posture, in press.

Wagenaar RC, van Emmerik REA. (2000) Resonant frequencies of arms and legs identify different walking patterns. J. Biomechanics; 33:853-861

Waters, R. L. and Mulroy, S. (1999) The energy expenditure of normal and pathologic gait. Gait and Posture 9: 207-231.

Webb D, Tuttle RH. (1994) Pendular activity of human upper limbs during slow and normal walking. American J. Physical Anthropology; 93:477-489

Weber W, Weber E. (1836) Mechanik der menschlichen Gehwerkzeuge. Gottingen. p. 426

Whittle, M. W. (1996) Gait Analysis: An Introduction, 2nd ed. Oxford: Butterworth-Heinemann.

Winter, D.A. (1990) Biomechanics and Motor Control of Human Movement, Second edition. John Wiley & Sons, Inc., Toronto.

Wisse, M., Frankenhuyzen, J.V. (2003) Design and construction of Mike; a 2D autonomous biped based on passive dynamic walking. In Proc. 2nd Int. Symp. on Adaptive Motion of Animals and Machines, Kyoto, Japan.

Wisse, M. (2004) Essentials of dynamic walking; analysis and design of two-legged robots. Ph.D. Thesis, Technische Universiteit Delft.

Zarrugh, M.Y., Todd, F.N., and Ralston, H.J., (1974) Optimization of Energy Expenditure During Level Walking. European Journal of Applied Physiology, 33: 293-306.